U.PORTO

FEUP FACULDADE DE ENGENHARIA
UNIVERSIDADE DO PORTO

Doctoral Program in Chemical and Biological Engineering

Development of effective disinfection strategies to control drinking water biofilms

Supervisor: Professor Manuel Simões

Co-Supervisors: Dr. Lúcia Simões

Dr. Peter Eaton

Isabel Maria Pereira de Oliveira

2023

This work was financially supported by: LA/P/0045/2020 (ALiCE), UIDB/00511/2020 and UIDP/00511/2020 (LEPABE), funded by national funds through FCT/MCTES (PIDDAC); Portuguese funds through FCT - Fundação para a Ciência e a Tecnologia, I.P., under the Pluriannual Financing Programme for R&D Units for the Centre of Biological Engineering of University of Minho (ref. UIDB/BIO/04469/2020); LABBELS – Associate Laboratory in Biotechnology, Bioengineering and Microelectromechanical Systems, LA/P/0029/2020; project HealthyWaters (NORTE-01-0145-FEDER-000069), supported by Norte Portugal Regional Operational Programme (NORTE 2020), under the PORTUGAL 2020 Partnership Agreement, through the European Regional Development Fund (ERDF); PT national funds (FCT/MCTES, Fundação para a Ciência e Tecnologia e Ensino Superior) through the project UIDB/50006/2020 | UIDP/50006/2020; and FCT PhD grant awarded to Isabel Maria Oliveira (SFRH/BD/138117/2018).

“Be curious. However difficult life may seem, there is always something you can do and succeed at. It matters that you don’t just give up.”

Stephen Hawking, at Oxford University Union speech in 2016

Acknowledgements

First and foremost, this project would not have been possible without the support of my supervisors. I would like to express my sincere gratitude to Professor Manuel Simões for supporting me since my undergraduate, for his invaluable patience and guidance through my PhD journey when I needed his support. I am deeply indebted for giving me the opportunities to improve my work and challenging me to grow as a scientist. I want to express my appreciation to Dr. Lúcia Simões for her insightful comments, support, and generous contribution of knowledge and expertise. In addition, this endeavour would not have been possible without Dr. Peter Eaton, who generously provided me with important resources to perform my work. His knowledge and experience were also very crucial for the planning and development of this project.

I would like to extend my gratitude to all the professional collaborations through my PhD journey. Dr. Inês Gomes and Dr. Anabela Borges, who took their time for discussions about anything that I was unsure about, I am thankful for their unlimited support and advice. Special thanks to Dr. Alexandra Plácido for her generous support and availability to help me during my experiments at FCUP. I am also grateful to Professor Maria da Conceição Rangel and Dr. Tânia Moniz for allowing me to develop part of my work in their research facilities and for their expertise to achieve valuable findings in this project.

Additionally, I want to thank BEL and LEPABE for the possibility to develop this work in their excellent facilities. Special thanks to all the BEL members, research assistants, and administrative staff that help me in different steps of my PhD journey. Especially to my lab- and PhD-mates Ana Cláudia Barros, Beatriz Magalhães, Diana Oliveira, Sara Faria, and Susana Fernandes, for their friendship, sharing of ideas, and moral support throughout these past 4 years.

I would be remiss in not mentioning my family and close friends for their continuous encouragement and love. My friends from the ‘PhD Peer Group’, who have become as my personal coaches through the COVID lockdown. Thanks of course to Rui, his kindness, patience, and emotional support have help me to keep my motivation and self-belief. Finally, I want to dedicate this thesis to my mother, whose love and inspiring resilience are with me in whatever I pursue.

Thesis outputs

Papers in international scientific journal with referees:

Oliveira IM, Gomes IB, Simões LC, Simões M. 2022. Chlorinated cyanurates and potassium salt of peroxymonosulphate as antimicrobial and antibiofilm agents for drinking water disinfection. Science of the Total Environment. 811:152355. doi: 10.1016/j.scitotenv.2021.152355.

Oliveira IM, Gomes IB, Plácido A, Simões LC, Eaton P, Simões M. 2023. The impact of potassium salt of peroxymonosulphate and chlorinated cyanurates on biofilms of *Stenotrophomonas maltophilia*: effects on biofilm control, regrowth and mechanical properties. Biofouling. In Press. doi: 10.1080/08927014.2023.2254704.

Oliveira IM, Gomes IB, Moniz T, Simões LC, Rangel M, Simões M. 2023. Realism-based assessment of the efficacy of potassium peroxymonosulphate on *Stenotrophomonas maltophilia* biofilm control. Journal of Hazardous Materials. 460: 132348. doi: 10.1016/j.jhazmat.2023.132348.

Oliveira IM, Gomes IB, Simões LC, Simões M. 2023. A systematic review of research advances on disinfection strategies for biofilm control in drinking water systems. Submitted.

Simões LC, **Oliveira IM**, Borges A, Gomes IB, Simões M. 2023. A procedure to harmonize the hydrodynamic force during microbial cultivation in shaking flasks. Journal of Microbiology and Biology Education. In Press. doi: 10.1128/jmbe.00099-23.

Sousa M, **Oliveira IM**, Correia L, Sousa CA, Braga DFO, Simões M. 2023 Far-UV-C radiation demonstrated bactericidal activity against adhered cells of *Escherichia coli* and *Staphylococcuc epidermidis*. Submitted.

Chapters in books:

Fernandes S, **Oliveira IM**, Gomes IB, Simões M. 2023. Surface disinfection – state of the art. In: Control/preventing of biological risks associated with food contamination during processing/distribution and consumer usage. Bénézech T and Faille C (eds.). ISTE SCIENCE PUBLISING LTD. In Press.

Oliveira IM, Fernandes S, Simões M, Gomes IB. 2023. Surface disinfection – new approaches. In: Control/preventing of biological risks associated with food contamination during processing/distribution and consumer usage. Bénézech T and Faille C (eds.). ISTE SCIENCE PUBLISING LTD. In Press.

Intellectual property:

Gomes IB, **Oliveira IM**, Fernandes S, Simões LC, Simões M. 2019. A head for a reactor for biofilm formation, reactor for biofilm formation, reactor for biofilm inactivation and removal from the adhesion surface, and related process for biofilm formation and process for biofilm inactivation and removal from the adhesion surface. Provisional patent application (PCT/IB2019/060443).

Abstracts in conferences:

Oliveira IM, Simões LC, Simões M. 2020. The effects of different biocides against selected drinking water-isolated bacteria in planktonic and sessile states. In: biofilms 9 international online conference, 29th September – 1st October 2020. Karlsruhe, Germany. doi: 10.5194/biofilms9-125. (Virtual poster presentation).

Oliveira IM, Simões LC, Simões M. 2021. Comparative antibiofilm efficacy of different disinfectants against *Acinetobacter calcoaceticus* and *Stenotrophomonas maltophilia* isolated from a drinking water distribution system. In: World Microbe Forum an ASM and FEMS collaboration, 20th – 24th June 2021. (Virtual poster presentation).

Oliveira IM, Simões LC, Simões M. 2021. Antimicrobial activity of chlorinated cyanurates and peroxymonosulphate against emerging pathogens isolated from drinking water. In: World Microbe Forum an ASM and FEMS collaboration, 20th – 24th June 2021. (Virtual poster presentation).

Oliveira IM, Simões LC, Simões M. 2022. The potential of OXONE as an alternative disinfectant to control drinking water biofilms. In: SUSTENG 2022 – 1st International Conference on Sustainable Chemical and Environmental Engineering, 31st August – 4th September 2022. Rethymno, Crete, Greece. ISBN: 978-618-86417-0-9. (Virtual oral presentation).

Oliveira IM, Simões LC, Eaton P, Simões M. Estudo da ação do OXONE em biofilmes de *Stenotrophomonas maltophilia* isolada de um sistema de distribuição de água potável. In: Microbiologia 2022 – Congresso internacional de microbiologia em língua portuguesa, 17th – 19th October 2022. (Virtual oral presentation).

Other publications:

Oliveira IM, Borges A, Borges F, Simões M. 2019. Repurposing ibuprofen to control *Staphylococcus aureus* biofilms. European Journal of Medicinal Chemistry. 166, 197-205. doi: 10.1016/j.ejmech.2019.01.046.

Abreu AC, Marín P, Aguilera-Sáez LM, Tristán AI, Peña A, **Oliveira IM**, Simões M, Valera D, Fernández I. 2019. Effect of a shading mesh on the metabolic, nutritional, and defence profiles of harvested greenhouse-grown organic tomato fruits and leaves revealed by NMR metabolomics. Journal of Agricultural and Food Chemistry. 67(46), 12972-12985. doi: 10.1021/acs.jafc.9b05657.

Oliveira IM, Borges A, Borges F, Simões M. 2019. The effects of ibuprofen on *Staphylococcus aureus* biofilm control. In: IC2AR – 3rd International Caparica Conference in Antibiotic Resistance, 10th – 13th June 2019. Caparica, Portugal. ISBN: 78-989-54470-0-8 (Awarded as Excellent Shotgun Communication Prize).

Oliveira IM, Borges A, Borges F, Simões M. 2019. Antibacterial and antibiofilm activities of ibuprofen against *Staphylococcus aureus*. 2019. In: DCE19 – 3rd Doctoral Congress in Engineering, Symposium on Chemical, Biological and Environmental Engineering, 27th – 28th June 2019. Porto, Portugal. ISBN: 978-972-752-255-2 (Oral presentation).

Oliveira IM, Borges A, Simões M. 2020. Chapter 14 – The potential of drug repurposing to face bacterial and fungal biofilm infections. In book: Recent Trends in Biofilm Science and Technology. 307-328. doi 10.1016/B978-0-12-819497-3.00014-3.

Abstract

More than a decade has passed since the declaration by the United Nations General Assembly that stated access to safe drinking water (DW) as a basic human right. Given its importance as a health and development issue, efforts have been done to increase the number of people with access to safely managed DW services. However, despite compliance with international guidelines for DW quality, drinking water distribution systems (DWDS) are subjected to biofilm development. The complex structure of biofilms ensures microbial protection from adverse conditions and provides a possible reservoir for pathogenic microorganisms that are not easily detected in bulk water. Although chlorine has been commonly used for DW treatment, the biofilm tolerance to chlorination and the production of harmful disinfection by-products highlight the need to search for new disinfection strategies to control DW biofilms.

Understanding microbial susceptibility to disinfectants is an important step for providing DW with adequate microbiological quality. Therefore, the antimicrobial activity of sodium dichloroisocyanurate (NaDCC), trichloroisocyanuric acid (TCCA), and pentapotassium bis(peroxymonosulphate) bis(sulphate) (OXONE) was evaluated against two emerging pathogens isolated from DW, *Acinetobacter calcoaceticus* and *Stenotrophomonas maltophilia*. Conventional hypochlorite-based disinfection was used for comparison. The dose and time-responses in planktonic bacteria were performed, as well as the assessment of the effects on cytoplasmic membrane integrity and physicochemical properties of bacterial surfaces. Minimum bactericidal concentrations (MBC) of 2.1 and 3.1 mg/L for NaDCC, 2.5 and 3.8 mg/L for TCCA, 340 and 690 mg/L for OXONE, and 0.80 and 1.0 mg/L for free chlorine were obtained against *S. maltophilia* and *A. calcoaceticus*, respectively. Kinetic modelling revealed that NaDCC and TCCA caused similar inactivation rates and the time for first log reduction by OXONE was less than 10 min, for both bacteria. All the disinfectants triggered significant bacterial cytoplasmic membrane destabilization, even at sub-lethal concentrations. Further, the effects of the selected disinfectants against 48 h-old biofilms formed on polyvinyl chloride (PVC) and stainless steel (SS) were also evaluated based on biofilm culturability and removal. NaDCC, TCCA, and OXONE had similar or better efficiencies in reducing biofilm culturability than free chlorine. OXONE was the most efficient disinfectant

against both bacterial biofilms, causing up to 4 log CFU/cm^2 reduction. However, biofilms of *S. maltophilia* were more tolerant to disinfection than those of *A. calcoaceticus*. Additionally, biofilm removal was invariably modest, for all the biofilms tested and disinfectants applied.

A deeper evaluation of the activity of the selected disinfectants on established *S. maltophilia* biofilms and in the prevention of biofilm regrowth after disinfection was performed. The viscoelastic properties of the biofilms and alterations in the structure were further evaluated by rheometry and atomic force microscopy (AFM) analysis. The disinfectants were generally more efficient against biofilms formed on SS than on PVC. The regrowth of biofilms on SS previously exposed to OXONE was limited by 5 and 4 log CFU/cm^2 in comparison to the unexposed biofilms and biofilms exposed to free chlorine, respectively. OXONE caused a reduction of the biofilm cohesiveness, revealed by a significant decrease of the complex shear modulus (G*) in comparison to unexposed biofilms or biofilms exposed to free chlorine. AFM analysis showed that biofilms after OXONE exposure had a fractured appearance and smaller bacterial aggregates dispersed on the top of the biofilm surface than in the control samples.

Following a realism-based approach, the effectiveness of OXONE to combat DW biofilms was validated against mature *S. maltophilia* biofilms formed in a simulated DWDS using a rotating cylinder reactor. Significant biofilm inactivation was observed after exposure to OXONE, with a reduction of culturable and non-damaged cells up to approximately 4 log. OXONE also presented better chemical stability in synthetic tap water (STW) than chlorine. The reactive species formed during the disinfection with OXONE in STW were further investigated by electron paramagnetic resonance analysis, revealing the presence of singlet oxygen and other non-identified radicals. Finally, the effects of OXONE on the growth of *Chlorella vulgaris* were studied, suggesting less ecotoxicity to the freshwater microalga than chlorine.

Collectively, the results of this project reinforce OXONE as a promising alternative to chlorine for the disinfection of DW biofilms. Although its routine use for DW requires further research on long-term safety for human consumption, OXONE may initially be indicated for temporary emergency disinfection of DW biofilms.

Resumo

Há pouco mais de uma década atrás, a Assembleia Geral das Nações Unidas declarou o acesso a água potável segura como um direito humano básico. Dada a sua relevância para a saúde humana e desenvolvimento das populações, vários esforços têm sido desenvolvidos para aumentar o número de pessoas com acesso a serviços de água potável geridos de forma segura. No entanto, apesar do cumprimento de diretrizes internacionais para a garantia de água potável de qualidade, os sistemas de distribuição de água potável estão sujeitos ao desenvolvimento de biofilmes. A estrutura complexa dos biofilmes garante a proteção microbiana contra condições adversas e fornece um possível habitat para microrganismos patogénicos que não são facilmente detetados nas análises de qualidade da água. Embora o cloro seja vulgarmente usado para o tratamento de água potável, a tolerância dos biofilmes à desinfeção e a produção de subprodutos nocivos decorrentes da reação do cloro com substâncias orgânicas justificam a necessidade de estudar estratégias alternativas para o controlo de biofilmes em água potável.

A compreensão da suscetibilidade microbiana aos desinfetantes constitui um passo importante para o fornecimento de água potável com qualidade microbiológica adequada. Neste projeto, a atividade antimicrobiana do dicloroisocianurato de sódio (NaDCC), ácido tricloroisocianúrico (TCCA) e bis(peroximonossulfato) bis(sulfato) de pentapotássio (OXONE) foi avaliada contra duas bactérias patogénicas emergentes isoladas de água potável, *Acinetobacter calcoaceticus* e *Stenotrophomonas maltophilia*. A desinfeção convencional com cloro livre foi usada para comparação. A relação dose-efeito e tempo de exposição das bactérias em estado planctónico aos desinfetantes foi estudada, bem como a avaliação dos efeitos na integridade da membrana citoplasmática e nas propriedades físico-químicas de superfícies bacterianas. As concentrações mínimas bactericidas obtidas contra *S. maltophilia* e *A. calcoaceticus* foram respetivamente de 2,1 e 3,1 mg/L para NaDCC, 2,5 e 3,8 mg/L para TCCA, 340 e 690 mg/L para OXONE e 0,80 e 1,0 mg/L para o cloro livre. O ajuste cinético das curvas obtidas revelou que o NaDCC e TCCA causaram taxas de inativação semelhantes, e que o tempo para a primeira redução logarítmica pelo OXONE foi inferior a 10 min, para ambas as bactérias. Todos os desinfetantes desencadearam uma destabilização significativa da membrana citoplasmática bacteriana, mesmo em concentrações sub-letais. Os efeitos dos

desinfetantes no controlo de biofilmes formados durante 48 h em policloreto de vinila (PVC) e aço inoxidável (SS) foram avaliados com base na capacidade de redução de células cultiváveis e remoção de biofilme. O NaDCC, TCCA e OXONE tiveram eficiências de redução de células cultiváveis dos biofilmes semelhantes ou melhores que a ação do cloro livre. O OXONE foi o desinfetante com melhor desempenho contra ambos os biofilmes de *S. maltophilia* e *A. calcoaceticus*, causando reduções até 4 log UFC/cm^2. No entanto, os biofilmes de *S. maltophilia* foram mais tolerantes à desinfeção que os de *A. calcoaceticus*. A remoção dos biofilmes foi invariavelmente modesta para todos os biofilmes testados e desinfetantes aplicados.

Posteriormente, foi realizada uma avaliação mais profunda da atividade dos desinfetantes selecionados no controlo de biofilmes pré-estabelecidos de *S. maltophilia* e na prevenção do recrescimento após a desinfeção. As propriedades viscoelásticas e alterações na estrutura dos biofilmes foram avaliadas por reometria e por microscopia de força atómica (AFM). Os desinfetantes foram geralmente mais eficientes contra biofilmes formados em SS do que em PVC. O recrescimento de biofilmes em SS previamente expostos ao OXONE foi limitado em 5 e 4 log UFC/cm^2, em comparação com os biofilmes não expostos ou biofilmes expostos ao cloro livre, respetivamente. O OXONE causou uma redução da coesão do biofilme, revelada pela diminuição significativa do módulo de rigidez complexo (G*), comparativamente aos valores obtidos para os biofilmes não expostos ou biofilmes expostos ao cloro livre. A análise por AFM mostrou que, após exposição ao OXONE, os biofilmes apresentaram uma aparência fraturada e com agregados celulares menores dispersos no topo da superfície do biofilme.

Seguindo uma abordagem de mimetização de condições reais, a eficácia do OXONE para o controlo de biofilmes foi validada contra biofilmes maduros de *S. maltophilia* formados num sistema de distribuição de água potável simulado por um reator de cilindros rotativos. Após exposição ao OXONE, observou-se uma inativação significativa do biofilme, com redução do número de células cultiváveis e de células não danificadas até aproximadamente 4 log. O OXONE também apresentou uma melhor estabilidade química em água da torneira sintética (STW) do que o cloro. As espécies reativas formadas durante a desinfeção com o OXONE em STW foram avaliadas por ressonância paramagnética eletrónica, revelando a presença de oxigénio singleto e outros radicais não identificados. Finalmente, os efeitos do OXONE foram estudados no crescimento de

Chlorella vulgaris, indicando uma menor ecotoxicidade para a microalga de água doce do que o cloro.

Coletivamente, os resultados deste projeto reforçam o OXONE como uma alternativa promissora em relação ao cloro para o controlo de biofilmes nos sistemas de distribuição de água potável. Embora o seu uso recorrente para a desinfeção de água potável exija mais estudos sobre a sua segurança para o consumo humano a longo prazo, o OXONE poderá inicialmente ser indicado para desinfeção de emergência temporária de biofilmes formados nos sistemas de água potável.

Table of contents

List of figures

List of tables

List of abbreviations

AFM – atomic force microscopy

AUC – area under the curve

BAC – biological activated carbon

BOM – biodegradable organic matter

BPD – Biocidal Product Directive

CDC – Centers for Disease Control

CSTR – Continuous stirred tank reactor

DBPs – disinfection by-products

DMPO – 5,5-dimethyl-1-pyrroline-*N*-oxide

DNEL – derived-no-effect level

DW – drinking water

DWDS – drinking water distribution systems

EC_{50} – median effective concentration for 50% of growth reduction

ECHA – European Chemicals Agency

EPA – Environmental Protection Agency

EPDM – ethylene- propylene-diene monomer

EPR – electron paramagnetic resonance

EPS – extracellular polymeric substances

GAC – granular activated carbon

HDPE – high-density polyethylene

LVR – linear viscoelastic region

MBC – minimum bactericidal concentration

NaDCC – sodium dichloroisocyanurate

NOAEL – no-observed-adverse-effect level

NSF – National Sanitation Foundation

nZVI – zero-valent iron

OXONE – pentapotassium bis(peroxymonosulphate) bis(sulphate)

PI – propidium iodide

PVC – polyvinyl chloride

RCR – rotating cylinder reactor

ROS – reactive oxygen species

SD – standard deviation

SS – stainless steel

STW – synthetic tap water

TCCA – trichloroisocyanuric acid

TDI – tolerable daily intake

UV – ultraviolet

WHO – World Health Organization

4-oxo-TEMP – 2,2,6,6-tetramethyl-4-piperidone hydrochloride

Chapter 1

Work outline

This chapter summarizes the relevance and motivation of the work, the main objectives, and a description of the organization of the thesis.

1.1 Relevance and Motivation

Access to safe drinking water (DW) is essential to health, a basic human right, and a component of effective policy for public health protection (UN General Assembly, 2010). The World Health Organization (WHO) states that a satisfactory water supply must be available to all, and every effort should be made to achieve DW that is as safe as practicable (WHO, 2022). However, an appreciable number of serious health concerns may occur because of chemical and microbial contamination of DW. The potential health problems of microbial (bacterial, viral, protozoan, or other biological) contamination are such that its control must always be of utmost importance and must never be compromised (WHO, 2022). In the pursuit of pathogen-free DW, disinfection practices are applied to remove the majority of microorganisms found in raw water. However, the treated water is not sterile, and low levels of microorganisms persist in drinking water distribution systems (DWDS) (Lugo et al., 2021; Novak Babič et al., 2020). In fact, more than 95% of the total biomass in DWDS can be found attached to pipe walls in the form of biofilms, while only up to 5% of the biomass is freely suspended in the bulk water (Chan et al., 2019; Liu et al., 2016; Simões and Simões, 2013).

Biofilms can be defined as microbial-derived sessile communities, constituted by cells that are attached to a substratum, interface, or each other, embedded in a matrix of extracellular polymeric substances (EPS), and exhibiting an altered phenotype concerning growth, gene expression, and protein production (Donlan and Costerton, 2002; Flemming and Wuertz, 2019). Biofilm-embedded microorganisms benefit from several advantages over planktonic cells. The extracellular matrix is capable of sequestering and concentrating environmental nutrients such as carbon, nitrogen, and phosphate. On the other hand, microorganisms in biofilms have the ability to evade multiple clearance

mechanisms, namely the exposure to disinfectants (Simões et al., 2010; Yuan et al., 2020). When the detachment of portions of biofilms occurs in DWDS, biofilm-embedded microorganisms enter into the bulk water, permitting a possible outbreak of disease (Hemdan et al., 2021; Simões and Simões, 2013; Zhang et al., 2018). Therefore, biofilms should be considered when DW microbial control strategies are being designed. However, currently there is no known affordable strategy able to successfully prevent or control biofilm formation (Simões and Simões, 2013; Simões et al., 2010).

Chemical control of microbial contamination is the most widely employed method, particularly for DWDS, as chemicals generally offer downstream residual control, which other methods cannot provide. Chlorine in the form of chlorine gas, sodium hypochlorite or calcium hypochlorite is the most widely used disinfectant for water treatment (Pichel et al., 2019; WHO, 2022). Nevertheless, the potential toxicity of chlorine gas, as a pulmonary irritant, as well as side reactions of chlorine compounds to form toxic disinfection by-products (DBPs) have caused some concerns about the use of chlorination as a method for microbial control (Andersson et al., 2019; Cahoon, 2019; Pichel et al., 2019). Additionally, it is known that the increase in microbial tolerance to conventional chlorination can occur (Luo et al., 2021; Mir et al., 1997). Furthermore, chlorination *per se* does not control the biofilms formed on the DWDS surfaces (Miller et al., 2015; Novak Babič et al., 2020; Pelleieux et al., 2016). This is in part due to the current DW guidelines for testing disinfectant effectiveness that are mainly based on experiments carried out with planktonic cultures, without mimicking the growth conditions found on surfaces where the disinfectants are required to act (European Standard, 1997).

Consequently, there is an urgent need to seek and develop new and alternative strategies to control the presence of biofilms in DWDS and minimize the environmental and public health impacts of traditional methods. On the other hand, the use of novel

disinfectants has been becoming more critical, especially in Europe, as a result of the Biocidal Product Directive. The Regulation No 528/2012 of the European Parliament and the Council (Regulation (EU) No 528/2012) has two major obvious consequences: i) a decrease in the number of available active biocides; ii) a decline in new product introductions – initial cost are significant and the return on investment takes longer. Therefore, the prudent use of disinfectants by knowing their exact activity against microorganisms, in both planktonic and sessile states, is fundamental to preserving their efficacy and preventing microbial tolerance.

Sodium dichloroisocyanurate (NaDCC), trichloroisocyanuric acid (TCCA), and potassium salt of peroxymonosulphate (OXONE) are being evaluated by the European Chemicals Agency (ECHA) for the disinfection of DW. Specifically, the initial application for approval of NaDCC and TCCA is under competent authority evaluation, while the initial application for approval of OXONE is under opinion development by the Biocidal Products Committee (ECHA, 2022a, 2022b, 2023a). In the United States, the Environmental Protection Agency (EPA) approval and National Sanitation Foundation (NSF) certifications allow the use of the chlorinated isocyanurates NaDCC and TCCA for routine treatment of DW (Kuechler, 2009; NSF, 2018). However, chlorinated isocyanurates are principally used to stabilize the residual chlorine in swimming pools, for industrial water treatment (*i.e.* cooling towers), and for sanitation in the food industry (Kuechler, 2009; Wahman, 2018). NaDCC and TCCA are alternative sources of chlorine since they have a high chlorine content bound to cyanuric acid, and in water, they are dissociated by a quick equilibrium reaction, providing a continuous release of free chlorine (Clasen and Edmondson, 2006; Wahman, 2018). OXONE is a chlorine-free oxidising agent. It has a broad application in the field of advanced oxidation processes for degradation of organic pollutants in wastewater or groundwater (Ghanbari and

Moradi, 2017; Lee et al., 2020). However, studies on OXONE disinfection are limited (Lee et al., 2020; Wacławek et al., 2017). Both chlorinated isocyanurates and OXONE are dry solids and very stable in this state, which makes them easy to handle and store (Clasen and Edmondson, 2006; Kuechler, 2009; Wacławek et al., 2017). Information on the mode of action of these compounds has not been sufficiently explored. Moreover, most of the available literature describing the antimicrobial action of NaDCC, TCCA, and OXONE is mainly focused on their effects on planktonic microorganisms. The real impact of these alternatives in water treatment interventions and control of DW biofilms has yet to be demonstrated.

1.2 Objectives

This PhD project aimed to understand the effects of new alternatives to hypochlorite-based disinfection on DW biofilms, with particular emphasis on biofilm control and prevention of regrowth. To obtain results with practicable significance, DW-isolated microorganisms and experimental conditions mimicking DWDS were used.

The specific objectives are provided below:

a. Evaluation of the antimicrobial activity of disinfectants, with an initial application for approval by ECHA, against DW-isolated bacteria based on relevant physiological indices.
b. Assessment of the most effective disinfectant to control DW biofilms by determination of the effects on biofilm culturability, removal, structure, and mechanical stability, as well as on biofilm regrowth events.

c. Realism-based validation of the performance of the selected disinfectant against mature biofilms formed in a bench-scale biofilm reactor mimicking real conditions found in a DWDS.
d. Study of the mode of action and possible advantages in terms of chemical stability and toxicity of the selected disinfectant in comparison to conventional hypochlorite-based disinfection.

1.3 Synopsis

This thesis is divided into seven main chapters that are summarized below.

Chapter 1 presents the relevance and motivation of the project as well as the main objectives of this work.

Chapter 2 is a literature review, with particular emphasis on the problems of biofilms in DWDS and its control. Firstly, some generic concepts and conventional technologies for water disinfection are presented. Current practices commonly applied to control biofilm growth in DWDS are described. Then, a systematic review is presented to assess the scientific knowledge gained from the research on the disinfection of DW biofilms in the last decade.

Chapter 3 describes in detail all the materials and methods used in the experimental work reported in this thesis.

The main results and respective discussion are presented in Chapters 4, 5, and 6. In Chapter 4 is included the evaluation of the antimicrobial activity of NaDCC, TCCA, and OXONE against two emerging pathogens, *Acinotobacter calcoaceticus* and *Stenotrophomonas maltophilia*. The dose and time-responses against planktonic bacteria were performed as well as the assessment of the effects on selected physiological indices

(membrane integrity and physicochemical properties of bacterial surface). Moreover, the effects of the selected disinfectants against 48 h-old single-species biofilms formed on two representative pipe materials were evaluated in terms of reduction in biofilm culturability and biofilm removal. The results presented in this chapter are published in the manuscript: Oliveira IM, Gomes IB, Simões LC, Simões M. 2022. Chlorinated cyanurates and potassium salt of peroxymonosulphate as antimicrobial and antibiofilm agents for drinking water disinfection. Science of the Total Environment. 811:152355.

Chapter 5 aims to derive an understanding of the action of OXONE and chlorinated isocyanurates against biofilms, particularly their effects on the structure and mechanical properties. The effects of the selected disinfectants in the prevention of biofilm regrowth after disinfection were also evaluated. *S. maltophilia* biofilms were studied in more detail in this chapter because they were found to be more tolerant to the selected disinfectants than those of *A. calcoaceticus* in the previous study. The results included in this chapter are in the process of production of the manuscript: Oliveira IM, Gomes IB, Plácido A, Simões LC, Eaton P, Simões M. 2023. The impact of potassium peroxymonosulphate and chlorinated cyanurates on biofilms of *Stenotrophomonas maltophilia*: effects on biofilm control, regrowth, and mechanical properties. Biofouling. In Press. doi: 10.1080/08927014.2023.2254704.

In chapter 6 a realism-based assessment of the potential of OXONE to control DW biofilms in comparison to chlorine disinfection is performed. The effects of OXONE were evaluated against 7 day-old *S. maltophilia* biofilms formed under conditions mimicking DWDS using the bench-scale biofilm reactor – rotating cylinder reactor (RCR). The chemical stability of OXONE and chlorine solutions in STW at 25 ºC was evaluated over 40 days. The reactive species produced during the OXONE disinfection in STW were identified by electron paramagnetic resonance (EPR) analysis. Additionally, the

ecotoxicity of the disinfectants was examined using a freshwater microalga as test organism, and considerations of possible toxicological profiles resulting from human consumption in DW are discussed. The main results included in this chapter are published in the manuscript: Oliveira IM, Gomes IB, Moniz T, Simões LC, Rangel M, Simões M. 2023. Realism-based assessment of the efficacy of potassium peroxymonosulphate on *Stenotrophomonas maltophilia* biofilm control. Journal of Hazardous Materials. 460: 132348.

The main conclusions of the overall study are outlined in chapter 7, as well as perspectives for further research.

Supplementary experimental work performed for optimization of the methods and other experimental results not included as the main results of the thesis are presented in the Annexes section.

The PhD project was performed mainly in the facilities of LEPABE – Laboratory for Process Engineering, Environment, Biotechnology, and Energy, at the Department of Chemical Engineering of the Faculty of Engineering of the University of Porto. The effects of selected disinfectants (from the product type 5 list of ECHA) at sub-lethal and lethal concentrations were assessed on relevant physiological indices of two DW bacteria that were already isolated from a DWDS at CEB – Centre of Biological Engineering of the University of Minho. All the techniques performed regarding objective a) were available and already validated at LEPABE. Most of the work of objectives b) and c) regarding the evaluation of the effects of disinfectants on biofilm control was developed at LEPABE, with exception of the study of the biofilm mechanical stability/cohesion that was accomplished at REQUIMTE/LAQV – Associated Laboratory for Green Chemistry of the Network of Chemistry and Technology, at the Department of Chemistry and Biochemistry of the Faculty of Sciences of University of Porto, and at Biointerfaces and

Nanotechnology core facility, at INEB – Instituto de Engenharia Biomédica. Initially, the changes in the biofilm mechanical properties (without and with disinfection exposure) were intended to be studied by atomic force microscopy (AFM)-based indentation technique followed by determination of Young's modulus, which would allow the biofilm characterization under non-destructive conditions. However, challenges related to the force-distance curve acquisition underwater and time limitations due to COVID-19 lockdowns forced the reformulation of the work plan. Consequently, AFM analysis was implemented for the topographic characterization (image acquisition) of the biofilms and additional rheometry analysis was employed for the determination of viscoelastic properties. Finally, the experimental work concerning objective d) was mainly performed at LEPABE, as well as in collaboration with Laboratory for Electron Paramagnetic Resonance Spectrometry from CEMUP – Centro de Materiais da Universidade do Porto - for identification of reactive species involved in the disinfection process with OXONE.

Chapter 2

Literature review

This chapter comprises a literature review with a special focus on biofilm issues and control in DWDS. First, some general concepts and traditional techniques for water disinfection are presented. State-of-the-art methods commonly used to control biofilm growth in DWDS are described. Then a systematic review is provided to assess the scientific knowledge gained from DW biofilm disinfection research over the past decade.

2.1 Introduction

In DW networks, multiple approaches are applied to treat the raw water and against any contamination resulting from the loss of integrity of the systems. Conventional DW treatment technologies include physical methods, particularly, flocculation and sedimentation, filtration, ultraviolet (UV) irradiation and pasteurization, and chemical methods, such as chlorination, chloramination, and ozonation. Only the activities associated with the destruction or inactivation of microorganisms can be denominated as disinfection treatments (*e.g.* chemical methods, irradiation, heat) (Cahoon, 2019; Ellis, 1991; Pichel et al., 2019). Generally, the disinfection of water can be grouped into two categories, the primary disinfection to eliminate the pathogens in the raw water supply, and secondary disinfection to minimize the effects of re-contamination during storage and distribution (Pichel et al., 2019). Treatment technologies can also be distinguished by their utility for point-of-use or larger distribution networks. DW systems typically serve multiple residences and users in more urbanized settings and are composed of pumping, water treatment plants, storage, and transmission line infrastructure. The combination of different strategies along the network are applied since the failure of one barrier can be compensated for the efficiency of the remaining barriers (LeChevallier and Au, 2004; WHO, 2022). **Figure 2-1** presents the different stages and technologies for water treatment that are usually implemented in urbanized DW systems, from source to household water mains.

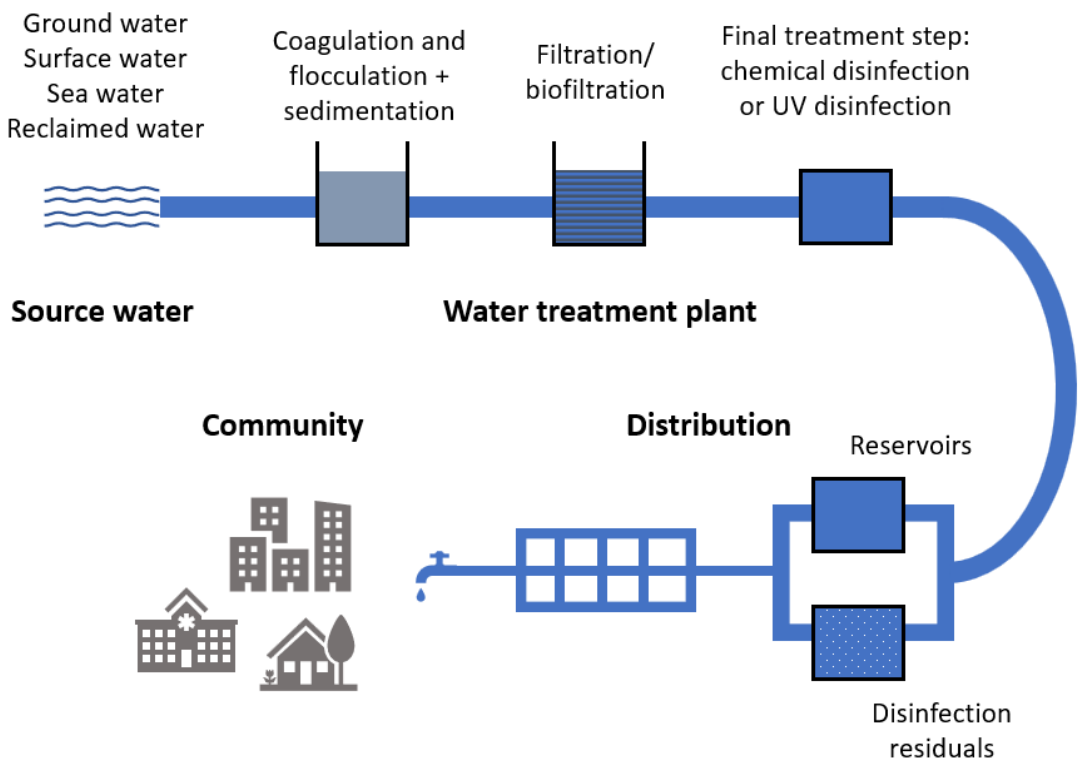

Figure 2-1 – Schematic representation of common urbanized DW systems with different stages and technologies for water treatment.

Regarding the chemical disinfection methods, the key technical advantages and limitations of different disinfectants that are used for water treatment are summarized in **Table 2-1**. Chlorination is the most commonly used method for DW disinfection (Pichel et al., 2019; WHO, 2022). Chlorine gas (Cl_2) or chlorine-related forms (sodium hypochlorite or calcium hypochlorite) are added to water, where it reacts to form hypochlorous acid (HOCl) and hypochlorite ion (OCl^-), usually termed as free chlorine (Ellis, 1991). Although both the undissociated hypochlorous acid and the hypochlorite ion are disinfecting agents, the hypochlorite ion is far less effective than the undissociated hypochlorous acid (Ellis, 1991). Therefore, the germicidal effect of chlorine in water is dramatically reduced as the pH rises above pH 7. The mechanism of inactivation appears to be primarily the destruction of the cytoplasmic membrane and the inhibition of the enzymatic activity. The selective permeability of the membrane is destroyed, respiration

is impaired, and irreparable damage is triggered to the metabolic functions and DNA (Ellis, 1991; Nizer et al., 2020). Haas and Engelbrecht (1980) proposed that both the cell membrane and physical damage of the DNA, possibly involving strand scission or cross-linkages, are the causative effects of the lethal lesions by chlorine. However, the increase in microbial tolerance to chlorine and the production of toxic DBPs are the main disadvantages of conventional chlorination (Andersson et al., 2019; Luo et al., 2021).

Chloramination is less effective than chlorination and consists of the addition of ammonia and chlorine in a controlled manner to react and form monochloramine (NH_2Cl), which must be generated at the point-of-use (U.S. EPA, 2011; Pichel et al., 2019). Chloramines are generally used as a secondary disinfectant during distribution, rather than for primary disinfection.

Chlorine dioxide (ClO_2) is a more powerful oxidizing agent than chlorine and chloramines, and it is less pH-dependent than that chlorine (Pichel et al., 2019). Another advantage of using chlorine dioxide in the water industry is its lack of reaction with ammonia, reducing the oxidation demand in water and allowing its dosing into lower-quality surface waters (Ellis, 1991). However, the principal concern with the use of chlorine dioxide in water treatment is the possible toxicity of the chlorite ion produced.

Ozone (O_3) used as a water disinfectant is the only real competitor to the employment of chlorine (Ellis, 1991). Its use in water treatment is a result of its electrophilic characteristics and is generated on-site by passing dry oxygen or air through a system of high-voltage electrodes (Ellis, 1991; Pichel et al., 2019). Vegetative bacteria are readily destroyed by ozone in water. A dose of 0.19 mg/L over 5 min was sufficient to kill all vegetative *Bacillus cereus*, *Bacillus megaterium*, and *Escherichia coli*, while the spores of *B. cereus* and *B. megaterium* required between 2.03 and 2.29 mg/L O_3 over a 5 min period to be inactivated (Broadwater et al., 1973; Ellis, 1991). However, ozone

concentration in water decays more rapidly than other disinfectants, so it is suitable as a primary disinfectant without residual protection against re-contamination in the distribution system (Pichel et al., 2019).

Table 2-1 – Comparison of different chemical methods for microbial disinfection of DW, adapted from the Environmental Protection Agency manual (2011).

Disinfectant	Advantages	Limitations
Chlorine (various forms)	Well understood disinfectant capability Established dosing technology Stable residual in clean networks Potential for using it for both primary disinfection and distribution It is commonly used in the oxidation and removal of iron and manganese in water treatment upstream of disinfection	By-product formation, taste and odour issues can affect acceptability
Chlorine dioxide	More effective than chlorine at higher pH Stable residual with no significant by-product issues Less taste and odour issues	Inorganic by-product formation (chlorate and chlorite) limits the dose of chlorine dioxide that can be applied Substantially more expensive than chlorine
Chloramines	No significant by-product issues The taste threshold is typically much greater than for chlorine alone	Considerably less effective than chlorine Not usually applied as a primary disinfectant Mixing with non-chloraminated supplies can cause taste and odour issues Good process control is required
Ozone	Strong oxidant and highly effective disinfectant compared with chlorine Benefits of destruction of organic micropollutants (pesticides, taste and odour compounds)	Complex, energy-intensive, and expensive equipment compared with chlorination Residual insufficiently long-lasting for distribution

Concerning physical technologies, UV irradiation constitutes another relevant disinfection method. UV-based disinfection of water is normally achieved by passing the water through tubes lined with UV lamps using wavelengths at about 255 nm (Ellis, 1991; Pichel et al., 2019). Unlike many chemical disinfectants, UV irradiation impacts no taste and odour to water and has no risk due to overdosing. The adverse effect on cells results primarily from photochemical damage to nucleic acids, and energy dissipation causes disruption of unsaturated bonds which appears to produce a progressive lethal biochemical change (Ellis, 1991; Sedgwick, 1973). Nevertheless, supplementary processes are required upstream to clarify the water and improve the effectiveness of the UV disinfection, and in addition, UV treatment does not have a residual effect in treated water, being only suitable for primary disinfection.

2.2 The occurrence of biofilms in DWDS and current practices for biofilm control

Biofilms are persistent microbial communities grown on any surface in contact with water, responsible for several undesirable effects on the water quality, including a possible source of waterborne opportunistic pathogens (Hemdan et al., 2021; Ma et al., 2020; Simões and Simões, 2013). These complex and organized microbial communities are composed of cells embedded in a self-produced matrix of EPS that provides integrity to the three-dimensional structure of biofilms and protection from adverse environmental conditions (Ciofu et al., 2022; Desmond et al., 2018).

Although a multiple-barrier approach is applied in water treatment plants and for management of DWDS, biofilms are ubiquitous along the water networks. Emtiazi et al. (2004) investigated the formation of natural biofilms in different sites of a DW production

system, covering biofilms from surface water, raw water after bank filtration, downstream of granular activated carbon filtration, after UV disinfection, as well as from the downstream municipal distribution system. Even though reductions in cell counts and enzyme activities of biofilms during the disinfection process from surface water to DW reflected an improvement in its trophic status, biofilms were detected directly after UV disinfection, from 1 to 2 m distance. Moreover, opportunistic pathogens such as atypical mycobacteria and *Legionella* spp. were found in DW biofilms, and *Pseudomonas aeruginosa* was sporadically detected, despite preceding filtration and UV disinfection.

Community composition studies have revealed that DW microbiota is complex, with wide variation in the identity and composition of microbial communities in DW biofilms. Given the high growth rates of bacteria, their relatively small size, adaptation capabilities, and ability to produce EPS, biofilm microbial communities in DWDS are generally dominated by that type of cells (Characklis and Marshall, 1990; Liu et al., 2016). Proteobacteria, particularly those belonging to the α, β, γ, and δ subclasses, have been found to generally dominate biofilms in DWDS (Liu et al., 2016; Proctor and Hammes, 2015; Wu et al., 2015). However, viruses, filamentous fungi, algae, and protozoa may also be present in DW biofilms. Single-species biofilms are rare, and in many cases, biofilm formation can be enhanced by the co-presence of microorganisms (Schwering et al., 2013; Simões et al., 2007b; 2023). For instance, in a full-scale chloraminated DWDS composed by cast-iron water mains it was found that *Mycobacteria* dominated the biofilm communities at the biofilm-bulk water interface, with the detection of both non-pathogenic *Mycobacterium frederiksbergense* and *Mycobacterium aurum* at a higher frequency, and the opportunistic pathogens *Mycobacterium haemophilum* and *Mycobacterium abscessus* at a low number (Gomez-Smith et al., 2015). On the other

hand, underneath of the corrosion tubercules, the biofilm communities were dominated by sulphate-reducing bacteria from the genus *Desulfovibrio* (Gomez-Smith et al., 2015).

The development of biofilms in the distribution systems is affected by several inter-related factors. The biodegradable organic matter (BOM) in water is metabolized by most aquatic microorganisms for energy sources and the production of cellular materials (Liu et al., 2016). The levels of BOM are unique to each distribution system depending on the water source, which significantly shapes the microbial community in the water networks (Hozalski et al., 1999; Pan et al., 2021; Sun et al., 2014; Wan et al., 2019). The presence of inorganic nutrients, such as phosphorus or nitrogen, also influences biofilm growth. Following phosphate addition, changes in the biofilm structure and microbial community can be observed (Batté et al., 2003). Biofilms have been shown to increase EPS production in response to phosphorus limitation. Additionally, the growth-enhancing effect of both planktonic cells and biofilm was observed with the addition of phosphate in water with low phosphorus content (Kim et al., 2014; Liu et al., 2016). Likewise, nitrogen content in water can also modulate the composition of microbial communities in biofilms (Navada et al., 2020; Song et al., 2021). The relative abundance of autotrophic bacteria is promoted by high nitrogen-to-carbon ratios, while predominantly heterotrophic bacteria growth is present at low nitrogen-to-carbon ratio (Liu et al., 2016; Ohashi et al., 1995). Biofilm development in DWDS can also be affected by trace metals such as iron and copper (Gomes et al., 2019; Hindré et al., 2008).

The development of biofilms in DWDS is also known to be altered by the choice of pipe materials. The corrosion products of materials susceptible to degradation such as iron- and copper-based materials have biofilm growth-promoting effects, as well as possible chemical reactions with disinfectant residuals leading to disinfectant depletion (Li et al., 2019; Liu et al., 2016). Most polymeric pipes have shown less biofilm growth

compared to those formed on corrosion-prone materials (Liu et al., 2016). Nevertheless, some studies have observed the leaching of emerging contaminants from plastic-based pipes into water that can threaten both human health and the environment (Mohammadi et al., 2022; Ye et al., 2020; Zhang et al., 2022). Microplastics of polyvinyl chloride (PVC), polyamide, polypropylene, polyethylene, and polyethylene terephthalate were commonly found in DW (Mohammadi et al., 2022). Zhang et al. (2022) demonstrated that ozone-exposed pipe materials predominantly released small-sized microplastics between 1 to 10 µm, being this release facilitated by the surface crack propagation and fragmentation in aged plastic pipe materials. Besides microplastics, DW in contact with polymer materials during transport and storage presented the highest mean concentrations of other emerging contaminants including bisphenol A, phthalates, nonylphenol, perfluoroalkyl, and polyfluoroalkyl substances (Mohammadi et al., 2022).

Another important operational condition that potentially affects biofilm growth is the flow-rate variation in DWDS. Different locations along the DW network systems have variable hydrodynamic conditions, oscillating from laminar to turbulent and conversely. At low flow rates, the nutrient transport and shear effects are decreased, stimulating the formation of more loosely attached and more-porous biofilms. On the other hand, turbulent flow and high-shear-stress conditions result in the growth of thinner, denser, and less-porous biofilms (Liu et al., 2016; Liu and Tay, 2002; Moreira et al., 2013). Even though the detachment of mature biofilms due to increased shear stress on the outer layers may be promoted by high flow rates.

The elimination of biofilms in water distributions is practically impossible to achieve and to date, no approach has shown complete success in eradicating them. The strategies implemented for biofilm prevention and control in DWDS are based on factors known to contribute to biofilm development, such as the concentration of nutrients in the water,

type and stability of the material used in DWDS, the hydrodynamic conditions in DWDS, and levels of disinfectant residual through the distribution system (Gagnon et al., 2002; Liu et al., 2016; Simões and Simões, 2013).

The balance between nutrient removal and residual disinfection has been a high priority for many water utilities because the presence of organic matter in water increases the disinfectant demand (Gagnon et al., 2002; Simões and Simões, 2013). For a balanced growth in DW, a generally accepted assumption is that carbon, nitrogen, and phosphorus must be present in a ratio of approximately 100:10:1, respectively (Camper, 1994; Gagnon et al., 2002; Simões and Simões, 2013). Therefore, the strategy of accomplishing high levels of BOM removal and subsequently delivering very low disinfectant residual concentrations has been becoming popular in Europe (Gagnon et al., 2002). For example, the Netherlands, Germany, Austria, and Switzerland, have taken the approach of distributing DW without the use of post-disinfection because of concerns associated with DBPs, taste and odour complaints, and public perception (Gagnon et al., 2002; Simões and Simões, 2013). The removal of BOM is mainly executed by biological treatment processes including fluidized bed filters, slow sand filters, biological activated carbon (BAC) filters, and soil-aquifer treatment systems. Additionally, ozone can also be applied to water before filtration with either a rapid sand filter or a BAC filter (Gagnon et al., 2002; Mirnasab et al., 2021; Peterson and Summers, 2021; Sinha and Mukherji, 2022). However, most water treatment plants strive to ensure the maintenance of a disinfectant residual throughout the distribution system. In fact, disinfectant residuals minimize the propensity of microorganisms for regrowth or re-inoculation from biofilms, reduce the risk of general contamination from exogenous intrusions, and serve as a sentinel of any rupture of the system integrity (Haas, 1999).

As explained above, chlorine is the most widely used disinfectant for water treatment and is also applied to control microbial accumulation in pipes and tanks. Chlorine inhibits the reversible-to-irreversible transition of cell attachment to surfaces by degrading cell-membrane functional groups and associated polymers, however, it is incapable of the complete inhibition of biofilm growth (Xue and Seo, 2013). Alternatively, chloramines are often used in distribution systems in which free chlorine residuals are difficult to maintain or to avoid excessive by-product formation (Liu et al., 2016). LeChevallier et al. (1990) conducted a study to evaluate the differences in disinfection efficiency between free chlorine and monochloramine for controlling biofilm growth in a model pipe system. Either free chlorine or monochloramine at low levels (1 mg/L) could reduce viable counts of more than 2 log reduction for biofilms grown on galvanized, copper, or PVC pipe surfaces. However, free chlorine residuals ranging from 3 to 4 mg/L were ineffective for biofilm control on iron pipes. Conversely, biofilms treated with monochloramine residuals (> 2 mg/L) exhibited more than 3 log reduction. Therefore, the accumulation of corrosion products on iron pipes was found to interfere with chlorine disinfection. On the other hand, although less reactive in comparison to chlorine against planktonic microorganisms, chloramines have been reported to have greater penetrating capacity in biofilms due to their relatively low tendency to react with EPS (LeChevallier et al., 1988; Liu et al., 2016). Nevertheless, the use of chloramine has been associated with the growth of certain nitrifying bacteria within the biofilm, due to the release of ammonia from chloramine decay (Li et al., 2014). Additionally, chlorine-resistant bacteria were also detected in full-scale chloraminated DWDS, including *Bdellovibrio*, *Bradyrhizobium*, *Peredibacter*, *Sphingomonas*, and *Hydrogenophaga* bacteria (Miao et al., 2022). The authors indicated that resistance was modulated by glutaminyl-tRNA biosynthesis given

the increase of relative abundance of glutamate-tRNA ligase after chloramine disinfection (Miao et al., 2022).

To avoid zones in the distribution network with high organic material sedimentation, and consequently abundant biofilm formation, the DWDS must be planned to reduce as much as possible the presence of zones of water stagnation and high water residence times in pipes (Liu et al., 2016; Simões and Simões, 2013). Flushing, pigging, and air-water scouring are considered to be the best routine management practices for biofilm control because they also remove any biomass killed or inactivated by disinfection (Liu et al., 2016).

2.3 Guidelines and regulations for DW disinfection

The management and monitoring of DW quality are based on guidelines and regulations that establish acceptable limit values for various potential contaminants and support the development and implementation of activities to ensure the protection of public health (Tsaridou and Karabelas, 2021). The WHO guidelines for DW quality provide information on water quality and health, including effective management approaches, which are commonly accepted through consensus and internationally adopted in the development of national policies and regulations (WHO, 2022). On the other hand, technical regulations are legislative documents issued by authorities that stipulate mandatory product and process characteristics, as well as applicable administrative provisions (Tsaridou and Karabelas, 2021). Within this regulatory context, the new European Union DW Directive (Directive (EU) 2020/2184) published in December 2020 repealed the previous Council Directive 98/83/EC on the quality of water intended for human consumption. This Directive (EU) 2020/2184 lays down rules for the

protection of "human health from the adverse effects of any contamination of water intended for human consumption by ensuring that it is wholesome and clean, and to improve access to water intended for human consumption" for all in the European Union.

Concerning microbiological contaminants in DW, the practical approach for setting DW system performance is based on the control of specific microbial indicators, assuming that there is a relationship between an indicator density and the potential health risks involved (Lugo et al., 2021; Tsaridou and Karabelas, 2021; WHO, 2022). The WHO guidelines provide a range of indicator organisms that should be considered for different purposes in DW monitoring, including validation of the treatment process, operational monitoring, and surveillance (WHO, 2022). *E coli* has traditionally been used to monitor DW quality as an indicator of faecal pollution and is a well-established parameter implemented in the verification or surveillance. Heterotrophic plate counts can be used as operational indicators of bacterial disinfection effectiveness and DWDS cleanliness and integrity. The presence of total coliforms in the distribution networks can reveal regrowth and possible biofilm formation or contamination from possible breaches in the system (WHO, 2022). However, viruses and protozoa more resistant to treatment technologies may be present in DW without the detection of traditional indicators. Therefore, the inclusion of indicators of persistent microbial contaminants, such as bacteriophages and bacterial spores, in the control and surveillance programs, should be considered (WHO, 2022).

Regarding Directive (EU) 2020/2184, no intestinal enterococci and *E. coli* numbers should be detected in 100 mL of DW supplied by distribution systems. For monitoring purposes and ensuring DW quality in remedial actions, the Directive (EU) 2020/2184 establishes that colony counts at 22 ºC should not present abnormal change and no coliform bacteria should be detected in 100 mL of DW supplied by distribution systems.

If the risk-based approach indicates the evaluation of *Clostridium perfringens*, including spores, the parametric value should be zero in 100 mL of DW. Additionally, if somatic coliphages are detected in raw water at more than 50 plaque forming units/100 mL, this operational parameter should be analysed in DW to determine log removal by the measures implemented and to assess whether the risk of a viral outbreak is adequately controlled (Directive (EU), 2020/2184; Tsaridou and Karabelas, 2021). Conversely to the previous Council Directive 98/83/EC, the new Directive (EU) 2020/2184 establishes the parametric value for *Legionella* less than 1000 CFU/L if it is included in the risk assessment of domestic distribution systems and remedial actions. In the case of infections and outbreaks, the legislation specifies that further measures could also be considered when below the parametric values, the source of the infection must be confirmed and *Legionella* species identified (Dettori et al., 2022; Directive (EU), 2020/2184). The adoption of a risk-based approach along the entire supply chain, including the domestic system, is one of the main innovations in this updated Directive, however, the responsibility for this risk assessment study relies principally on the DW provider and distributer (Directive (EU), 2020/2184; Tsaridou and Karabelas, 2021).

Chemicals used in water treatment may give rise to contaminants in the final water. Disinfectant residuals are deliberately added to water and their presence confers a benefit, but the treatment processes should be optimized to control the residual levels and to control the formation of DBPs. The Directive (EU) 2020/2184 does not specifically determine that water supplies should be disinfected, nor residual disinfection is required, although it indicates disinfection when necessary. If disinfection is included in the treatment or distribution of DW, the member states shall ensure that the efficiency of the disinfection used is validated, the DBPs levels are kept as low as possible without neglecting the disinfection, and the treatment chemicals are safe and properly managed

to avoid adverse effects on consumer health. European Union member states may adopt standards and monitoring requirements more stringent than those imposed by the Directive (EU) 2020/2184. For example, Portugal requires primary disinfection for water treatment and secondary disinfection during distribution (Decreto-Lei n.º 152/2017). The maximum guideline values recommended by WHO for disinfectants used in water treatment that are of health significance in DW are 5 mg/L for free chlorine, 3 mg/L for monochloramine, and 50 mg/L for sodium dichloroisocyanurate (WHO, 2022). In the case of chlorination, a residual concentration of free chlorine ≥ 0.5 mg/L after at least 30 min contact time at pH < 8.0 should be ensured for effective disinfection. Moreover, the WHO states that a minimum residual concentration of free chlorine of 0.2 mg/L should be present at the point of delivery (WHO, 2022). The potential toxicity from chlorine dioxide is protected by the provisional guideline values for chlorite (0.7 mg/L) and chlorate (0.7 mg/L), which are the primary DBPs resulting from the use of chlorine dioxide as a disinfectant (WHO, 2022). The new Directive (EU) 2020/2184 establishes that the levels of chlorate and chlorite shall be measured if disinfectant methods that generate these compounds are used, setting a parameter value of 0.25 mg/L for both chemicals (Dettori et al., 2022; Directive (EU), 2020/2184). However, particularly when chlorine dioxide is used for disinfection, parametric values are more flexible up to 0.70 mg/L. The Directive (EU) 2020/2184 also stipulates the quantification of total trihalomethanes and haloacetic acids, which are two principal DBPs classes, when a disinfection method is included in the treatment and distribution of DW (Directive (EU), 2020/2184; Tsaridou and Karabelas, 2021). The parametric value for haloacetic acids is 60 µg/L, comprising the sum of five representative substances: monochloroacetic acid, dichloroacetic acid, trichloroacetic acid, monobromo acetic acid, and dibromo acetic acid (Dettori et al., 2022; Directive (EU), 2020/2184). For the case of total trihalomethanes,

100 µg/L is defined as a parametric value, including the sum of concentrations of chloroform, bromoform, dibromochloromethane, and bromodichloromethane (Directive (EU), 2020/2184).

2.4 Research on DW biofilm disinfection in the last decade

A systematic review was performed to access the knowledge gained from the research on the disinfection of DW biofilms in the last decade. The systematic quantitative literature review was accomplished according to the method described by Pickering and Byrne (2014) and Li et al. (2019). Research articles were searched on Web of Science™ (Clarivate) in the advanced topic search using the keywords "drinking water" OR "potable water" AND biofilm AND disinfection. Only original English written research articles published between January 2013 and December 2022 were considered. This list included 326 journal articles. After manually screening the titles and abstracts, 135 full-text articles were assessed for eligibility and then 77 articles were selected for detailed assessment (**Figure 2-2**). Selection criteria included the requirement that i) the research studies described the DWDS (real or simulated) and characteristics of the water when tap water was used for biofilm formation; ii) microbial or physicochemical changes in the biofilm had to be addressed; iii) differences in water treatment (preferable with primary or secondary disinfection) had to be studied, and iv) a clear definition of disinfectants concentrations tested.

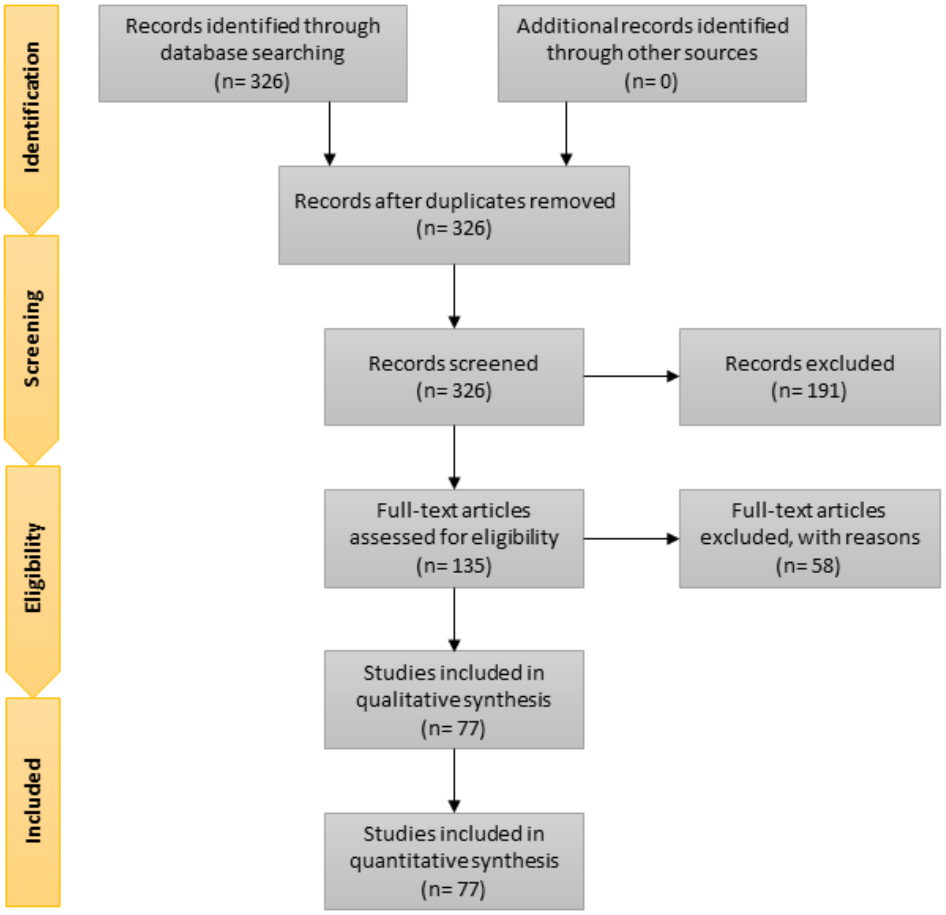

Figure 2-2 – Flow diagram of the different phases of the systematic review implemented, according to PRISMA recommendations (Moher et al., 2009).

The 77 studies from the last decade included in this review were conducted in 22 different countries, with the United States of America and China being the two countries with the highest number of publications (**Figure 2-3**). Following this rank are Canada and Portugal, each with six publications, and the United Kingdom and France, each with five studies. From 2013 to 2022, the most published years were 2019 and 2022, with 12 and 10 articles, respectively.

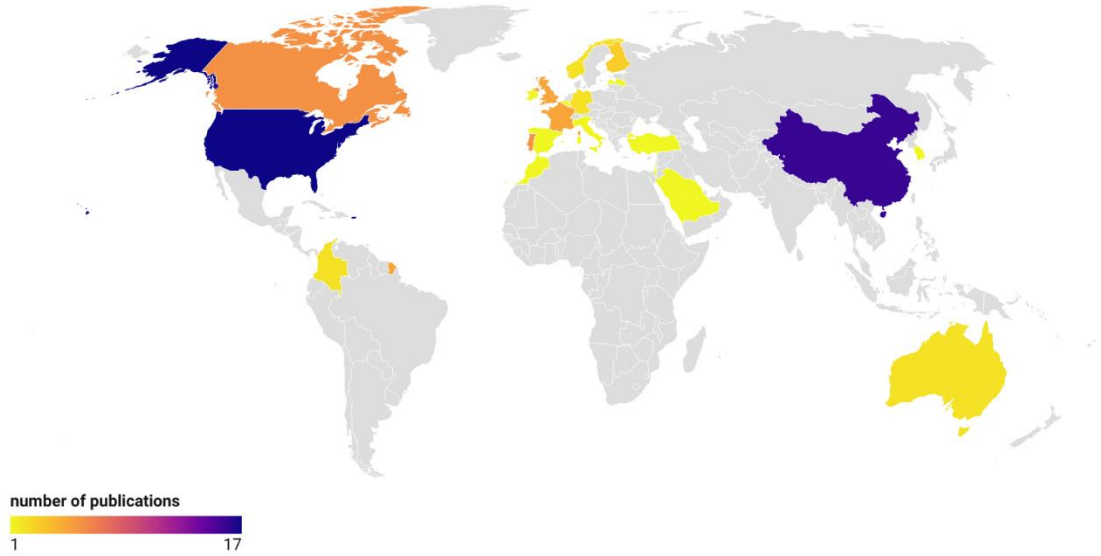

Figure 2-3 – World map representing the number of publications per country under the topic of disinfection of DW biofilms.

2.4.1 Methods for biofilm formation and monitoring biofilms within DWDS

The preferable methods implemented to study DW biofilms were through the use of benchtop laboratory devices (**Figure 2-4 (a)**), principally annular reactors, Centers for Disease Control (CDC) biofilm reactors, 96-well microtiter plates or Calgary biofilm devices, and microtiter plates with coupons of different materials. Other devices, such as Propella^{TM} reactor, rotating disc reactor, parallel plate flow chamber, flow cell system, and RCR were also applied, but at a lower frequency. The characterization and description of the limitations and advantages of these devices for studying biofilms in DWDS were extensively reviewed by Gomes et al. (2014). They are mainly used in laboratory-scale experiments, nevertheless, these devices mimic the conditions found in real DWDS, for example, environmental factors (temperature, concentration of nutrients and disinfectants), hydrodynamic conditions, and type of surface materials. Additionally, to

promote biofilm formation, the benchtop laboratory devices can be supplied with tap water, supplemented water, or an appropriate broth medium. **Table 2-2** summarizes the experimental conditions reported in the selected articles to form and study the simulated DW biofilms with the use of benchtop laboratory devices.

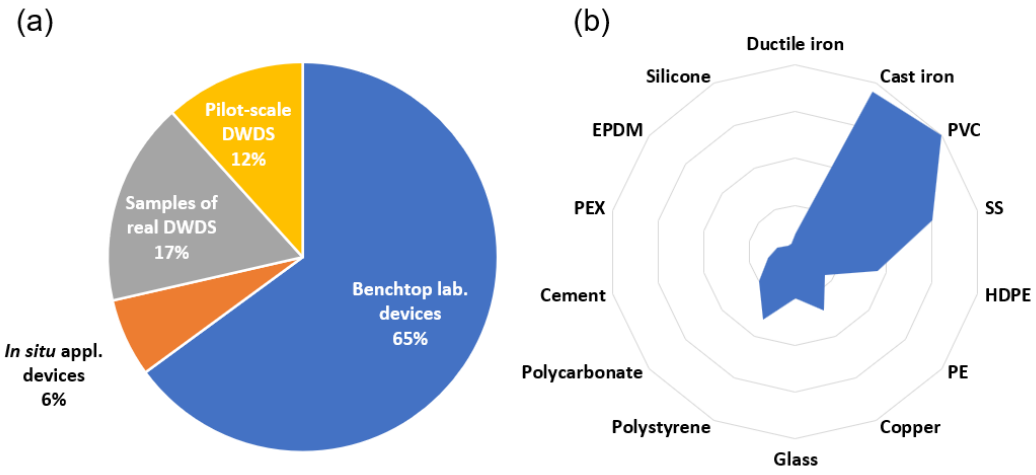

Figure 2-4 – Methods used to study DW biofilms (benchtop laboratory devices, pilot-scale DWDS, samples of real DWDS, and *in situ* application devices) (a) and different surface materials evaluated (b). PVC – polyvinyl chloride; SS – stainless steel; HDPE – high-density polyethylene; PE – polyethylene; PEX – cross-linked polyethylene; EPDM – ethylene-propylene-diene monomer rubber.

Moreover, 17% of the selected articles evaluated the biofilm growth in real DWDS by scraping the surfaces of water mains (Aggarwal et al., 2018; Alfredo, 2021; Cruz et al., 2020; Inkinen et al., 2021, 2019; Kelly et al., 2014; Waak et al., 2019; Wu et al., 2015); in hospital shower hoses through swab samples of the showerheads (Soto-Giron et al., 2016; Stüken et al., 2018); in dental units by cutting and collecting the PVC tubes that supplied the units (Dallolio et al., 2014); in DWDS within broiler farms by swabbing the sample surface at the end of the pipes, openings at the drinking cups, and inside pressure regulators (Maes et al., 2019); and in an aircraft DW system through swab samples of coupling and tubing surfaces (Szabo et al., 2019). However, considering the

heterogeneity of the biofilm distribution along the DW networks and the discrepancy of water properties in different locations, representative sampling constitutes a challenge (Liu et al., 2016). On the other hand, when it is intended to analyse biofilm samples of the water mains, the opportunities for the sampling process are dependent on pipe substitution and maintenance operations. Alternatively, the adaption of *in situ* devices placed as a by-pass or directly connected to the DWDS, and the biofilm formation in pilot-scale DW networks were also reported in the selected research articles. The *in situ* application devices included the Pennine Water Group coupon sampling device (Calero-Preciado et al., 2022; Fish et al., 2020; Fish and Boxall, 2018), biofilm incubators with glass beads (Bertelli et al., 2018), and unconventional equipment analogous to a two-tiered "chandelier" with steel coupons for biofilm formation in groundwater wells (Murray et al., 2015). The pilot-scale distribution facilities consisted of parallel loops of pipes with 1 to 270 m lengths from different materials and fed by DW (Álvarez-Arroyo et al., 2022; Farhat et al., 2022; Inkinen et al., 2017; Jungfer et al., 2013; Li et al., 2014; Meier and Bendinger, 2016; Pérez et al., 2019; Pérez and Susa, 2017).

Among all the selected articles, the surface materials most studied for biofilm formation were PVC, cast iron, and stainless steel (SS) (**Figure 2-4 (b)**). High-density polyethylene (HDPE), copper, and polystyrene were also tested, but at a lower frequency. These materials are representative of pipe materials used in DWDS and household plumbing systems (Liu et al., 2016), except for polystyrene which reflected the limitation of the platform used for biofilm formation, *i.e.*, 96-well microtiter plates and Calgary biofilm device.

Table 2-2 – Methods for biofilm formation with benchtop laboratory devices.

Benchtop laboratory devices	Microbial colonization	Surface material	Primary water disinfection and/or residual disinfectant	Other operational conditions	References
Annular reactor	Autochthonous microorganisms present in groundwater source for DW	Cast iron	Chlorine at 0.1 m/L or chlorine with UV pre-treatment (40 mJ/cm^2)	T = 25 ºC Biofilm formation for 1 year Shear stress = 0.25 Pa HRT = 6 h	(Liu et al., 2019a)
	Autochthonous microorganisms present in DW	Cast iron	Chorine at 0-0.08 mg/L or chlorine with UV pre-treatment (40 mJ/cm^2)	Biofilm formation for 250 or 300 days Shear stress = 0.25 Pa (corresponding to a water velocity of 0.3 m/s in a 100 mm Ø smooth pipe) HRT = 6 h	(Wang et al., 2017; Zhu et al., 2014)
	Autochthonous microorganisms present in DW and further *Legionella pneumophila* inoculation (≈6.7 log CFU/mL)	Copper and PVC	Chlorine at 1 mg/L	T = 19-20 ºC Biofilm formation for 1.5-2 years Rotational speed of 110 to 120 rpm (corresponding to a velocity of 0.3 m/s in a 12.7-25.4 mm Ø pipe) HRT = 10 min Then, 5 d incubation with *L. pneumophila* in batch mode in a beaker under agitation	(Buse et al., 2019)
	Autochthonous microorganisms present in DW	PVC	Chlorine at 0.02-0.08 mg/L	T = 45 ºC (lower limit for domestic hot water) Shear stress = 0.08 Pa HRT = 4 h	(Li et al., 2020)
	Autochthonous microorganisms present in DW	Cast iron	Chlorine at 1 mg/L or with UV/H_2O_2 pre-treatment (500 mJ/cm^2; 1 mg/L)	Biofilm formation for 90 days Rotational speed of 50 rpm HRT = 48 h	(Huo et al., 2021)
	Autochthonous microorganisms present in DW	Cast iron	Chlorine at 0.04-0.1 mg/L of chlorine with ozone pre-treatment (0.55 mg/mg dissolved organic carbon)	Biofilm formation for 250 days Rotational speed of 50 rpm HRT = 6 h	(Wang et al., 2018)

Table 2-2 (cont.) – Methods for biofilm formation with benchtop laboratory devices.

Benchtop laboratory devices	Microbial colonization	Surface material	Primary water disinfection and/or residual disinfectant	Other operational conditions	References
Annular reactor	Autochthonous microorganisms present in DW	Cast iron	Phosphate-enhanced ozone/biofiltration (2.18 mg O_3/mg dissolved organic carbon) and secondary chlorination (2.8 mg/L)	Biofilm formation for 1.5-2 years Shear stress = 0.25 Pa HRT = 6 h	(Xing et al., 2018)
	Autochthonous microorganisms present in groundwater source for DW	Cast iron and polycarbonate	Untreated or groundwater treated with ion exchange, followed by chorine at 0.2 mg/L or chlorine with UV pre-treatment (40 mJ/cm^2)	Biofilm formation for 4 weeks without chlorination, followed by 12 weeks with disinfection Shear stress = 0.25 Pa	(Rand et al., 2013)
	Autochthonous microorganisms present in reclaimed water	Cast iron	Chorine at 0.05-1.10 mg/L or chlorine with UV pre-treatment (60 mJ/cm^2)	Biofilm formation for 305 days (first 30 days without disinfection) Shear stress = 0.25 Pa HRT = 6 h	(Wang et al., 2014)
	Autochthonous microorganisms present in DW	Cast iron, SS, copper, PVC, and HDPE	chlorine at 0.8 mg/L or chloramine at 1 mg/L	Biofilm formation for 8 weeks Shear stress = 0.25 Pa HRT = 1.7 h	(Li et al., 2020a)
	Autochthonous microorganisms present in DW	Cast iron and polycarbonate	No disinfectant residual for 4 weeks, followed by 2 phases of chlorine at 0.2 and 1 mg/L	T = 21 ºC Biofilm formation for 16 weeks Shear stress = 0.25 Pa HRT = 2 h	(Sharafimasooleh et al., 2016)
	Autochthonous microorganisms present in DW	PVC	No disinfectant residual, or chlorine at 0.4 mg/L or chloramine at 1.0 mg/L	T = 24 ºC Biofilm formation for 6 weeks Shear stress = 0.154 Pa HRT = 1.9 h	(Wang et al., 2013)
	Autochthonous microorganisms present in DW	Cast iron	Chlorine at 0.08 mg/L or chlorine with UV pre-treatment (40 mJ/cm^2)	Biofilm formation for 350 days	(Zhu et al., 2020)

Table 2-2 (cont.) – Methods for biofilm formation with benchtop laboratory devices.

Benchtop laboratory devices	Microbial colonization	Surface material	Primary water disinfection and/or residual disinfectant	Other operational conditions	References
Annular reactor	Autochthonous microorganisms present in DW	Cast iron	Chorine at 0.05 mg/L or combination with ozone pre-treatment at 0.34 and 0.64 mg/L or O_3-BAC-Cl_2 system	T = 25 ºC Biofilm formation for 6 months Rotational speed of 50 rpm HRT = 6 h	(Liu et al., 2019b)
	Autochthonous microorganisms present in DW	Polycarbonate	Chlorine at 1 mg/L with addition of either 1 mg/L PO_4^{3-} or 24-48 mg/L SiO_2	Biofilm formation for 1 year Rotational speed of 50 rpm HRT = 2 h	(Munoz et al., 2022)
Rotating disc reactor	Autochthonous microorganisms present in DW	HDPE and glass	Chlorine < 0.02 mg/L	T = 20 ºC Biofilm formation for 2 months Shear stress = 0.2-1 Pa	(Mathieu et al., 2014)
	Autochthonous microorganisms present in DW and further bacteriophage (MS2, GA, and Qβ) inoculation ($\approx 10^6$ eqPFU/mL)	HDPE	Chlorine < 0.05 mg/L	Biofilm formation for 2 months Shear stress = 1 Pa (corresponding to a velocity of 0.5 m/s in a 20 cm Ø pipe) HRT = 24 h Then, the reactor was spiked with phages for adhesion (3 h) in batch mode	(Pelleieux et al., 2016)
CDC biofilm reactor	Multi-species cultures isolated from a local water utility (2×10^5 CFU/mL)	PVC	No chlorine residuals or 3 phases of disinfection (Cl_2 or NH_2Cl): 50 days at 0.5 mg/L, followed by 25 days at 2 mg/L, and finally 25 days at 4 mg/L	T = 24 ºC Biofilm formation for 6 months without disinfection, followed by 100 d with disinfection HRT = 12 h	(Wang et al., 2021)
	P. aeruginosa ($\approx 10^{10}$ cells/mL)	Polycarbonate	No disinfectant residual	Biofilm formation for 5 days Stirred at 100 rpm HRT = 1.7 h	(Ma et al., 2022)
	Autochthonous microorganisms present in DW	Cement, PVC, and HDPE	No disinfectant residual or chloramine at 1.7 mg/L (total chlorine)	Biofilm formation for 28 months Stirred at 125 rpm HRT = 4.5 h	(Aggarwal et al., 2018)

Table 2-2 (cont.) – Methods for biofilm formation with benchtop laboratory devices.

Benchtop laboratory devices	Microbial colonization	Surface material	Primary water disinfection and/or residual disinfectant	Other operational conditions	References
CDC biofilm reactor	Autochthonous microorganisms present in groundwater source for DW	PVC	No disinfectant residual for 1 year, then chlorine or chloramine at 4 mg/L	Biofilm formation for 1 year Stirred at 125 rpm (Re = 2384) Biofilm disinfection for 3 or 6 months in stirred or non-stirred conditions	(Shen et al., 2017, 2016)
	P. aeruginosa (unknown cellular density of the inoculum)	Polycarbonate	No disinfectant residual	T = 23 ºC Biofilm formation: 24 h in batch mode with 300 mg/L TSB, followed by 24 h in CSTR mode with 100 mg/L TSB Stirred at 250 rpm HRT = 0.83 h	(Gora et al., 2019)
	Autochthonous microorganisms present in DW	SS and PE	Chlorine at 0.5 and 1.0 mg/L from chlorine gas or on-site generated chlorine	T = 21.6 ºC Biofilm formation for 70 days Stirred at 100 rpm HRT = 30 min	(Choi et al., 2022)
	Autochthonous microorganisms present in groundwater source for DW	PVC	No disinfectant residual for 2 weeks, followed by chloramine at 7.5 to 9.1 mg/L (total chlorine) for 8 weeks	Biofilm formation for 10 weeks Flow rate at 2.6 mL/min	(Ling and Liu, 2013)
	Single-species cultures of *P. aeruginosa* and *Staphylococcus aureus* (≈3 × 10^6 CFU/mL)	PVC	No disinfectant residual	T = 20 and 37 ºC Biofilm formation for 24, 48 and 72 h Stirred at 125 rpm	(Garvey et al., 2015)
RCR	Single- and dual-species cultures of *A. calcoaceticus* and *S. maltophilia* (≈10^7 CFU/mL)	PVC	No disinfectant residual	Biofilm formation for 7 days Shear stress = 1 Pa (0.34 m/s water velocity on the cylinder surface) HRT = 10 h	(Gomes et al., 2018a)
	S. maltophilia (2 ×10^7 cells/mL)	Copper alloys and SS	No disinfectant residual	Biofilm formation for 7 days Shear stress = 0.1 Pa HRT = 10 h	(Gomes et al., 2020)

Table 2-2 (cont.) – Methods for biofilm formation with benchtop laboratory devices.

Benchtop laboratory devices	Microbial colonization	Surface material	Primary water disinfection and/or residual disinfectant	Other operational conditions	References
Calgary biofilm device and 96-well microtiter plates	*Pseudomonas alloputida* ($OD_{600\ nm}$=0.1)	Polystyrene	No disinfectant residual or 10 to 250 mg/L nanoparticles of zero-valent iron (nZVI) and its derivates (carboxymethyl cellulose- nZVI, oxidized-nZVI and Fe_3O_4)	T = 30 ºC Biofilm formation for 24 h	(Yu et al., 2022)
	Single- and multi-species cultures of bacterial strains isolated from DWDS [(1:30) dilution of suspension with turbidity equal to 1.0 McFarland standard]	Polystyrene	No disinfectant residual	T = 25 ºC Biofilm formation between 20 h to 9 days Agitation at 125 rpm	(Schwering et al., 2013)
	Single- and multi-species cultures of *Sphingomonas* sp., *Acidovorax defluvii*, *Acinetobacter* sp., *B. cereus*, and *Microbacterium laevaniformans* (≈10^6 cells/mL)	Polystyrene	No disinfectant residual	T = 25 ºC Biofilm formation for 24, 48, and 72 h Agitation at 150 rpm	(Zhu et al., 2020a; Zhu et al., 2021)
	Single- and multi-species cultures of *A. calcoaceticus* (≈10^8 cells/mL) and filamentous fungi *Penicillium brevicompactum* and *P. expansum* (≈10^5 spores/mL)	Polystyrene	No disinfectant residual	T = 25 ºC Adhesion for 2 or 4 h and biofilm formation for 24 or 48 h Shear stress = 0.05 and 1.6 Pa	(Simões et al., 2023)
	P. aeruginosa (suspension with turbidity equal to 0.5 McFarland standard)	Polystyrene	Chlorine at 0, 0.5, 0.7, and 1 mg/L	T = 37 ºC Biofilm formation for 3 days	(Kekeç et al., 2016)

Table 2-2 (cont.) – Methods for biofilm formation with benchtop laboratory devices.

Benchtop laboratory devices	Microbial colonization	Surface material	Primary disinfection and/or residual disinfectant	Other operational conditions	References
Calgary biofilm device and 96-well microtiter plates	Single-specie culture of *P. putida* and mixed microbial community isolated from DW (unknown cellular density of the inoculum)	Polystyrene	No disinfectant residual for 4 days, followed by chloramine at 0.5 to 32 mg/L (total chlorine) for 2 days	T = 30 and 37 ºC Biofilm formation for 6 days Static conditions	(Ng et al., 2021)
	Mixed-species nitrifying cultures	Polystyrene	No disinfectant residual	T = 25 ºC Biofilm formation for 72 h Agitation 100 rpm	(Keshvardoust et al., 2020)
Microtiter plates with coupons	Single-species cultures of *A. calcoaceticus* and *S. maltophilia* (≈10^6 CFU/mL)	PVC and SS	No disinfectant residual	T = 25 ºC Biofilm formation for 48 h Agitation 150 rpm	(Oliveira et al., 2022)
	Single-species cultures of *L. pneumophila* serogroup 1 and *L. pneumophila* serogroup 2-15 (≈10^6 CFU/mL)	Galvanized steel and PVC	No disinfectant residual or, after 18 or 30 days, chlorine at 50, 100, 150, and 200 mg/L	T = 37 ºC Biofilm formation for 45 days	(Assaidi et al., 2020)
	Single- and dual-species cultures of *A. calcoaceticus* and *S. maltophilia* (≈10^8 CFU/mL)	PVC	No disinfectant residual	T = 23 ºC Adhesion for 2 h and biofilm formation for 24 h Agitation 120 rpm	(Gomes et al., 2016)
	Single-species cultures of *Aeromonas* sp. isolated from DW, *Aeromonas hydrophila* and *P. aeruginosa* (≈10^8 CFU/mL)	SS	No disinfectant residual or disinfection with 1% of amphoteric surfactants and diamines or 0.75% of chlorine compounds	T = 4 and 20 ºC Biofilm formation for 48 h	(Craveiro et al., 2015)
	P. aeruginosa ($OD_{600\ nm}$=0.4)	HDPE coated with encapsulated phages	No disinfectant residual	T = 30 ºC Biofilm formation for 72 h	(Zuo et al., 2022)

Table 2-2 (cont.) – Methods for biofilm formation with benchtop laboratory devices.

Benchtop laboratory devices	Microbial colonization	Surface material	Primary water disinfection and/or residual disinfectant	Other operational conditions	References
Parallel plate flow chamber	Single-species cultures of 3 *P. aeruginosa* strains and a wild-type *P. putida* ($\approx 10^{10}$ cells/mL)	Glass	No disinfectant residual	T = 22 ºC Biofilm formation for 6 days Flow rate = 0.2 mL/min	(Xue et al., 2014)
	Single-species cultures of 3 *P. aeruginosa* strains, wild-type, alginate-deficient and alginate-overproducing mutants ($\approx 10^{10}$ cells/mL)	Glass	No disinfectant residual or chlorine at 0.5 mg/L	Bacterial adhesion for 2 h without flow Biofilm formation for 6 days Flow rate = 1 mL/min HRT = 0.1 min	(Xue and Seo, 2013)
Flow cell system	Autochthonous microorganisms present in DW	HDPE	Dechlorinated DW containing 50 mg/L NH_3-N for stable nitrification process, then (3:1) and (5:1) Cl_2/NH_3-N mass ratios	T = 16 ºC After stable nitrification process, two phases of chloramination, each for 33 days Shear stress from 0.018 to 0.286 Pa	(Shi et al., 2019)
Propella reactor	Autochthonous microorganisms present in DW	Cast iron, PVC, and SS	No disinfectant residual	T = 20 ºC Biofilm formation for 1 month in cast iron and 10 months in PVC and SS Water velocity = 0.13 m/s HRT = 12 h	(Gosselin et al., 2013)
	Autochthonous microorganisms present in DW and further *E. coli* inoculation ($\approx 10^6$ cells/mL)	SS	No disinfectant residual	Biofilm formation for 2-3 weeks (until 1.8-2 $\times 10^6$ cells/cm^2) Then, the reactor was spiked with *E. coli* for bacterial adhesion (1 h)	(Mezule et al., 2015)

2.4.2 Disinfection strategies for biofilm prevention and control

In the overall range of publications from the last decade, chlorination continues to be the most commonly studied strategy for biofilm prevention and control (**Figure 2-5**). Chlorine in the form of chlorine gas, sodium hypochlorite, or calcium hypochlorite, was used as primary and secondary disinfection of water and subsequent control of microbial regrowth along the DW networks, as well as a direct strategy for control of pre-established biofilms. Nevertheless, it is important to mention that the use of chlorine as a reference disinfectant for comparison to other strategies or in combination with other disinfectants has contributed to its high relative frequency of implementation in the selected studies. Among the literature, other disinfectants have been evaluated such as chloramine, UV irradiation, hydrogen peroxide, chlorine dioxide, ozone, and others, but at a lower frequency.

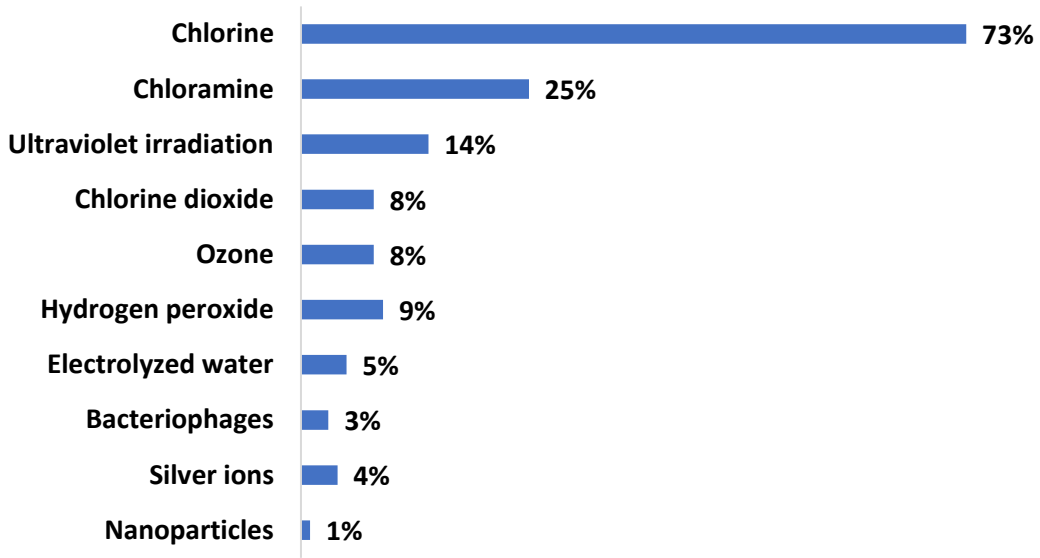

Figure 2-5 – Disinfection strategies reported in the last decade for biofilm prevention and control in DW. The values represent the relative frequency of implementation in the literature.

Chlorine

A significant number of studies have focused their objectives on evaluating the impact of chlorination on the microbial community developed in DW biofilms. According to Pérez et al. (2019) in chlorinated DWDS with low flow conditions and high chlorine residuals, it is likely that a higher number of γ-proteobacteria can be observed than at sites further away from the treatment plant with lower chlorine residuals. On the other hand, fluctuations in the relative abundance of γ-proteobacteria probably will be higher at the end of the DW network if changes in water velocity do occur, as a consequence of bacterial detachment from the biofilm (Pérez et al., 2019). However, among the operational conditions evaluated, such as distance, time of stabilization, water velocity, and level of disinfectant residual, chlorine was found to be the most influential factor for the bacterial community, as it favoured the group characterized by its pathogenicity (Pérez et al., 2019). Performing a metagenomic approach, Soto-Giron et al. (2016) demonstrated that the predominant taxon in microbial communities growing on hospital shower hoses supplied by DW containing 0.8 mg/L free chlorine was *Mycobacterium* sp., closely related to *Mycobacterium rhodesiae* and *Mycobacterium tusciae*. Additionally, genes associated with disinfectant tolerance and a lower abundance of virulence determinants associated with colonization and evasion of the host immune system were also detected in the biofilm community (Soto-Giron et al., 2016). Furthermore, sub-inhibitory concentrations of chlorine and type of pipe material (PVC and copper) collectively resulted in a selective pressure to enrich antibiotic-resistant bacteria within the microbial biofilm populations (Khan et al., 2019; Soto-Giron et al., 2016).

Shock chlorination was demonstrated to change the biofilm cohesiveness by reducing the number of contact points within the biofilm EPS network structure after exposure of mature DW biofilms to 10 mg/L for 1 h (Mathieu et al., 2014). The damages also included

a decrease in biofilm cluster volumes and detachment of bacterial cells in combination with low shear stress (Mathieu et al., 2014). Nevertheless, Xue and Seo (2013) highlighted that detached *P. aeruginosa* cell clusters were still able to survive and initiate biofilm redistribution, even in the presence of chlorine at recommended minimal residual for DWDS (0.5 mg/L). Moreover, high concentrations of chlorine can lead to high water quality deterioration, which can be observed by the increase of inorganic loads and discoloration, a major cause of water quality complaints (Fish et al., 2020).

A recent study evaluated the impacts of water temperature increase due to climate change on the efficacy of biofilm control by shock chlorination combined with flushing (Calero-Preciado et al., 2022). An increase in water discoloration and alterations in the biofilm community structure were observed by the increase of water temperature from 16 to 24 ºC. The implementation of flushing procedures or combined with high concentrations of chlorine decreased the discoloration potential and allowed a reduction of the relative abundance of bacterial biofilm community (Calero-Preciado et al., 2022). However, the authors concluded that the addition of shock chlorination as a strategy for managing biofilms seemed to be not beneficial because no difference between the interventions was observed (Calero-Preciado et al., 2022).

Chloramine

The effects of chloramination on microbial communities of DW biofilms were also widely reported in the literature (Aggarwal et al., 2018; Cruz et al., 2020; Li et al., 2020a; Ling and Liu, 2013; Wang et al., 2013). The presence of chloramine residual allowed a reduction of biofilm accumulation and shaped the biofilm community by selecting *Mycobacterium*- and *Shingopyxis*-like taxon, while the biofilm community developed without chloramine was more diverse and dominated by *Nitrospira* population (Aggarwal et al., 2018). Conversely, another study revealed that biofilm communities in

chloraminated systems were dominated by α-proteobacteria and β-proteobacteria (Li et al., 2020a). The presence of antibiotic biosynthesis-related pathways, such as tetracycline, bovobiocin, ansamycin, butirosin, and neomycin biosynthesis, were also found in biofilm communities (Li et al., 2020a). Chloraminated DWDS located in urbanized metropolis with tropical conditions were affected by the auto-decomposition of chloramine to free ammonia, promoting the growth of nitrifiers within the biofilms (Cruz et al., 2020). Furthermore, metabolically active ammonia-oxidizing bacteria were responsible to mediate the decay of chloramine, protecting the members of mixed-species biofilms from chloramine disinfection (Keshvardoust et al., 2020).

A comparative study between biofilms under chlorinated and chloraminated DW demonstrated the lower efficacy of chloramine in biofilm removal than chlorine, even at the highest concentration tested (4 mg/L) for 25 days (Wang et al., 2021). However, chloramine disinfection showed to be beneficial for the prevention of high levels of DBPs at different chloramine residuals (Wang et al., 2021), as well as for the control of *Legionella* spp. in the DW biofilms (Wang et al., 2013). A significant reduction in biofilm biomass and thickness of more than 80% was reported for the disinfection of DW biofilms under high concentrations of chloramine (between 7 to 9 mg/L), even though membrane-intact cells within the biofilms were still detected (Ling and Liu, 2013). Actually, Ng et al. (2021) suggested that the persistent bacteria found after chloramine disinfection have the ability to easily enter a viable but non-culturable state and form biofilms mainly constituted by protein EPS. Additionally, sub-lethal disinfection with chloramine resulted in biofilms being more resistant to chloramination, given the increase of the inhibitory concentration of the exposed biofilm cultures in comparison to the untreated biofilm cultures (Ng et al., 2021).

UV irradiation

The effects of combined UV irradiation for primary disinfection of water followed by the addition of chlorine residuals have been evaluated on biofilms developed in these DWDS. Valuable results were reflected in the water quality, with the inactivation of heterotrophic bacteria and opportunistic pathogens in the bulk phase, reduction of the required initial chlorine dose, as well as decreased iron release from cast iron surfaces (Liu et al., 2019a; Wang et al., 2014). However, no significant differences were observed in biofilm growth, suggesting an inefficiency of UV irradiation and residual chlorine for biofilm control in cast iron distribution networks (Rand et al., 2013; Wang et al., 2014). Moreover, opportunistic pathogens such as *Legionella* spp., *Mycobacterium* spp., *P. aeruginosa*, *Acanthamoeba* spp., and *Aeromonas* spp. present in the biofilms, corrosion products, and loose deposits were shown to be tolerant to combined UV and chlorine or chlorine alone disinfection (Liu et al., 2019a). Within biofilms developed in UV-disinfected DW, the expression of *rec*A SOS responsive gene, which is the main mechanism to repair DNA injuries, was also reported (Jungfer et al., 2013).

The impacts of UV/chlorine disinfection have also been studied on the microbial composition of the biofilm communities (Wang et al., 2014, 2017; Zhu et al., 2014). Combined UV and chlorine disinfection induced bacteria from the genus *Dechloromonas* to be dominant in the biofilms, which were responsible for the decrease of corrosion rate through their redox cycling of iron, enhancing the precipitation of iron oxides and formation of Fe_3O_4 (Wang et al., 2017; Zhu et al., 2014). Additionally, Wang et al. (2014) also detected the presence of the iron-oxidizing bacterium *A. defluvii* and the iron-reducing bacteria uncultured *Rhodoferax* sp. and uncultured *Geobacter* sp. in biofilms of UV/chlorine distribution systems.

A recent study indicated that the use of an advanced oxidation process with the combination of UV (500 mJ/cm^2) and hydrogen peroxide (1 mg/L) before granular activated carbon (GAC) filtration allowed to control opportunistic pathogens in biofilms formed in DWDS (Huo et al., 2021). This multi-barrier process promoted the reduction of the number of *L. pneumophila*, *Mycobacteria avium*, and *P. aeruginosa* in the bulk water and biofilms, as well as induced a lower chlorine-tolerance of the biofilm-embedded cells by decreasing the content of proteins found within the biofilm matrix (Huo et al., 2021).

Other disinfection strategies

Dental units supplied by municipal DW are also subjected to biofilm formation within their water networks. Dallolio et al. (2014) investigated the efficacy of different strategies to control biofilms in dental units, including an intermittent disinfection protocol with a peroxidic system (peracetic acid, peracetyl ions, and hydrogen peroxide) and two continuous disinfection protocols with hydrogen peroxide combined with silver ions and chloride dioxide, respectively. Compared to non-disinfected dental units, the different protocols allowed the decrease of the number of heterotrophic bacteria in the bulk water and the reduction of biofilm thickness (Dallolio et al., 2014). However, the continuous disinfection protocols were demonstrated to be more efficient, promoting the total eradication of *P. aeruginosa* (Dallolio et al., 2014). Conversely, Meier and Bendinger (2016) reported that the efficacy of chlorine, hydrogen peroxide, or chlorine dioxide in controlling the regrowth of opportunistic pathogens in DW plumbing systems is affected by the operating temperature, pipe surface material, and water quality. Generally, at 11 ºC all the disinfectants were able to suppress the regrowth of *L. pneumophila* and *P. aeruginosa* in biofilms and bulk water, while at 37 ºC both pathogens were detected in a culturable state (Meier and Bendinger, 2016). The presence of high nutrient levels in the

water and the use of ethylene-propylene-diene monomer (EPDM) rubber pipes also limited the action of these disinfectants. Nevertheless, non-culturable cells were observed in treated biofilms even in favourable disinfectant operating conditions (Meier and Bendinger, 2016).

The impacts of primary disinfection of water with ozone followed by post-chlorination have also been evaluated on the development of biofilms in the DW networks. Likewise UV/chlorine disinfection, the ozone/chlorine disinfection was demonstrated to promote changes in the content of corrosion-related bacteria within biofilms formed in these DWDS (Wang et al., 2018). An abundance of iron-oxidizing and iron-reducing bacteria were detected in the water systems disinfected with ozone combined with chlorination, in comparison to those only disinfected with chlorine (Wang et al., 2018). The alterations in the microbial community of biofilms in the ozone/chlorine systems promoted an increase of Fe_3O_4 formation in the corrosion scales of cast iron surfaces that became more stable than the ones formed in the chlorinated systems. Therefore ozone/chlorine disinfection was beneficial to inhibit corrosion and iron release in these DWDS (Wang et al., 2018). Even though a decrease in the gene copy number of *M. avium* and *L. pneumophila* within the biofilms was observed (Wang et al., 2018), typical opportunistic pathogens, such as *Legionella* spp., *Mycobacterium* spp., *P. aeruginosa*, *Acanthamoeba* spp., and *Aeromonas* spp. were still positively detected in biofilms of DW treated with ozone/chlorine disinfection or ozone combined with BAC biofiltration followed by chlorination (Liu et al., 2019a; Wang et al., 2018). Besides the inability to prevent biofilm formation in chlorinated DWDS, the use of ozone before water ultrafiltration resulted in the increase of DBPs formation, such as trihalomethanes and haloacetic acids (Álvarez-Arroyo et al., 2022).

Alternatively to conventional DW chlorination, electrochemical water disinfection can also generate free chlorine from the electrolysis of water in the presence of high concentrations of salts (Choi et al., 2022; Mezule et al., 2015; Murray et al., 2015). Other oxidative species such as ozone, hydrogen peroxide, and oxygen free radicals can also be formed (Choi et al., 2022; Mezule et al., 2015), and, therefore, the term "mixed oxidants" disinfectant solution has been similarly reported in the literature to designate this disinfection strategy (Choi et al., 2022; Murray et al., 2015; Szabo et al., 2019). Mezule et al. (2015) reported that electrolyzed water was efficient in decreasing the culturability and respiratory activity of *E. coli* in the planktonic state up to 5 and 2 log reduction, respectively. Biofilm-associated *E. coli* was more tolerant to disinfection with a 3 log decrease in culturability and the presence of 30% of cells able to divide (Mezule et al., 2015). Moreover, electrolyzed water was demonstrated to be more effective than chlorine gas in reducing the total heterotrophic bacteria present within biofilms formed on polyethylene surfaces (Choi et al., 2022). Although this strategy resulted in a lower $HOCl/OCl^-$ ratio, the weak reactivity of OCl^- with the biofilm matrix allowed to effectively penetrate into the biofilms (Choi et al., 2022).

A comparative study between different disinfection strategies, such UV irradiation, hydrogen peroxide, ozone, and electrolyzed water, was performed for the control of biofilms from groundwater wells (Murray et al., 2015). The authors concluded that hydrogen peroxide at 1 or 6% (v/v) caused the most effective disinfection with a reduction of biofilm culturability up to 3.1 log, followed by electrolyzed water and ozone with 1.4 and 1.0 log reduction, respectively (Murray et al., 2015).

Bacteriophages, also known as phages, are small viruses that exclusively and selectively target prokaryotic cells. Specifically, the lytic phages are first absorbed on the bacterial surface by a viral tail strand that binds to specific receptors, such as

lipopolysaccharides, proteins, sugar molecules, and fimbriae. The phage then enters the cell and takes over the metabolism of the host cell. After phage replication, new phages are released by endolysin-mediated cell lysis (an enzyme encoded by phage capable of degrading the bacterial cell wall), making a new cycle of infection possible (Parasion et al., 2014; Tian et al., 2021). For this reason, lytic phages have a cost-effective bactericidal capacity, even at a low single dosage, and are considered an environment-friendly strategy for biofilm control (D'Accolti et al., 2021; Parasion et al., 2014). Bacteriophages have been used in several fields for controlling bacterial pathogens in agriculture, the food industry, aquaculture, and medicine (D'Accolti et al., 2021; Moye et al., 2018). Recently, at least two investigations with bacteriophages for water systems have been conducted (Magin et al., 2019; Zuo et al., 2022). After 14 h of exposure to specific lytic bacteriophages, biofilm reduction of 24 h-old *P. aeruginosa* biofilms formed on SS coupons achieved up to 1.7 log (Magin et al., 2019). Additionally, the authors also observed that bacteriophages were effective in limiting the spread of detached biofilm cells in the bulk phase (Magin et al., 2019). However, similarly to other disinfectant solutions, the action of bacteriophages was higher against planktonic bacteria than in biofilms. To circumvent the diffusion limitations through the biofilm matrix, Zuo et al. (2022) proposed a targeted delivery of bacteriophages by encapsulation of phages in chitosan cross-linked with tri-polyphosphate and 3-glycidoxypropyltrimethoxysilane. The encapsulated-phage coating on HDPE surfaces allowed a biofilm biomass reduction of more than 90%, as well as a significant reduction of the biofilm surface area coverage and the ratio of the viable/damaged cells (Zuo et al., 2022).

Finally, a promising strategy has been recently proposed to control biofilm formation in water systems and to prevent the emergence of antimicrobial resistance through the use of a nanomaterial-based approach (Yu et al., 2022). The exposure of *P. alloputida* to 10

mg/L of engineered nanoscale zero-valent iron (nZVI) and derivates, including carboxymethyl cellulose-modified nZVI and oxidized nZVI nanoparticles, revealed a significant inhibitory effect on biofilm formation (Yu et al., 2022). The nZVI nanoparticles also promoted the removal of pre-established 24 h-old *P. alloputida* biofilms. Moreover, both nZVI and carboxymethyl cellulose-modified nZVI hindered the acquisition of *P. alloputida* resistance to ampicillin, ciprofloxacin, and tetracycline during a 30-day antimicrobial resistance emergence assay. The mechanism of action of nZVI nanoparticles was suggested to be through the overproduction of reactive oxygen species, cytoplasmic membrane destabilization, and inhibition of efflux pumps (Yu et al., 2022).

2.4.3 Challenges for innovation in DW biofilm disinfection

The presence of biofilms in DWDS constitutes an important problem for DW suppliers given the potential source of microbial contamination, deterioration of water quality, including the taste and odour, and promotion of pipe corrosion. The biofilm matrix protects the embedded cells from disinfection and facilitates the recovery and growth of microbial cells injured by environmental stress and disinfection (Liu et al., 2016; Simões and Simões, 2013). Moreover, the higher biofilm tolerance to disinfection in comparison to the planktonic cell state (Mezule et al., 2015; Rand et al., 2013; Wang et al., 2014) poses a significant difficulty in the surveillance of public health risks present in the DW networks. The presence of opportunistic pathogens namely *Legionella* spp., *Mycobacterium* spp., *P. aeruginosa*, *Acanthamoeba* spp., and *Aeromonas* spp. (Liu et al., 2019a; 2019b; Wang et al., 2018) and detection of antibiotic biosynthesis-related pathways and virulence determinants (Li et al., 2020a; Soto-Giron et al., 2016) in microbial communities of DW biofilms developed in conventional disinfected DWDS have been frequently reported. Additionally, sub-inhibitory concentrations of chlorine or

chloramine, which are possible to be observed in network locations further away from the treatment plants, may create a selective pressure to enrich antibiotic-resistant bacteria in the DW biofilms (Khan et al., 2019; Soto-Giron et al., 2016) or promote biofilm resistance to disinfection (Ng et al., 2021). Therefore, to ensure an optimized control of microbial recontamination in DWDS it is important to choose a disinfectant presenting adequate chemical stability though the DW network. On the other hand, it has been observed that an effective strategy for biofilm control is not necessarily achieved by the use of a disinfectant with the best activity against microbial cells in a planktonic state (Choi et al., 2022). The reaction with the EPS components and consequent lower chemical diffusion through the biofilm hinder the action of disinfectants against biofilms (Xue et al., 2014). For that reason, an appropriate understanding of the mechanisms involved in the interaction of disinfectants with biofilms, including biofilm matrix and embedded cells, will advance the accomplishment of effective strategies for biofilm control in DWDS.

Lastly, when designing a new approach for the disinfection of DW biofilms, specifically with the use of chemical agents, it is important to not undervalue the public perception of the solution and the regulatory requirements for approval, particularly the Biocidal Product Directive (Regulation (EU) No 528/2012) in the European Union. Chemical agents for water disinfection are also classified as biocidal products, and so, the practical application of these strategies is dependent on the approval process defined by the Regulation on the supply and use of biocidal products in the European Union. The Biocidal Product Directive tries to ensure that the biocidal products are effective and do not present unacceptable risks to humans, animals, or the environment (Regulation (EU) No 528/2012).

Chapter 3

Materials and Methods

This chapter describes the materials and methods used to perform the work presented in chapters 4 to 6.

3.1 Bacteria and culture conditions

Acinetobacter calcoaceticus (031) and *Stenotrophonomas maltophilia* (028) were previously isolated from a DWDS in Braga (Portugal) and used as model microorganisms in diverse studies to understand DW biofilm formation and to develop control strategies (Gomes et al., 2016, 2020; Simões et al., 2007a, 2007b, 2010a). Community composition studies have revealed that DW microbiota is complex, however, Proteobacteria have been found to dominate biofilms in DWDS, mainly those belonging to α, β, γ, and δ subclasses (Liu et al., 2016; Proctor and Hammes, 2015). Both *A. calcoaceticus* and *S. maltophilia* belong to the subclass γ- Proteobacteria and are recognized as emerging and opportunistic multi-drug resistant pathogens, often associated with nosocomial infections (Brooke, 2012; Gales et al., 2001; Gröschel et al., 2020; Menetrey et al., 2021).

Bacteria were grown overnight in batch cultures using R2A broth (peptone 0.5 g/L (Merck, Darmstadt, Germany), glucose 0.5 g/L (Merck, Darmstadt, Germany), magnesium sulphate heptahydrate 0.1 g/L (Labkem, Mataró, Spain), sodium pyruvate 0.3 g/L (VWR Chemicals, Solon OH, USA), yeast extract 0.5 g/L (Merck, Darmstadt, Germany), casein hydrolysate 0.5 g/L (Oxoid, Basingstoke, UK), starch soluble 0.5 g/L (Acros Organics, Morris Plains NJ, USA) and di-potassium phosphate trihydrate 0.4 g/L (Fisher Scientific, Leicestershire, UK)) at 25 ± 2 °C and under agitation (150 rpm). Cells were harvested by centrifugation at 3220 × *g*, 10 min, washed, and resuspended in phosphate-buffered saline (PBS) pH 7.4 or 10 × diluted R2A broth to achieve the bacterial concentration required for further experiments [see **Annex A** for optical density (OD_{610nm}) to bacterial concentration (CFU/mL) relationship].

3.2 Disinfectants

Three disinfectants (sodium dichloroisocyanurate – NaDCC – from Acros Organics (Morris Plains NJ, USA); trichloroisocyanuric acid – TCCA – from Sigma-Aldrich (St. Louis MO, USA), and pentapotassium bis(peroxymonosulphate) bis(sulphate) - OXONE - from Sigma-Aldrich (St. Louis MO, USA)) were selected from the product type 5 Article 95 List of the Biocidal Products Regulation published by ECHA (2020). Calcium hypochlorite – $Ca(OCl)_2$ – from Merck (Darmstadt, Germany) was used as a reference disinfectant whose action is based on free chlorine release (WHO, 2022). Therefore, throughout this work $Ca(OCl)_2$ is also described as free chlorine. The free chlorine concentration was determined using the HI96701 free chlorine portable photometer (Hanna Instruments) according to the DPD (N,N-diethyl-p-phenylenediamine) colourimetric method (Meireles et al., 2017). The stock solutions were aseptically and freshly prepared in ultrapure water and stored at 4 ºC.

3.3 Dose-response relationship and determination of minimum bactericidal concentration (MBC)

The dose-response relationship and the bactericidal activity against planktonic cells were evaluated according to the European Standard EN 1276 with some modifications (European Standard, 1997). The pre-cultures grown as previously described were adjusted to a cellular density of approximately 10^8 CFU/mL in PBS. Afterwards, 1 mL of the cell suspension was added to 1 mL of sterile distilled water and 8 mL of the disinfectant solution prepared in ultrapure water at 1.25 times the required test concentration. The range of concentrations was between 1/32 and 1/8 of the maximum

guideline values for DW disinfection: 50 mg/L for NaDCC (WHO, 2022), 30 mg/L for TCCA (NSF, 2018), and 5500 mg/L for OXONE. In the case of $Ca(OCl)_2$ the concentrations were between 0.10 and 5.0 mg/L of free chlorine. Control samples were performed by replacing the disinfectant solution with ultrapure water. After 30 min of exposure at room temperature (23 ± 2 ºC), the disinfectant neutralization was performed through the dilution-neutralization method using a neutralizer solution [30 g/L of polysorbate 80 (VWR Chemicals, Solon OH, USA), 30 g/L of saponin (VWR Chemicals, Leuven, Belgium), 1 g/L of L-histidine (Merck, Darmstadt, Germany), 3 g/L of lecithin (Alfa Aesar, Karlsruhe, Germany), 5 g/L of sodium thiosulphate (Labkem, Mataró, Spain) in 0.0025 M phosphate buffer] (European Standard, 1997). Therefore, 100 µL of the test mixture was added to 800 µL neutralizer and 100 µL of sterile distilled water. At the end of a further 5 min of incubation, the neutralized test mixture was 10-fold serially diluted in sterile saline solution (8.5 g/L NaCl), and 10 µL of each dilution was placed on R2A agar plates. Colony counting was carried out after 48 h of incubation at 25 ± 2 ºC, and log CFU/mL was determined. The detection limit was 2.7 log CFU/mL. The antimicrobial activity was evaluated by the assessment of the logarithmic reduction (log reduction) as log N_0/N, where N_0 and N are the CFU/mL counts for disinfectant unexposed (control) and exposed bacteria, respectively. MBC was considered to be the lowest concentration in which complete growth absence was detected. The neutralizer toxicity and the dilution-neutralization efficacy were validated for each of the disinfectants and bacteria (see **Annex B**).

3.4 Bacterial inactivation over time and kinetic modelling

The evaluation of bacterial inactivation over time was performed as described for the determination of the dose-response relationship, with some modifications. The disinfectant solutions were tested at MBC and at a concentration that caused only partial inactivation. The selection of the sub-lethal concentrations for each disinfectant was based on approximately a 3 to 4 log reduction in bacterial culturability from the above experiments. Different exposure times were evaluated: 5, 10, 20, 30, 45, 60, 90, and 120 min at room temperature (23 ± 2 ºC). Control samples were performed by replacing the disinfectant solution with ultrapure water. The bacterial inactivation was then evaluated by the quantification of log CFU/mL.

The bacterial inactivation data generated in this study was then fitted to different disinfection models through the use of GinaFiT, a freeware excel plug-in developed by (Geeraerd et al., 2005).

The biphasic model was considered an adequate disinfection model to describe the action of NaDCC and TCCA, which can be formulated as follows (Cerf, 1977; Geeraerd et al., 2005):

$$log(N) = log(N_0) + log(f \cdot e^{-k_{max1}t} + (1-f) \cdot e^{-k_{max2}t}) \quad (1)$$

Herein, N is the number of survivors, N_0 is the inoculum size, t is the time, f is the fraction of the initial population in a major subpopulation, $(1-f)$ is the fraction of the initial population in a minor subpopulation (which is more resistant than the previous one), and k_{max1} and k_{max2} are the specific inactivation rates of the two populations, respectively.

Conversely, the double Weibull model was used to describe bacterial inactivation with OXONE. The model can be written as follows (Coroller et al., 2006; Geeraerd et al., 2005):

$$N(t) = \frac{N_0}{1+10^{\alpha}}\left[10^{-\left(\frac{t}{\delta_1}\right)^p+\alpha} + 10^{-\left(\frac{t}{\delta_2}\right)^p}\right] \quad (2)$$

Where, α is the fraction of the first subpopulation remaining in the total population, δ_1 and δ_2 are the time to first log reduction of the first and second subpopulation, and p is the shape parameter of the inactivation curve ($p < 1$ for convex, $p > 1$ for concave). The parameter α varies from negative infinity to positive infinity and was introduced based on logit transformation of the ratio f, which provides insufficient discrimination and varies from 0 to 1.

$$\alpha = log\ \left(\frac{f}{1-f}\right) \quad (3)$$

The goodness of fit of the different kinetic models was evaluated based on the root mean squared error (RMSE) between the predicted and observed log inactivation values.

3.5 Assessment of membrane integrity

The Live/Dead *Bac*Light™ kit (Invitrogen, Waltham MA, USA), which comprises two nucleic acid-binding stains, SYTO 9 and propidium iodide (PI), was used to assess membrane integrity by selective stain exclusion according to Borges et al. (2013).

After 30 min of exposure to each disinfectant at MBC and at a concentration that caused only partial inactivation (as described in subsection **3.4**), 1 mL of the neutralized test mixture was filtered through a black polycarbonate membrane (pore size 0.22 µm) and then stained with 250 µL of SYTO 9 and 50 µL of PI. The dyes were left to react for

7 min in the dark, and then the membrane was prepared on *Bac*Light mounting oil, as described in the manufacturer's instructions. A LEICA DMLB2 epifluorescence microscope (LEICA Microsystems) coupled with a LEICA DFC300 FX camera and a 100× oil immersion fluorescence objective was used for the observation of stained bacteria. LEICA IM50 Image Manager software was used to acquire images, for their processing and archiving. Both total and PI-stained cells on each membrane were estimated from counts of 15 fields of view. The percentage of PI-stained cells was determined as damaged cells/total cells (%).

3.6 Physicochemical characterization of bacterial membranes

Bacterial lawns were prepared for sessile drop contact angle measurements as described by Busscher et al. (1984). After 30 min of exposure to each disinfectant at MBC and at a concentration that caused only partial inactivation, as described in subsection **3.4**, 30 mL of each bacterial suspension was filtered using a sterile cellulose nitrate membrane filter, pore size 0.45 μm (Advantec).

Determination of contact angles was performed automatically using a Contact Angle System OCA 15 Plus (Dataphysics Instruments) video-based optical measure instrument, allowing image acquisition and data analysis. The measurements were carried out at room temperature (23 ± 2 ºC) using three different liquids: water, the polar formamide (Merck) and the apolar 1-bromonaphthalene (Sigma). Three independent experiments were performed for each condition.

Hydrophobicity was evaluated after contact angles measurement following the approach of van Oss et al. (1987, 1988, 1989), where the degree of hydrophobicity of a

given surface (s) is expressed as the free energy of interaction between two entities of that surface when immersed in water (w), ΔG_{sws} (mJ/m^2). If the interaction between the two entities is stronger than the interaction of each entity with water, $\Delta G_{sws} < 0$, the material is considered hydrophobic. Conversely, if $\Delta G_{sws} > 0$, the material is hydrophilic. ΔG_{sws} can be calculated through the surface tension components of the interacting entities according to equation 4:

$$\Delta G_{sws} = -2\left(\sqrt{\gamma_s^{LW}} - \sqrt{\gamma_w^{LW}}\right)^2 + 4\left(\sqrt{\gamma_s^+\gamma_w^-} + \sqrt{\gamma_s^-\gamma_w^+} - \sqrt{\gamma_s^+\gamma_s^-} - \sqrt{\gamma_w^+\gamma_w^-}\right) \quad (4)$$

Where, γ^{LW} accounts for the Lifshitz-van der Waals component of the surface free energy, and γ^+ and γ^- are the electron acceptor and electron donor parameters of the Lewis acid-base component (γ^{AB}), respectively, with $\gamma^{AB} = 2\sqrt{\gamma^+\gamma^-}$.

The surface tension components of the surface can be obtained by measuring the contact angles of the three pure liquids, with known surface tension components, followed by the simultaneous resolution of three equations of the type of equation 5, one for each liquid:

$$(1 + cos\ \theta)\gamma_w^{Tot} = 2\left(\sqrt{\gamma_s^{LW}\gamma_w^{LW}} + \sqrt{\gamma_s^+\gamma_w^-} + \sqrt{\gamma_s^-\gamma_w^+}\right) \quad (5)$$

Where, θ is the contact angle and $\gamma^{Tot} = \gamma^{LW} + \gamma^{AB}$. The liquids' surface tension components were obtained from the literature (Janczuk et al., 1993).

3.7 Evaluation of the effects of disinfectants on biofilm control

3.7.1 Biofilm formation

Polyvinyl chloride (PVC) and stainless steel (SS) coupons (1 × 1 cm) were used as substrata for biofilm formation and were selected as a representative pipe material from DW networks (Simões et al., 2007a). The coupons were cleaned in sequential ultrasonic baths (Transsonic T420, Elma, Singen, Germany) in a commercial detergent solution in distilled water for 30 min, followed by ethanol at 70% (v/v) for 30 min (SS) or 1 min (PVC), and ultrapure water for 30 min to remove any organic or inorganic contaminant on the surfaces. Afterwards, they were sterilized by ultraviolet light for 90 min.

The coupons were inserted in 24-well microtiter plates and 2 mL of cell suspension was added to each well. The bacterial cultures were used as inoculum with a cellular density of approximately 10^6 CFU/mL in 10 × diluted R2A broth. Biofilm formation was allowed to occur for 48 h at 25 ± 2 °C and 150 rpm, with medium refreshment at the end of 24 h. After incubation, the coupons were carefully immersed in PBS to remove loosely attached cells and biofilms were tested on their behaviour to chemical treatment.

3.7.2 Biofilm exposure to disinfectants and biofilm regrowth

The effects of the selected disinfectants on biofilms were assessed in terms of culturability and total cells, according to Gomes et al. (2016). Coupons with biofilms were exposed to disinfectants at MBC or 10 × MBC for 30 min, by adding 2 mL of the disinfectant solutions into each well of the 24-well microtiter plates. After chemical exposure, the disinfectants were neutralized through the dilution-neutralization method using the neutralizer solution described in subsection **3.3** (European Standard, 1997). After this, biofilms were resuspended and homogenized in PBS by vortexing for 2 min,

followed by 2 min in an ultrasound bath (frequency 35 kHz). For culturability assessment, 10 × serial dilutions in sterile saline solution (8.5 g/L NaCl) were performed and 10 µL of each dilution were plated on R2A agar. Colony counting was carried out after 48 h of incubation at 25 °C. The results are presented as log CFU/cm^2. For the determination of total cells, 1 mL of the biofilm suspensions was filtered through a 0.22 µm black polycarbonate membrane and bacteria were stained with 400 µL of 4',6-diamidino-2-phenylindole (DAPI – Merck, Darmstadt, Germany) at 0.5 µg/mL for 10 min in the dark (Gomes et al., 2016). A LEICA DMLB2 epifluorescence microscope (LEICA Microsystems) coupled with a LEICA DFC300 FX camera and a filter sensitive to DAPI fluorescence (359 nm excitation filter in combination with a 461 nm emission filter) were used for the observation of stained bacteria. LEICA IM50 Image Manager software was used to acquire images, for their processing and archiving. Fifteen micrographs per sample were obtained to estimate the log cells/cm^2.

To evaluate the effects of chemical treatment on biofilm regrowth, after 30 min exposure to the selected disinfectants the coupons with treated biofilms were carefully immersed in PBS to remove loosely attached cells and inserted in new 24-well microtiter plates, each well containing 2 mL of 10 × diluted R2A broth. The biofilms were incubated for an additional 24 h at 25 ± 2 °C, 150 rpm, and finally analysed for determination of culturability and total cells as explained above.

At least three independent experiments were performed with the use of two coupons for each test condition.

3.7.3 Atomic Force Microscopy

The 48-h old *S. maltophilia* biofilms on SS coupons were equally prepared and treated as mentioned in subsections **3.7.1** and **3.7.2**. After chemical exposure, biofilms were

rinsed with PBS, followed by ultrapure water, and dried for 1 h at 37 °C. Samples were imaged in air, using a TT-AFM atomic force microscope from AFM Workshop, and ACT (AppNano) probes in vibrating (tapping) mode. At least six areas per sample were imaged to obtain representative results, and typical images are shown here. The data analysis was performed using the free and open-source software Gwyddion 2.51. The surface area of the cell clusters in the images of each condition was measured using the mask editor and grain measure tools. Then, the histogram descriptive statistics was assessed by using the program GraphPad Prism 9 for Windows. The results of the surface area of cell clusters on the surface of biofilms were represented by violin-plots.

3.8 Determination of viscoelastic properties of biofilms

3.8.1 Biofilm formation and treatment

The colony biofilm method was used to grow 48 h-old *S. maltophilia* biofilms for rheometry analysis. This methodology has been used in previous rheological studies due to the ease of culturing and mechanical evaluation (Gloag et al., 2018; Jones et al., 2011). In this study, colony biofilms were developed according to Fernandes et al. (2022). The bacterial culture was diluted to a cellular density of approximately 10^8 CFU/mL in PBS. Polycarbonate filter membranes (25 mm, 0.2 μm pore size) Nuclepore^{TM} Track-Etched (Whatman Inc, UK) that had been previously autoclaved were used as the substrate to grow the biofilms. Sterilized membranes were placed onto R2A agar plates and a drop of 40 μL of the cell suspension was then pipetted onto the centre of each filter membrane. The plates were incubated at 25 ± 2 °C for 48 h, with the membrane-supported biofilms transferred to fresh culture medium agar at the end of 24 h.

These culture conditions allowed the formation of colony biofilms with diameters of approximately 8 mm and thicknesses of 70-170 μm. Colony biofilms were characterized in terms of culturability, total cells, and content of extracellular proteins and polysaccharides. Colony biofilms were removed from the filter membranes by resuspending in 5 mL of extraction buffer [0.76 g/L of $Na_3PO_4 \cdot 12H_2O$ (Merck, Darmstadt, Germany), 0.4 g/L of $Na_2HPO_4 \cdot 2H_2O$ (Chem-lab, Belgium), 0.53 g/L of NaCl and 0.08 g/L of KCl, pH 7] and vigorously vortexed for 2 min. The culturability assessment and determination of total cells were performed as described in subsection **3.7.2**. Proteins and polysaccharides content were quantified after extraction using Dowex® Marathon© resin (Na^+ form, strongly acidic, 20-50 mesh (Sigma-Aldrich, Steiheim, Germany) according to Frølund et al. (1996) and Gomes et al. (2020). The extraction occurred under 400 rpm at 4 °C for 4 h. Then, the extracellular components were separated from the cells through centrifugation at 3220 ×g for 5 min. The total amounts of proteins and polysaccharides present in the biofilm matrix were assessed. The quantification of proteins was performed by Peterson's modification of the micro Lowry method, using bovine serum albumin as standard (Lowry et al., 1951; Peterson, 1977). The polysaccharides were quantified according to the phenol-sulfuric method, using glucose as the standard (Dubois et al., 1951).

The exposure of colony biofilms to the selected disinfectants was performed by carefully dipping a 2 × 2 cm filter paper from Whatman Inc (UK) in each disinfectant solution at 10 × MBC, then placing the membrane containing the 48 h-old colony biofilms on the top of the filter paper for 30 min. Following the chemical exposure, the membrane was placed onto R2A agar plate to neutralize the disinfectants.

3.8.2 Rheometry analysis

A Kinexus Rheometer connected with rSpace software (Malvern Instruments Ltd, UK) was used for the rheological testing. The rheometer was fitted with an 8 mm SS parallel plate geometry and the measurements were performed at 25 °C. The membranes containing the colony biofilms were cut with an 8 mm biopsy punch and positioned directly in the centre of the base plate so that the 8 mm rheometer head completely covered the biofilm sample. For setting the gap before analysis, colony biofilms were compressed until a normal force was detected by lowering the head by a small interval, followed by an equilibrium period of a few seconds. Each biofilm sample was tested only once and up to five replicate colony biofilms were analysed for each test condition.

Oscillatory strain sweeps were performed by incrementing the shear strain from 0.01-1000% at a constant frequency of 1 Hz. The viscoelastic parameters of the biofilms [shear stress, and storage (G'), loss (G'') and complex shear (G*) moduli] were measured and the linear viscoelastic region (LVR) was determined for each test condition. Afterwards, oscillatory frequency sweeps were performed by incrementing the frequency from 0.1-100 Hz at a constant shear strain of 0.3%.

3.9 Validation of the effects of OXONE on biofilms using a benchtop biofilm reactor

3.9.1 Biofilm formation in the rotating cylinder reactor (RCR)

S. maltophilia was selected for this study since it was more tolerant to biofilm inactivation in the microtiter plate experiments. *S. maltophilia* was grown in two 1 L Erlenmeyer flasks containing 250 mL of R2A broth and was incubated overnight at 25 ±

2 ºC and 120 rpm. Cells were harvested by centrifugation at 3220 ×*g*, 10 min, washed, and resuspended in 500 mL of R2A broth.

Mature biofilms were formed according to Gomes et al. (2020) with some modifications, using a RCR under conditions mimicking DWDS. The RCR (**Figure 3-1**) was an aerobic biofilm reactor composed of a cylindrical vessel with a 5 L working volume and a cover that fitted the vessel and supported a triple shaft system connected by a timing belt, where three cylinders were fixed to each shaft. An overhead stirrer (Hei-TORQUE 400, Heidolph Instruments GmbH & Co. KG, Schwabach, Germany) provided the simultaneous rotation, at the same speed and direction, of the cylinders that were immersed in a bacterial suspension. PVC cylinders were used for biofilm formation with a sampling area of 39.27 cm^2 (d = 2.5 cm; l = 5 cm) per cylinder. This material was chosen given the lower efficiency of OXONE action on biofilms formed on PVC than on SS in the microtiter plate experiments.

The reactor was inoculated with 500 mL of bacterial suspension and diluted with sterile synthetic tap water (STW) to a final volume of 5 L and a final cellular density of approximately 2.5×10^7 CFU/mL. STW was used to mimic tap water and was composed of 100 mg/L $NaHCO_3$ (Merck, Darmstadt, Germany), 13.4 mg/L $MgSO_4 \cdot 7H_2O$ (Labkem, Barcelona, Spain), 0.7 mg/L K_2HPO_4 (VWR BDH CHEMICALS, Leuven, Belgium), 0.3 mg/L KH_2PO_4 (VWR BDH CHEMICALS, Leuven, Belgium), 0.01 mg/L $(NH_4)_2SO_4$ (Panreac, Barcelona, Spain), 0.01 mg/L NaCl (Merck, Darmstadt, Germany), 0.001 mg/L $FeSO_4 \cdot 7H_2O$ (VWR BDH PROLABO, Leuven, Belgium), 1 mg/L $NaNO_3$ (VWR BDH CHEMICALS, Leuven, Belgium), 27 mg/L $CaSO_4$ (Labkem, Barcelona, Spain), and 1 mg/L humic acids (Sigma-Aldrich, Sintra, Portugal) (U.S. EPA, 2011; Gomes et al., 2018). The cylinders rotated under constant speed equivalent to a liquid flow of 0.1 m/s and 0.1 Pa of shear stress on the cylinder surface, similar to typical conditions in plumbing

systems (Fu et al., 2021; Gomes et al., 2020; Husband and Boxall, 2011; Ragain et al., 2019). The RCR operated under batch conditions for 7 h to promote initial bacterial adhesion. Afterwards, silicone tubing and a peristaltic pump operating at 0.5 L/h were used to continuously feed the reactor with 10 × diluted R2A broth from a polypropylene 50 L feed carboy, ensuring a constant dilution rate of 0.1 h^{-1}. The RCR operated for 7 days to obtain mature and steady-state biofilms (Gomes et al., 2020; Lemos et al., 2015; Simões et al., 2005).

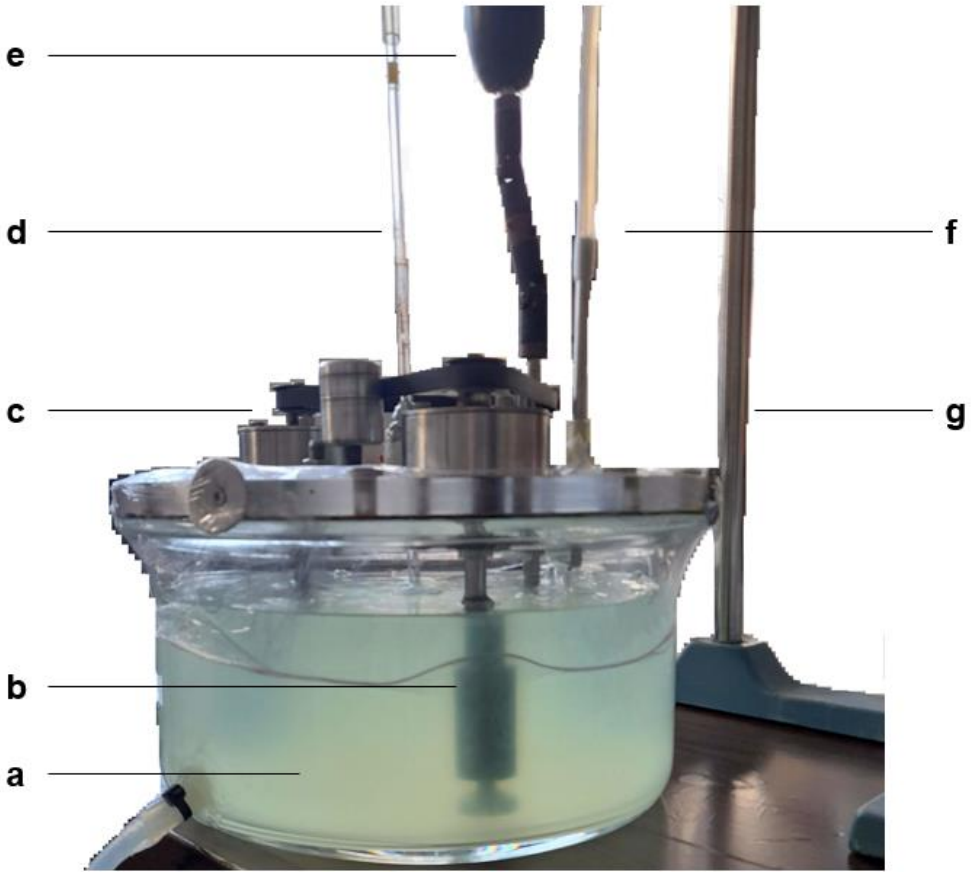

Figure 3-1 – Representative photograph of the rotating cylinder reactor. **a** – 5 L vessel with bacterial suspension; **b** – rotating cylinder for biofilm formation; **c** – triple shaft system connected by a timing belt; **d** – inlet of filter sterilized air; **e** – stirring overhead; **f** – inlet of diluted R2A broth; **g** – support for stirring system.

The shear stress (τ_w) on the cylinder surface was assessed by equation 6 (Altman et al., 2009):

$$\tau_w = \frac{f_{friction}\,\rho\,v^2}{2} \quad (6)$$

Where $f_{friction}$ is the Fanning friction factor, ρ is the fluid density (1000 kg/m^3) and v is the fluid velocity (m/s).

The linear velocity of the fluid (0.1 m/s) on the cylinder surface is given by equation 7, where *N* is the rotational speed of the cylinder (rpm) and *D* is the cylinder diameter (0.025 m):

$$v = N\pi D \quad (7)$$

The Fanning factor is calculated according to equation (8) (Gabe and Walsh, 1983):

$$f_{friction} = 0.158\,Re_a^{-0.3} \quad (8)$$

Where the Reynolds number of agitation (Re_a) is obtained from equation (9) (Mancilla et al., 2019), where μ is the fluid dynamic viscosity (0.001 kg/m/s):

$$Re_a = \frac{D^2 N \rho}{\mu} \quad (9)$$

3.9.2 Biofilm characterization

At the end of the operation time, each cylinder was removed from the RCR and carefully washed in STW to remove non-adhered bacteria. Then, biofilms formed in the RCR were characterized in terms of wet mass, culturability, total and intact membrane bacteria, and content of extracellular proteins and polysaccharides. The wet mass was obtained by the difference between the mass of the cylinder with biofilm and the mass of the cylinder without biofilm. The biofilms were removed from the cylinder surfaces by scrapping four times for 1 min using 5 mL pipette tips and rinsing each time with 2.5 mL of extraction buffer, resuspending the biofilms in a total of 10 mL of extraction buffer.

The suspensions were further vigorously vortexed for 2 min to homogenize. To assess culturable bacteria, the procedure was performed as described in subsection **3.7.2**. For determination of total cells and those with no damaged membrane, 1 mL of biofilm suspension was filtered through a 0.22 µm black polycarbonate membrane and bacteria were stained with Live/Dead *Bac*Light™ bacterial viability kit (Invitrogen, Waltham MA, USA). Volumes of 250 µL of SYTO 9 and 50 µL of PI were added to the black polycarbonate membrane and left in the dark for 10 min. The samples were analysed using a LEICA DMLB2 epifluorescence microscope connected to a LEICA DFC300 FX camera (LEICA Microsystems). The optical filter combination for optimal viewing of the stained preparations consisted of a 515-560 nm excitation filter combined with a dichromatic mirror at 580 nm and a suppression filter at 590 nm. Bacteria with intact membranes (green stained cells) and the total number of cells (sum of green and red stained cells) were assessed by cell counting of a minimum of 15 fields of view. The results are presented as log cells/cm^2 and the detection limit of the method is 4.8 log cells/cm^2. For the quantification of EPS, the procedure was performed as described in subsection **3.8.1**.

3.9.3 Biofilm exposure to disinfectants

Solutions of OXONE and free chlorine were prepared in STW at 10 × MBC of each disinfectant against *S. maltophilia*. Cylinders with biofilms were carefully washed in STW to remove non-adhered bacteria. Then, biofilms were exposed to 200 mL of OXONE or free chlorine solutions for 30 min in a 250 mL glass beaker. At the end of the exposure time, the cylinders were carefully immersed in STW to wash the disinfectants, followed by a similar procedure as described above, which included scrapping and resuspending the biofilms in 10 mL of neutralizer solution (described in subsection **3.3**)

to neutralize residual disinfectants (European Standard, 1997). The samples were analysed in terms of culturability, the presence of cells with non-damaged membranes and total cells, as described previously. Unexposed biofilms (control samples) were performed by replacing the disinfectant solution for STW.

3.10 Chemical stability of OXONE and free chlorine solutions

The stability of OXONE and free chlorine solutions were evaluated as the depletion of each disinfectant at 25 ± 2 ºC for 40 days. The solutions were prepared in STW (described in subsection **3.9.1**) and ultrapure water at 10 × MBC of each disinfectant against *S. maltophilia* and stored in light-protected flasks.

The concentration of OXONE was determined by spectrophotometric measurement using 2,2'-azino-bis(3-ethylbenzothiazoline-6-sulfonic acid) diammonium salt (ABTS, Sigma-Aldrich, Saint Louis MO, USA) as indicator and according with the method described by Zou et al. (2019). The stock solution of ABTS was prepared at 50 mM in ultrapure water and stored at 4 ºC. Phosphate buffer solution at 50 mM and pH 7 was prepared by mixing 38.5 mL of KH_2PO_4 (VWR BDH CHEMICALS, Leuven, Belgium) stock solution (0.5 M) with 61.5 mL of $K_2HPO_4 \cdot 3H_2O$ (Fisher Scientific, Leicestershire, UK) stock solution (0.5 M) and diluting the combined stock solutions to 1 L with ultrapure water. The OXONE standards solutions were freshly prepared in ultrapure water in the range of 50 to 1000 mg/L. For measuring the OXONE concentration, the procedure was as follows: 2.25 mL of phosphate buffer solution and 0.125 mL of ABTS solution were firstly added into appropriately labelled test tubes; then 0.125 mL of OXONE standard solutions or water samples containing OXONE were orderly added into the test

tubes; the mixed solutions were left to react for 10 min at room temperature (23 ± 2 ºC) in the dark; and finally, the absorption value of the mixed solutions at 415 nm were recorded using a spectrophotometer (V-1200 Spectrophotometer VWR, Leuven, Belgium). The mixed solution without OXONE (*i.e.*, replacing with 0.125 mL of ultrapure water) was used as the blank solution. When necessary, the water samples containing OXONE were appropriately diluted in ultrapure water before the reaction.

The over time depletion of free chlorine was evaluated with an HI96701 free chlorine portable photometer (Hanna Instruments) according to the DPD (N,N-diethyl-p-phenylenediamine) colourimetric method (Meireles et al., 2017).

When possible, a linear regression was performed to the experimental data to quantify the disinfectant depletion. The slope of the linear model corresponded to the disinfectant loss rate $\left(\frac{dC}{dt}\right)$ (mg/L/day) and the Y-intercept represented the estimated initial value of disinfectants (mg/L). Additionally, the half-life $t_{1/2}$ (days) for the free chlorine to be reduced by 50% was calculated from the linear models. The goodness of fit was evaluated based on the coefficient of determination (R^2).

3.11 Electron paramagnetic resonance studies

The electron paramagnetic resonance (EPR) spectroscopic studies were performed aiming to identify the reactive oxygen species (ROS) formed during the disinfection of *S. maltophilia* by OXONE at MBC in STW.

EPR spectra were recorded using a Bruker ELEXSYS E500 spectrometer, available at Laboratory for Electron Paramagnetic Resonance Spectrometry (CEMUP – Centro de Materiais da Universidade do Porto), operating at 9 GHz (X-band) using the following general experimental conditions, as specified below for each type of radical detection.

Xepr software (Bruker) was used for spectra acquisition and Easyspin-5.2.35 for computational simulations and calculation of the Spin Hamiltonian parameters. The relative amount of radical formed was estimated by the integration of EPR signal (area under the curve, AUC) using Origin 2015 software (Rebelo et al., 2019). All experiments were carried out under room light (only artificial light at constant intensity was present) and samples were protected from the light with aluminium foil.

For the investigations regarding the production of singlet oxygen radical ($^1O_2$), a stock solution of 2,2,6,6-tetramethyl-4-piperidone hydrochloride (4-oxo-TEMP – Sigma-Aldrich, Darmstadt, Germany) spin trap was freshly prepared before analysis at 14 mg/mL in distilled water. Then, 70 µL of 4-oxo-TEMP solution was added into 1 mL of bacterial test mixture as described in subsection **3.3**, except for the presence of interfering substance, in which sterile distilled water was replaced by STW (at 10 × its final concentration). An aliquot was quickly collected and placed in a capillary tube, which was then placed in the quartz EPR tube for spectra acquisition. Spectra were recorded at defined time points (0, 10, 20, and 30 min of disinfection) and at the following general experimental conditions: room temperature (20 ± 2 ºC), modulation frequency of 100 kHz, microwave power 6 mW, modulation amplitude 4 Gauss (G), 60 dB of receiver gain, acquisition time of 50 seconds and 5 scans.

To study the production of superoxide ($O_2^{\bullet-}$), hydroxyl ($HO^{\bullet}$), and sulphate ($SO_4^{\bullet-}$) radicals, a stock solution of 5,5-dimethyl-1-pyrroline-*N*-oxide (DMPO – TCI chemicals, Portland OR, USA) spin trap was freshly prepared before analysis at 18 mg/mL in distilled water. Then, 70 µL of DMPO solution was added into 1 mL of bacterial test mixture as described above. An aliquot was quickly collected and placed in a capillary tube, which was then placed in the quartz EPR tube for spectra acquisition. Spectra were recorded at defined time points (0, 10, 20, and 30 min of disinfection) and at the following

general experimental conditions: room temperature (20 ± 2 ºC), modulation frequency of 100 kHz, microwave power 4 mW, modulation amplitude 4 G, 60 dB of receiver gain, acquisition time of 220 seconds and 5 scans.

3.12 Ecotoxicity tests – impact of OXONE and free chlorine on freshwater microalga

The preliminary ecotoxicity tests were carried out with the freshwater unicellular green alga *Chlorella vulgaris* AGF002 (AllMicroalgae, Leiria, Portugal). *C. vulgaris* was used as test organism given the ease of culturing in laboratory and the existence of previous studies that reported short-term toxicity tests considering this microalga (Albuquerque et al., 2022; Silva et al., 2009). In the present study, the test organism was exposed to OXONE and free chlorine at 0.5 mg/L in STW for 72 h. This concentration was chosen regarding the recommended chlorine residual at the point of delivery between 0.2 and 0.5 mg/L for water that is centrally treated (WHO, 2022).

The test was carried out in accordance with the OECD 201 guideline (OECD, 2011) and Vale et al. (2022), with some modifications. The microalga was maintained in a solid OECD medium with 15 g/L agar (Merck, Darmstadt, Germany) at 4 ºC in the dark. The pre-cultures were prepared each week by inoculating 40 mL OECD medium in 100 mL Erlenmeyer flasks with microalgal cells. They were incubated at 25 ± 2 ºC for 3 days on an orbital shaker at 100 rpm under continuous "cool white" fluorescent light with a colour temperature of 4000-4200 K and an intensity of 3.6 cd at the surface of the flasks. The temperature, irradiation, and pH (7.5 ± 0.5) were monitored and kept constant throughout the experiment. The cultures were obtained by inoculating the cells from the pre-cultures at an initial concentration of 1×10^6 cells/mL in 100 mL OECD medium, in 250 mL

Erlenmeyer flasks. The cultures were incubated for 2 days under the conditions described for the pre-cultures. After incubation, the microalgal cells were harvested by centrifugation at 3220 ×g for 5 min and resuspended in STW.

Growth kinetic curves were obtained by the exposure of *C. vulgaris* to the selected disinfectants in the exponential growth phase, at a final concentration of 1×10^6 cells/mL, in 250 mL Erlenmeyer flasks containing STW supplemented with the nutrient components of OECD medium to a final volume of 100 mL. As a control sample, microbial cells were incubated in the same medium in the absence of the disinfectants. The cultures were incubated for 72 h under the same growth conditions (temperature and light) as described above, except for agitation that was performed by filtrated air bubbling.

Microalga cell density was determined measuring the optical density at 750 nm ($OD_{750\ nm}$) at 0, 24, 48, and 72 h and further converted to cellular concentration (X, in cells/mL) using the following equation (Vale et al., 2022):

$$OD_{750\,nm} = (3.92 \times 10^{-8}) \times X + 1.34 \times 10^{-2} \quad (10)$$

The specific growth rate (μ, d^{-1} or h^{-1}) was determined from equation 11:

$$\mu = \frac{lnX_f - lnX_i}{t_f - t_i} \quad (11)$$

Where X_f and X_i are the cellular concentration at the times t_f and t_i, respectively, the end and beginning of the exponential growth phase.

3.13 Statistical analysis

The experimental data were analysed using the program GraphPad Prism 9.5.0 for Windows. At least three independent experiments were performed in duplicate for each

test condition. Both mean and standard deviation (SD) within samples were calculated. Statistical calculations were based on a confidence level ≥ 95% ($P < 0.05$), which was considered statistically significant. The ANOVA test followed by Tukey's multiple comparisons test was performed for the statistical analysis of the most of experimental data, assuming normal distribution and that all the groups were sampled from populations with homogeneity of variance. The Brown-Forsythe and Welch ANOVA test followed by Dunnett's T3 multiple comparisons test was performed for the statistical analysis of the data from the rheological testing, assuming normal distribution and that the groups were sampled from populations with different variances

Chapter 4

Chlorinated cyanurates and OXONE as antimicrobial and antibiofilm agents against DW bacteria

The present chapter comprises the evaluation of the antimicrobial activity of NaDCC, TCCA, and OXONE against two emerging bacterial pathogens isolated from DW, *A. calcoaceticus* and *S. maltophilia*. Free chlorine was used for comparison and as reference DW disinfectant. The dose and time-responses against planktonic bacteria were performed as well as the assessment of the effects on selected physiological indices (membrane integrity and physicochemical properties of bacterial surface). Moreover, the effects of the selected disinfectants against 48 h-old biofilms formed by *A. calcoaceticus* and *S. maltophilia* were evaluated in the reduction of biofilm culturability and in biofilm removal.

4.1 Results and Discussion

4.1.1 Antimicrobial activity against planktonic bacteria – dose-response relationship and MBC

The antimicrobial activity of the selected disinfectants was found to be dose-dependent against both *A. calcoaceticus* and *S. maltophilia* (**Figure 4-1**). The increase in concentration led to an increase in antimicrobial activity until a total reduction of cell culturability was reached. MBC was considered to be the lowest concentration at which complete growth absence was detected, and the values obtained for each disinfectant and bacteria are summarised in **Table 4-1**. The ranking by dose efficiency against both bacteria was as follows: free chlorine from $Ca(OCl)_2$ > NaDCC > TCCA > OXONE. *S. maltophilia* was more susceptible than *A. calcoaceticus*, with total log reduction obtained for lower doses of each disinfectant. Gomes et al. (2016) reported an opposite trend, with planktonic *S. maltophilia* being significantly more tolerant to sodium hypochlorite (NaOCl) than *A. calcoaceticus*. These opposite results may denote that the action of chlorine-based disinfectants is not species-dependent. The results also reinforce that chlorinated cyanurates are less effective disinfectants against planktonic bacteria in comparison to the use of free chlorine alone (Murphy et al., 2015; Wahman, 2018; Wojtowicz, 2001).

Planktonic cultures of *P. aeruginosa* were not able to grow after 6 h of exposure to 5% (v/v) NaDCC (Morgenthau et al., 2012). Moreover, the antimicrobial effects against planktonic *P. aeruginosa* after exposure for 30 min to NaDCC solutions at 50% (v/v) or higher were equally effective as 5% bleach. On the other hand, to reduce the concentration of *A. calcoaceticus* over 6 log, the minimum inhibitory concentration of NaDCC was *circa* 1100 mg/L (Penna et al., 2001). Another work regarding the chlorination of

greywaters demonstrated that products containing $Ca(OCl)_2$, NaDCC, or TCCA reduced the mesophile microorganisms at least 5 and 4 log CFU after 30 min and 30 h, respectively (Chaillou et al., 2011).

Table 4-1 – Minimum bactericidal concentrations (MBC) and sub-lethal concentrations (mg/L) of NaDCC, TCCA, OXONE, and free chlorine from $Ca(ClO)_2$ against *A. calcoaceticus* and *S. maltophilia*.

	A. calcoaceticus		***S. maltophilia***	
	MBC (mg/L)	**Sub-lethal concentration (mg/L)**	**MBC (mg/L)**	**Sub-lethal concentration (mg/L)**
NaDCC	3.1	2.1	2.1	1.6
TCCA	3.8	1.9	2.5	1.1
OXONE	690	340	340	280
Free chlorine	1.0	0.50	0.80	0.40

Regarding the antimicrobial activity of OXONE, a disinfectant product containing pentapotassium bis(peroxymonosulphate) bis(sulphate) at concentrations above 5000 mg/L reduced the levels of *Aeromonas salmonicida*, *Yersinia ruckeri*, *Carnobacterium piscicola*, and *Lactococcus garvieae* more than 5 log CFU/mL after a contact time of 30 min (Verner-Jeffreys et al., 2009). Moreover, 3 h exposure to 1000 mg/L of a commercial disinfectant containing 40-55% of pentapotassium bis(peroxymonosulphate) bis(sulphate) reduced approximately 3 log CFU/mL of a *Vibrio* spp. and 3 log $TCID_{50}$/mL (the 50% tissue culture infectious dose) of viral nervous necrosis virus in seawater (Ciulli et al., 2017).

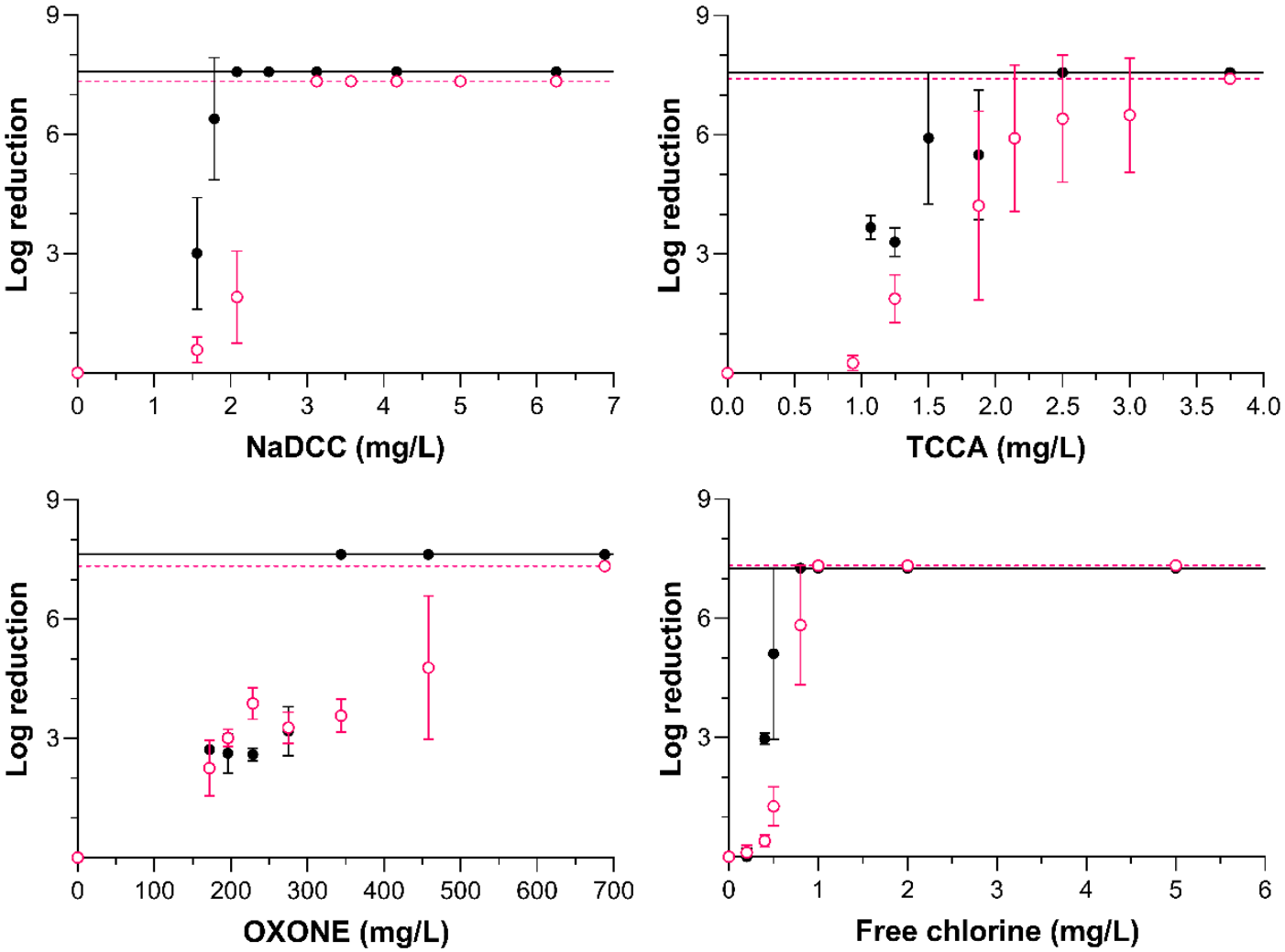

Figure 4-1 – Dose-response relationship after 30 min of exposure to NaDCC, TCCA, OXONE, and free chlorine from $Ca(ClO)_2$ against *A. calcoaceticus* (open circles) and *S. maltophilia* (closed circles). The dashed line and solid line represent the N_0 for *A. calcoaceticus* and *S. maltophilia*, respectively.

The differences between the studies can be explained by the use of other products, some of them applying commercially available disinfectants that often contain a blend of ingredients, and due to alternative methods for the determination of antimicrobial activity. Moreover, nutrient availability during disinfectant exposure is also distinct among the different studies. In the present study, the European Standard EN 1276 (1997) was followed without interfering substances, to avoid neutralization or potentiation of disinfectant action during the antimicrobial incubation time. The selected disinfectants were also tested in their unformulated state.

4.1.2 Antimicrobial activity against planktonic bacteria – time-response

The evaluation of bacterial inactivation over time was performed for each disinfectant at two different concentrations: MBC and a concentration causing partial inactivation (**Table 4-1**). The results of *A. calcoaceticus* and *S. maltophilia* inactivation for each disinfectant are presented in **Figure 4-2** and **Figure 4-3**, respectively. The comparative analysis of the experimental data did not reveal differences in the inactivation of *A. calcoaceticus* by NaDCC, TCCA, and OXONE, with total inactivation at the end of the 60 min exposure to the disinfectants (**Figure 4-2**). On the other hand, in the case of *S. maltophilia*, a total inactivation was observed after 45 min of exposure to OXONE, while for TCCA a complete log reduction was not obtained until 120 min exposure (**Figure 4-3**).

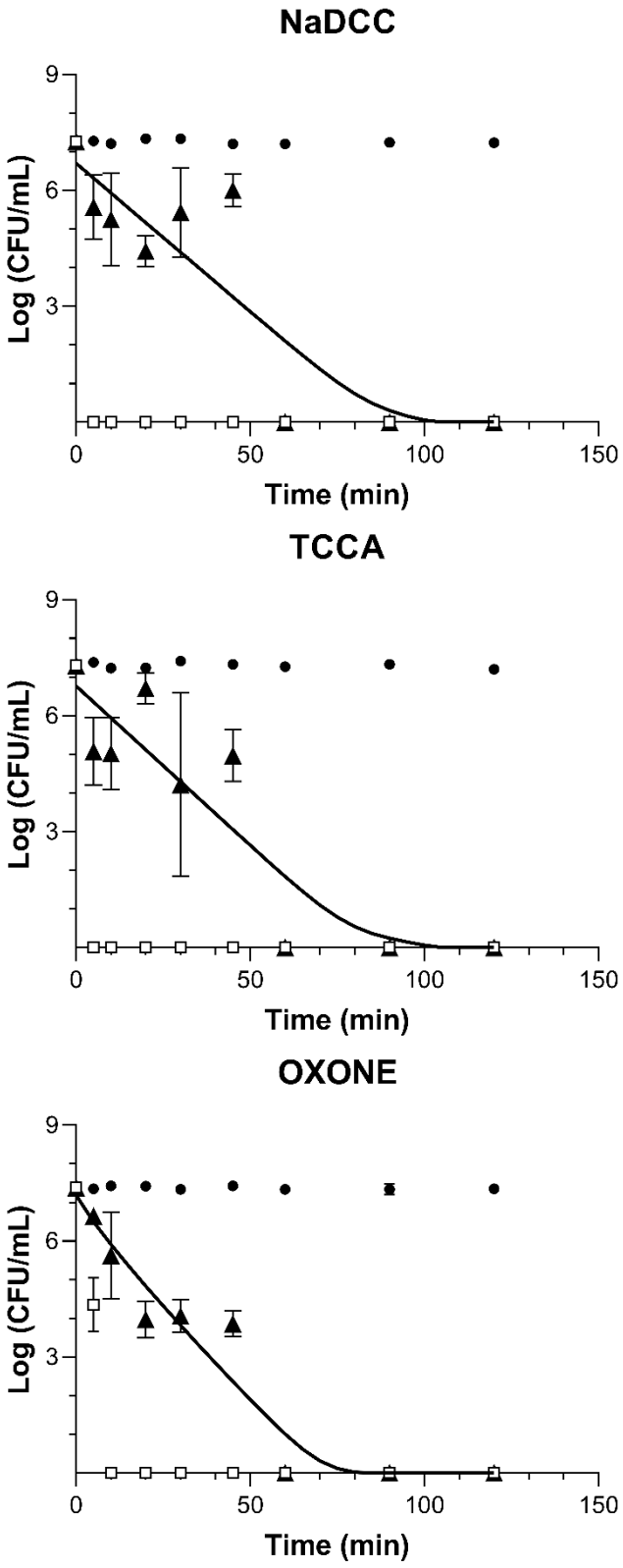

Figure 4-2 – *A. calcoaceticus* inactivation by NaDCC, TCCA, and OXONE at MBC (open squares), sub-lethal concentration (closed triangles), and 0 mg/L (closed circles). The lines represent the disinfection models fitted to the experimental data for the sub-lethal concentrations. The biphasic model was applied for NaDCC and TCCA, and the double Weibull model for OXONE.

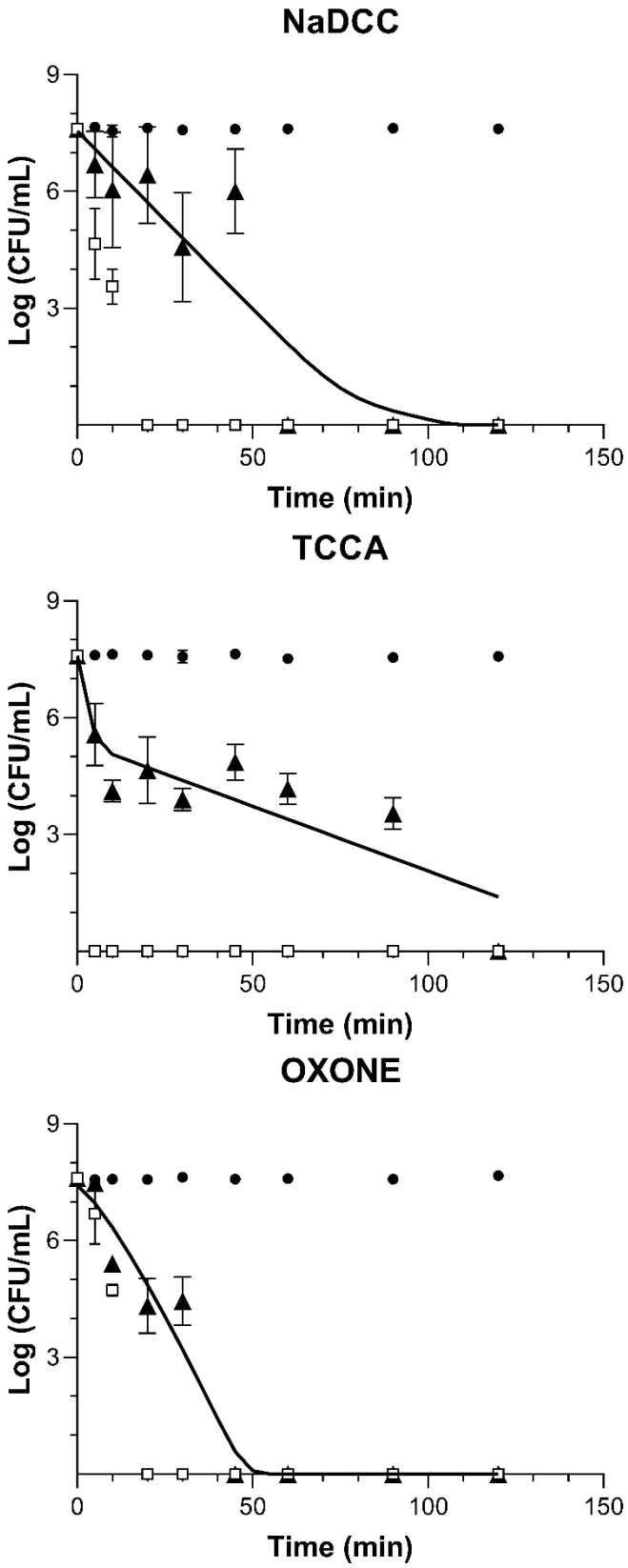

Figure 4-3 – *S. maltophilia* inactivation by NaDCC, TCCA, and OXONE at MBC (open squares), sub-lethal concentration (closed triangles), and 0 mg/L (closed circles). The lines represent the disinfection models fitted to the experimental data for the sub-lethal concentrations. The biphasic model was applied for NaDCC and TCCA, and the double Weibull model for OXONE.

The bacterial inactivation data generated in this study for the sub-lethal concentrations were then fitted to different disinfection models: the biphasic model, for NaDCC and TCCA, and the double Weibull model, for OXONE. To describe all shapes of inactivation kinetics, both models assume that the population is composed of two groups that differ in their levels of tolerance to stress (Cerf, 1977; Coroller et al., 2006; Geeraerd et al., 2005). One major subpopulation that is initially more sensitive to stress (represented by the initial steep constant decline in the biphasic model or the first wave in the double Weibull model) and one minor subpopulation that is more tolerant to stress (represented by the final smoother constant decline in the biphasic model or the second wave in the double Weibull model). The goodness of fit of the different kinetic models was evaluated based on the RMSE between the predicted and observed log inactivation values. **Table 4-2** summarizes the statistical measures and the parameter values obtained when applying the models to the experimental data set.

A brief analysis of the kinetic parameters regarding the action of NaDCC and TCCA on bacterial inactivation demonstrates that *S. maltophilia* appeared to be more susceptible to these disinfectants than *A. calcoaceticus*. The specific inactivation rates, k_{max1} and k_{max2}, of *S. maltophilia* were higher for both disinfectants than these of *A. calcoaceticus*. For both disinfectants and bacteria, the fraction of initially major subpopulation - *f*, the least tolerant to stress, was equal or close to 1, indicating that all the bacterial population of *A. calcoaceticus* or *S. maltophilia* was similarly susceptible to NaDCC or TCCA. Nevertheless, the inspection of the inactivation curve of *S. maltophilia* by TCCA (**Figure 4-3** TCCA) shows a clear initial shorter decline in time, which corresponds to a subpopulation more susceptible to the disinfectant. The following smoother decline is representative of the tolerant minor subpopulation.

Table 4-2 – Statistical measures and parameter values when applying the biphasic model on the experimental data of bacterial inactivation over time with NaDCC and TCCA, and the double Weibull model on the experimental data for OXONE. The parameter values are presented together with their Asymptotic Standard Error. NQ, not quantifiable.

Biphasic model	**RMSE**	**Log N_0 (CFU/mL)**	**k_{max1} (1/min)**	**k_{max2} (1/min)**	**f**	
NaDCC						
A. calcoaceticus	1.7	6.7 ± 1.0	0.18 ± 0.08	0.03 ± 0.25	1.0 ± 0.0	
S. maltophilia	1.6	7.6 ± 0.9	0.21 ± 0.07	0.04 ± 0.18	1.0 ± 0.0	
TCCA						
A. calcoaceticus	1.6	6.8 ± 0.9	0.19 ± 0.07	0.03 ± 0.19	1.0 ± 0.0	
S. maltophilia	1.1	7.6 ± 1.1	1.1 ± 1.1	0.08 ± 0.03	0.99 ± 0.02	
Double Weibull model	**RMSE**	**Log N_0 (CFU/mL)**	**δ_1 (min)**	**δ_2 (min)**	**α**	**p**
OXONE						
A. calcoaceticus	0.92	7.2 ± 0.9	7.6 ± 7.6	NQ	7.2 ± 6.0	0.88 ± 0.40
S. maltophilia	0.82	7.4 ± 0.8	9.3 ± 5.9	NQ	7.5 ± 1.9	1.2 ± 0.5

Concerning the action of OXONE, the time for the first log reduction - δ_1, was similar for both *A. calcoaceticus* and *S. maltophilia*. However, the parameter p for *A. calcoaceticus* (0.88 ± 0.40) and *S. maltophilia* (1.2 ± 0.5) defined different shapes of the inactivation curves. For *A. calcoaceticus,* the $p < 1$ produced a convex shape to the first part of the inactivation curve (**Figure 4-2** OXONE). For *S. maltophilia,* the $p > 1$ caused a concave shape to the first part of the inactivation curve (**Figure 4-3** OXONE). A deeper analysis of this parameter indicates that *A. calcoaceticus* ($p < 1$) bacterial cells became more tolerant to OXONE during the inactivation process, while *S. maltophilia* ($p > 1$) bacterial cells became more susceptible over time.

Comparing the goodness of fit of the different kinetic models on the experimental data set, the double Weibull model showed to be more appropriable to the inactivation of *A. calcoaceticus* and *S. maltophilia* by OXONE (RMSE < 1). The RMSE values of the double Weibull model were lower than those obtained when applying the biphasic model to the inactivation of both bacteria by NaDCC and TCCA (RMSE > 1). Meireles et al. (2017) conducted a study to evaluate the antimicrobial effects of different chlorine-based disinfectants against *E. coli*. The inactivation curves of NaOCl, neutral electrolyzed oxidizing water, ClO_2, and NaDCC were fitted to the Gompertz model (Gompertz, 1825) to determine the time-kill kinetic parameters: k_{CFU}, the maximum antimicrobial rate, and λ_{CFU}, the lag time for antimicrobial action evaluated by log CFU/mL decrease. In planktonic cultures, NaOCl demonstrated to be the fastest disinfectant causing antimicrobial action, with the shortest λ_{CFU} (2.5 to 13 min). NaDCC was the disinfectant requiring higher time (48 to 72 min) to promote log CFU/mL decrease. On the other hand, NaDCC and ClO_2 had the highest antimicrobial rates.

4.1.3 Effects on bacterial cytoplasmic membrane integrity

PI uptake was determined to assess the effects of NaDCC, TCCA, and OXONE on cytoplasmic membrane integrity (**Table 4-3**). The disinfectants were tested at MBC and sub-lethal concentrations. PI is commonly used as an indicator of cytoplasmic membrane integrity because it is a nucleic acid stain to which the cell membrane is usually impermeable (Abreu et al., 2013; Borges et al., 2013; Simões et al., 2007).

Table 4-3 – Permeability of *A. calcoaceticus* and *S. maltophilia* to PI (%) after 30 min of exposure to NaDCC, TCCA, and OXONE at sub-lethal concentration and MBC.

	PI-stained cells (%)	
	A. calcoaceticus	*S. maltophilia*
Control	9.3 ± 8.9	4.1 ± 6.9
NaDCC sub-lethal conc.	100 ± 0.0	100 ± 0.1
MBC	100 ± 0.0	100 ± 0.0
TCCA sub-lethal conc.	41 ± 25	58 ± 21
MBC	99 ± 3	100 ± 0.2
OXONE sub-lethal conc.	99 ± 1	97 ± 8
MBC	100 ± 0	100 ± 0.0

Table 4-3 shows that all disinfectants caused significant changes in the permeability of *A. calcoaceticus* and *S. maltophilia* to PI ($P < 0.05$), even at sub-lethal concentrations. The incubation with NaDCC and OXONE at MBC for 30 min promoted 100% of PI uptake in both bacteria. A 100% PI uptake was also observed after *S. maltophilia* exposure to TCCA at MBC. OXONE at sub-lethal concentrations also caused a high percentage of membrane damage ($P < 0.05$), with 99 ± 1% PI uptake for *A. calcoaceticus* and 97 ± 8% PI uptake for *S. maltophilia*. The lowest percentages of PI uptake were obtained after exposure to TCCA at sub-lethal concentrations ($P < 0.05$), with 41 ± 25%

PI uptake for *A. calcoaceticus* and 58 ± 21% PI uptake for *S. maltophilia*. The analysis of the results allowed to conclude that NaDCC, TCCA, and OXONE triggered cytoplasmic membrane destabilization, even at sub-lethal concentrations that only caused a 3 to 4 log reduction of bacterial culturability. As chlorine-based disinfectants, NaDCC and TCCA cause cytoplasmic membrane destabilization due to the physiological changes resulting from chlorination. Haas and Engelbrecht (1980) also demonstrated that the cell membrane is affected as a result of exposure to chlorine.

Complementary, the study of the selected disinfectants at MBC and sub-lethal concentrations was performed on the physical and chemical characteristics of *A. calcoaceticus* and *S. maltophilia* membranes (**Table 4-4** and **Table *4-5***). Despite the significant damages caused by the selected disinfectants on bacterial membranes (**Table 4-3**), in general, no significant alteration was observed in bacterial hydrophobicity, surface tension, and ability to accept and donate electrons. Statistically significant alterations were only found for TCCA, curiously the less effective on membrane damage (lower PI uptake). TCCA reduced *A. calcoaceticus* ability to donate electrons and reduced the polar component of *S. maltophilia* as well as increased *S. maltophilia* hydrophobicity.

Table 4-4 – Hydrophobicity ΔG_{sws} and surface tension parameters (γ^{LW} Lifshitz-van der Waals, γ^{AB} Lewis acid-base, γ^{+} electron acceptor and γ^{-} electron donor components) of *A. calcoaceticus* after exposure to disinfectants for 30 min. * Represents statistically significant differences ($P < 0.05$) in comparison to the control sample.

	Surface tension parameters (mJ/m^2)				**ΔG_{sws} (mJ/m^2)**
	γ^{LW} (apolar)	**γ^{AB} (polar)**	**γ^{+}**	**γ^{-}**	
Control	37.8 ± 1.2	4.8 ± 1.6	0.1 ± 0.1	48.7 ± 8.0	31.3 ± 9.9
NaDCC sub-lethal conc.	39.4 ± 2.8	0.0 ± 0.0	0.0 ± 0.0	39.1 ± 4.9	18.9 ± 6.4
MBC	40.1 ± 2.0	0.0 ± 0.0	0.0 ± 0.0	35.5 ± 1.0	12.8 ± 2.8
TCCA sub-lethal conc.	40.5 ± 1.6	0.7 ± 0.7	0.0 ± 0.0	**25.2 ± 1.3***	-5.8 ± 3.2
MBC	41.0 ± 1.3	4.5 ± 0.4	0.1 ± 0.1	38.7 ± 3.6	16.4 ± 6.8
OXONE sub-lethal conc.	41.2 ± 0.7	0.0 ± 0.0	0.0 ± 0.0	48.9 ± 6.6	32.4 ± 9.9
MBC	40.5 ± 1.3	0.0 ± 0.0	0.0 ± 0.0	43.7 ± 6.5	17.1 ± 2.3
Free chlorine sub-lethal conc.	38.1. ± 1.8	3.8 ± 5.3	0.5 ± 0.7	29.5 ± 9.0	19.7 ± 26.0
MBC	35.4 ± 1.7	0.6 ± 0.6	0.0 ± 0.0	44.1 ± 3.6	27.5 ± 5.9

Table 4-5 – Hydrophobicity ΔG_{sws} and surface tension parameters (γ^{LW} Lifshitz-van der Waals, γ^{AB} Lewis acid-base, γ^{+} electron acceptor and γ^{-} electron donor components) of *S. maltophilia* after exposure to disinfectants for 30 min. * Represents statistically significant differences ($P < 0.05$) in comparison to the control sample.

	Surface tension parameters (mJ/m^2)				**ΔG_{sws} (mJ/m^2)**
	γ^{LW} (apolar)	**γ^{AB} (polar)**	γ^{+}	γ^{-}	
Control	42.0 ± 0.3	10.6 ± 1.5	1.2 ± 0.5	31.4 ± 9.0	-6.7 ± 4.8
NaDCC sub-lethal conc.	42.1 ± 0.2	4.2 ± 1.4	0.1 ± 0.1	32.6 ± 0.7	5.7 ± 0.9
MBC	41.8 ± 0.2	6.7 ± 0.8	0.4 ± 0.2	28.7 ± 5.0	-5.8 ± 5.6
TCCA sub-lethal conc.	42.3 ± 0.3	6.9 ± 0.5	0.4 ± 0.1	35.8 ± 4.3	15.9 ± 1.1
MBC	42.1 ± 0.1	**0.0 ± 0.0***	0.0 ± 0.0	43.3 ± 0.0	**24.4 ± 0.1***
OXONE sub-lethal conc.	42.8 ± 0.2	6.2 ± 1.1	0.3 ± 0.1	35.2 ± 2.0	9.0 ± 3.3
MBC	42.1 ± 0.2	9.0 ± 0.9	0.7 ± 0.0	34.0 ± 7.7	15.1 ± 9.2
Free chlorine sub-lethal conc.	42.0 ± 0.5	5.8 ± 3.3	0.7 ± 0.5	35.4 ± 2.3	10.0 ± 3.0
MBC	41.8 ± 0.3	7.1 ± 2.1	0.6 ± 0.3	27.1 ± 7.3	-12.8 ± 3.0

4.1.4 Effects on 48 h-old *A. calcoaceticus* and *S. maltophilia* biofilms

The 48 h-old single-species biofilms on PVC and SS were exposed for 30 min to NaDCC, TCCA, OXONE, and free chlorine at MBC of each disinfectant against *A. calcoaceticus* and *S. maltophilia*. Then, disinfectants were evaluated in terms of biofilm culturability (**Figure 4-4**) and removal (**Figure 4-5**). *A. calcoaceticus* and *S. maltophilia* formed biofilms regardless of the substrata. Comparing the results of CFU numbers in the control of biofilms (**Figure 4-4**), *A. calcoaceticus* and *S. maltophilia* had similar numbers of log CFU/cm^2 on PVC ($P > 0.05$): 7.5 ± 0.2 and 7.4 ± 0.1 log, respectively. On the other hand, a significant statistical difference was observed between *A. calcoaceticus* and *S. maltophilia* biofilms on SS, with a higher value of log CFU/cm^2 for *A. calcoaceticus* (7.8 ± 0.1) than for *S. maltophilia* (7.3 ± 0.2) ($P < 0.05$). Concerning the results of total cells (**Figure 4-5**), *A. calcoaceticus* formed biofilms with higher cell densities than *S. maltophilia* for both substrata ($P < 0.05$). On SS, *A. calcoaceticus* formed biofilms with 8.8 ± 0.2 log cells/cm^2 and *S. maltophilia* with 8.1 ± 0.3 log cells/cm^2. On PVC, the *A. calcoaceticus* cell density was 8.5 ± 0.3 log cell/cm^2 and for *S. maltophilia* was 8.0 ± 0.2 log cell/cm^2. Conversely, in another study, S. *maltophilia* developed a higher number of log CFU/cm^2 on PVC than *A. calcoaceticus*, in both single and dual-species of 24 h-old biofilms (Gomes et al., 2016). The significant differences in experimental conditions, particularly the distinct growth media and nutrient availability, may justify these non-consensual results. In adhesion assays, *A. calcoaceticus* produced higher biomass on SS and PVC than *S. maltophilia* (Simões et al., 2007a). In the present study, the action of the disinfectants was tested against single-species biofilms formed by the selected DW bacteria on two representative pipe materials from DW networks, using the microtiter

plates as a reactor system. Although several other devices try to mimic the conditions found in real pipe networks, microtiter plates allowed to form biofilms with CFU and cell densities closer to the levels reported within DWDS, generally in the order of 10^6 CFU/cm^2 and 10^7 cells/cm^2 (Långmark et al., 2005; Olson and Nagy, 1984; Pedersen, 1990).

In terms of culturability (**Figure 4-4**), biofilm exposure to the selected disinfectants for 30 min promoted a decrease in the CFU levels up to a 4 log reduction ($P < 0.05$). *A. calcoaceticus* biofilms were more susceptible to the action of disinfectants than those of *S. maltophilia*, oppositely to the results obtained for the planktonic state. In Gomes et al. (2016), *A. calcoaceticus* formed biofilms more susceptible to NaOCl than those of *S. maltophilia*. Independently of the surface material, the exposure of *A. calcoaceticus* biofilms to OXONE at 690 mg/L caused approximately 4 log reduction in culturability, presenting the best disinfection action in comparison to free chlorine, NaDCC and TCCA ($P < 0.05$). The treatment with NaDCC at 3.1 mg/L and TCCA at 3.8 mg/L caused 1 and 2 log reduction in the CFU values of *A. calcoaceticus* biofilms, respectively ($P < 0.05$), regardless of the surface material. Moreover, these disinfectants allowed a significant statistical reduction of the CFU levels of *A. calcoaceticus* biofilms on SS than with the exposure to free chlorine ($P < 0.05$). The analysis of the effects on *S. maltophilia* biofilms revealed that the treatment with OXONE at 340 mg/L caused a culturability reduction significantly higher than free chlorine and NaDCC on both SS and PVC ($P < 0.05$). The highest CFU reduction of *S. maltophilia* biofilms was 2 log after the treatment with OXONE in biofilms formed on SS. The exposure to free chlorine at 0.8 mg/L, NaDCC at 2.1 mg/L, and TCCA at 2.5 mg/L caused 1 log reduction in the CFU values of *S. maltophilia* biofilms on both surface materials ($P < 0.05$). In general, the alternative

disinfectants were equally effective or better than the action of free chlorine, in terms of culturability reduction.

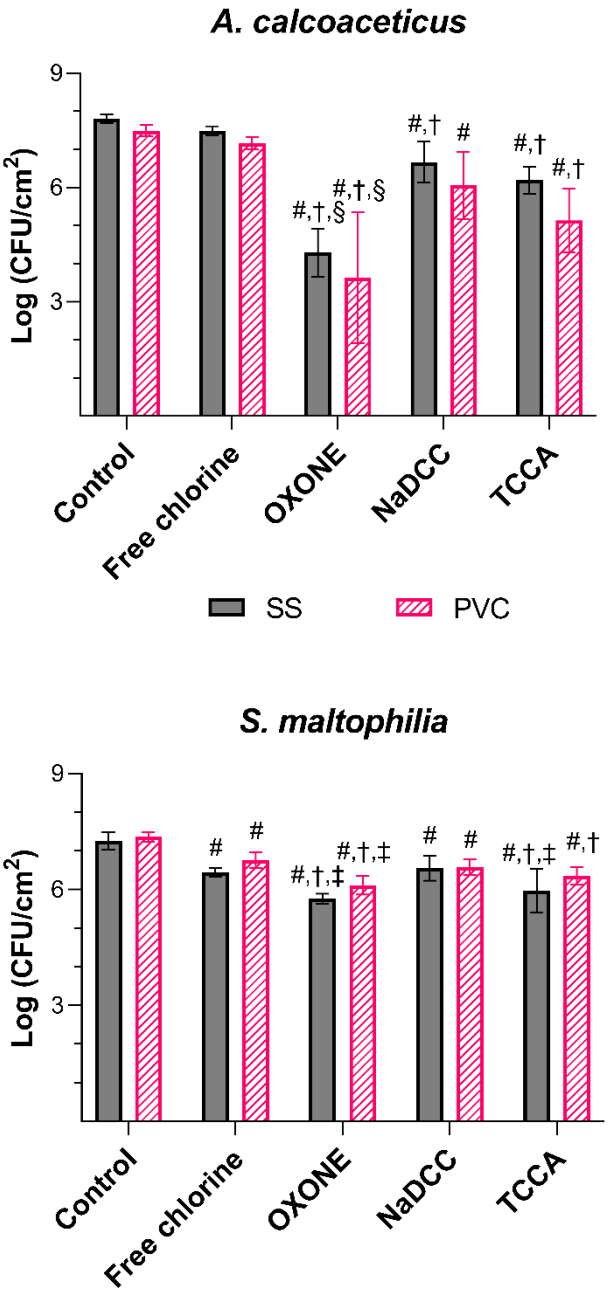

Figure 4-4 – Log CFU/cm^2 of 48 h-old *A. calcoaceticus* and *S. maltophilia* biofilms formed on SS (solid-grey bars) and PVC (patterned bars) coupons after 30 min exposure to NaDCC, TCCA, OXONE, and free chlorine at MBC. The MBC against *A. calcoaceticus* and *S. maltophilia* were, respectively, 1.0 and 0.80 mg/L for free chlorine, 690 and 340 mg/L for OXONE, 3.1 and 2.1 mg/L for NaDCC, 3.8 and 2.5 mg/L for TCCA. # Indicates statistically significant differences to control/unexposed biofilms. † Indicates statistically significant differences to biofilms exposed to free chlorine. § Indicates statistically significant differences to biofilms exposed to NaDCC or TCCA. ‡ Indicates statistically significant differences to biofilms exposed to NaDCC.

The analysis of the results of total cells (**Figure 4-5**) revealed that despite the effectiveness of the selected disinfectants on bacterial inactivation, the biofilms were generally resistant to removal. Indeed, the log cells/cm^2 levels in *S. maltophilia* biofilms after exposure to disinfectants were generally not statistically different from the control samples ($P > 0.05$). In the case of *A. calcoaceticus* biofilms, all disinfectants caused a decrease in the number of total cells ($P < 0.05$), except free chlorine at 1.0 mg/L against biofilms formed on SS. However, the selected disinfectants only allowed a modest biofilm removal, with values below 1 log. The highest level of biofilm removal was obtained for *A. calcoaceticus* biofilms on SS after exposure to OXONE at 690 mg/L with a 0.6 log removal ($P < 0.05$). Moreover, this condition had a better action on biofilm removal than free chlorine, NaDCC, or TCCA ($P < 0.05$). The biofilm resistance to removal by the selected disinfectants is similar to a previous comparative study of oxidizing disinfectants against *S. aureus* dry-surface biofilms (Chowdhury et al., 2019). Among other disinfectants, biofilms were treated for 5 min with chlorine-based products, which included Chlorclean, a tableted hospital-grade disinfectant containing NaDCC formulated with sodium toluenesulfonate (a foaming anionic surfactant) and adipic acid, and an unformulated NaDCC tablet, both at an equivalent concentration of 1000 mg/L chlorine (Chowdhury et al., 2019). A 2.8 log reduction in biofilm culturability was observed, but the efficacy of these products on biofilm protein removal was limited to < 30% (Chowdhury et al., 2019).

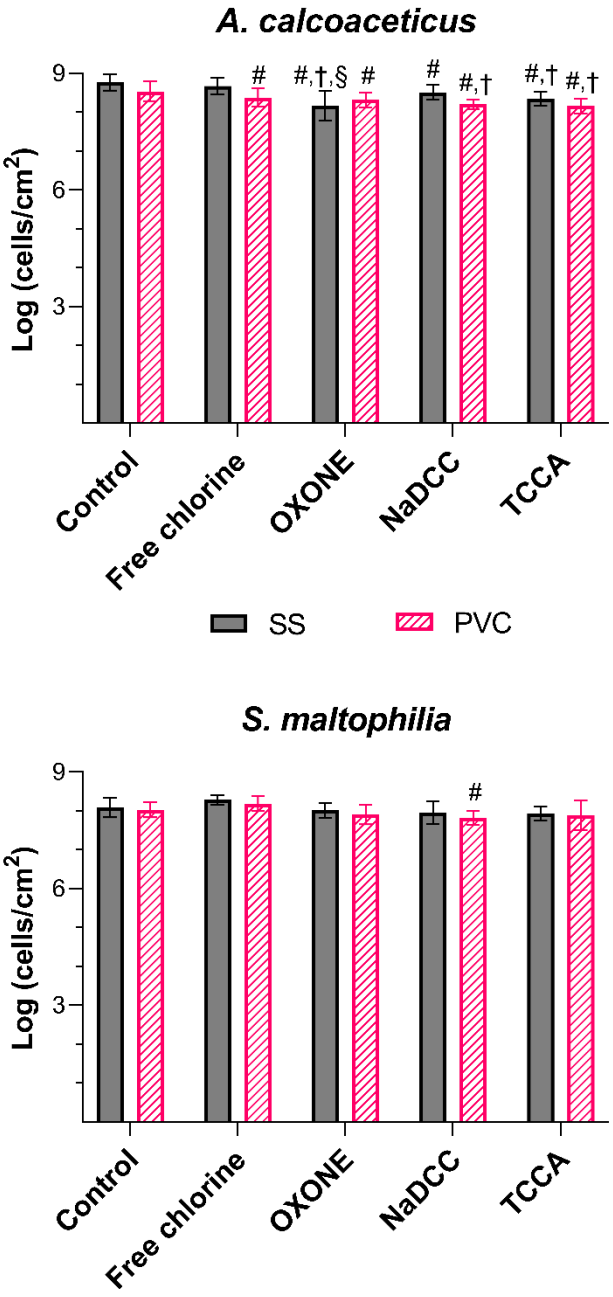

Figure 4-5 – Log cells/cm^2 of 48 h-old *A. calcoaceticus* and *S. maltophilia* biofilms formed on SS (solid-grey bars) and PVC (patterned bars) coupons after 30 min exposure to NaDCC, TCCA, OXONE, and free chlorine at MBC. The MBC against *A. calcoaceticus* and *S. maltophilia* were, respectively, 1.0 and 0.80 mg/L for free chlorine, 690 and 340 mg/L for OXONE, 3.1 and 2.1 mg/L for NaDCC, 3.8 and 2.5 mg/L for TCCA. # Indicates statistically significant differences to control/unexposed biofilms. † Indicates statistically significant differences to biofilms exposed to free chlorine. § Indicates statistically significant differences to biofilms exposed to NaDCC or TCCA.

There are few reports concerning the action of NaDCC, TCCA, and OXONE against biofilms. Farkas et al. (2014) compared the action of NaDCC and NaOCl against 90 days-

old biofilms on polypropylene coupons grown in a DW facility. After 2 h of exposure, none of the disinfectants was able to completely inactivate the opportunistic pathogens and faecal bacteria present in the biofilms. NaDCC was modestly more effective than NaOCl in biofilm control. This higher efficacy of NaDCC in comparison to NaOCl was verified by Yu et al. (2013) against *P. aeruginosa* biofilms grown on polyamide reverse osmosis membranes. In the present study, OXONE was found to be the best disinfectant with antimicrobial activity against both *A. calcoaceticus* and *S. maltophilia* biofilms. It caused a 2 to 4 log reduction in the biofilm culturability, although in the dose-response relationship from the experiments with planktonic bacteria OXONE was classified as the lowest efficient. Aarnisalo et al. (2000) showed that two potassium persulfate-based disinfectants promoted 5 log CFU/cm^2 reduction against three *Listeria monocytogenes* strains after 5 min of exposure, while NaDCC and NaOCl caused 2.2 and 1.5 log reduction, respectively. These results propose that OXONE might be of significance to control both Gram-negative and Gram-positive bacteria.

4.2 Conclusions

The antimicrobial and antibiofilm action of NaDCC, TCCA, and OXONE was extensively analysed. In sum, the dose-response analysis with planktonic cells demonstrated that *S. maltophilia* was more susceptible than *A. calcoaceticus* to the disinfectants tested and that their efficiency can be ranked as follows: free chlorine > NaDCC > TCCA > OXONE. Time-response evaluation demonstrated that NaDCC and TCCA had similar inactivation rates against both bacteria. The values of the parameter *f* equal or close to 1, indicated that both *A. calcoaceticus* and *S. maltophilia* were similarly susceptible to both disinfectants. Moreover, OXONE was able to inactivate 90% of both

bacterial populations after 10 minutes. However, *S. maltophilia* became more susceptible to OXONE during the disinfection process, while the opposite was observed for *A. calcoaceticus*. The selected disinfectants triggered significant bacterial cytoplasmic membrane destabilization, even at sub-lethal concentrations.

NaDCC, TCCA, and OXONE had similar or better efficiencies in reducing biofilm culturability than free chlorine, with reductions up to 4 log. OXONE was the most efficient disinfectant in causing the inactivation of both bacterial biofilms. It had the best performance against biofilms regardless of the surface material, with 2 to 4 log CFU/cm^2 reduction. However, biofilm removal was invariably modest (always < 1 log), for all the biofilms tested and disinfectants applied.

Chapter 5

The impact of OXONE and chlorinated cyanurates on *S. maltophilia* biofilms: effects on biofilm control, regrowth and mechanical properties

The main purpose of the present chapter was to elucidate the action of OXONE and chlorinated isocyanurates against biofilms, particularly their effects on the structure and mechanical properties. The effects of the selected disinfectants in the prevention of biofilm regrowth after disinfection were also evaluated. The activity of NaDCC, TCCA, and OXONE was compared to the action of free chlorine that was used as reference DW disinfectant. *S. maltophilia* was selected for this study since, in the previous study, its biofilms were more tolerant to the selected disinfectants than *A. calcoaceticus* biofilms.

5.1 Results and Discussion

5.1.1 Biofilm control and regrowth after disinfection

The effects of NaDCC, TCCA, OXONE, and free chlorine on biofilm culturability and total cells of 48 h-old *S. maltophilia* biofilms after 30 min exposure to the disinfectants at 10 × MBC are represented in **Figure 5-1 (a)** and **Figure 5-2 (a)**, respectively. *S. maltophilia* formed biofilms regardless of the surface material (SS or PVC), with CFU and cell densities approximately equal to the levels reported within DWDS, usually with approximately 10^6 CFU/cm^2 and 10^7 cells/cm^2 (Långmark et al., 2005; Olson and Nagy, 1984; Pedersen, 1990). The unexposed biofilms presented values of 7.2 ± 0.3 and 7.2 ± 0.1 log CFU/cm^2 on SS and PVC, respectively. The exposure to the selected disinfectants promoted a reduction in biofilm culturability up to 7 log ($P < 0.05$). The highest log reductions were obtained for biofilms on SS with exposure to OXONE, NaDCC and TCCA (7, 5, and 7 log reduction, respectively) and for biofilms on PVC with exposure to TCCA (6 log reduction). The biofilms on SS and PVC exposed to free chlorine and biofilms on PVC exposed to NaDCC and OXONE presented reductions in culturability between 2 and 4 log. Noteworthy, the action of OXONE, NaDCC, and TCCA against biofilms on SS was significantly more effective in reducing the biofilm culturability than the action of free chlorine ($P < 0.05$), which showed a reduction in biofilm culturability in the order of 2 log. Additionally, for biofilms on SS, the reduction of biofilm culturability was significantly more effective with the exposure to OXONE and TCCA than the exposure to NaDCC ($P < 0.05$). For biofilms on PVC, the action of TCCA was significantly more effective in reducing the biofilm culturability than the action of free chlorine and NaDCC ($P < 0.05$). However, regarding the effects on total cells, the biofilms exposed to the disinfectants presented cell densities in the same

magnitude of the unexposed biofilms, with approximately 8 log cells/cm^2, suggesting that these disinfectants were able to inactivate a significant number of sessile bacteria on SS and PVS but were not able to remove bacteria from the surface.

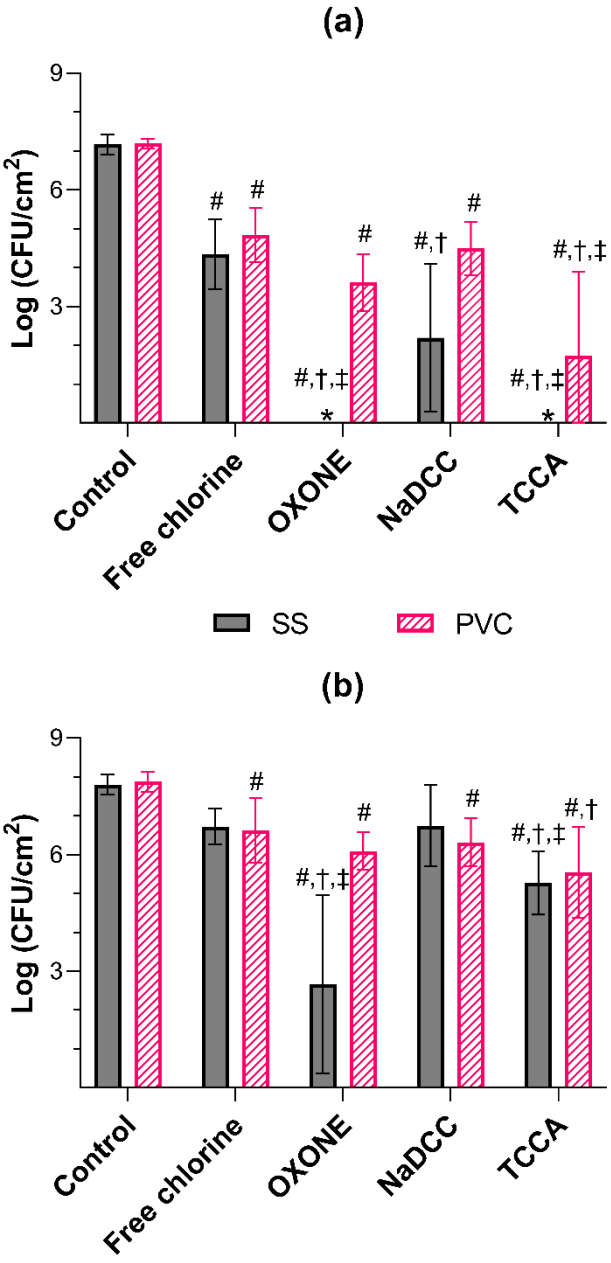

Figure 5-1 – The effects of free chlorine, OXONE, NaDCC and TCCA at 10 × MBC on the culturability of 48 h-old *S. maltophilia* biofilms formed on SS (solid-grey bars) and PVC (patterned bars) coupons. (**a**) After biofilm exposure to the selected disinfectants for 30 min. (**b**) Regrowth for 24 h of biofilms previously exposed to the selected disinfectants for 30 min. * Below the detection limit of 2.7 log CFU/cm^2. # Indicates statistically significant differences to control/unexposed biofilms. † Indicates statistically significant differences to biofilms exposed to free chlorine. ‡ Indicates statistically significant differences to biofilms exposed to NaDCC.

To examine the impact of biofilm exposure to the selected disinfectants on regrowth, the biofilms were incubated for 24 h with nutrient repositioning after the chemical treatment. The results of log CFU/cm^2 and log cells/cm^2 are shown in **Figure 5-1 (b)** and **Figure 5-2 (b)**, respectively. The exposure to the selected disinfectants did not prevent biofilm regrowth when compared with the results immediately after chemical exposure (**Figure 5-1 (a)**) and 24 h after biofilm regrowth (**Figure 5-1 (b)**). However, the regrown biofilms on SS and PVC previously exposed to OXONE and TCCA presented numbers of log CFU/cm^2 statistically significantly lower than the biofilms unexposed to the disinfectants ($P < 0.05$). For the regrown biofilms previously exposed to NaDCC, a statistically significant difference in comparison to the unexposed biofilms was only obtained for biofilms formed on PVC ($P < 0.05$) with a 2 log difference. The exposure to OXONE promoted the best efficacy in limiting biofilm regrowth on SS, with 5 log difference in comparison to the unexposed biofilms ($P < 0.05$), and 4 log difference in comparison to the biofilms exposed to free chlorine or NaDCC ($P < 0.05$). Regardless of the surface material used, the regrown biofilms previously exposed to TCCA presented a difference in biofilm culturability in the order of 2 log in comparison to the unexposed biofilms ($P < 0.05$) and a difference in the order of 1 log in comparison to the biofilms exposed to free chlorine ($P < 0.05$). Regarding the quantification of total cells, independently from the tested conditions, had a cellular density of approximately 8 log cells/cm^2, with a log difference less than 0.6 log in comparison to the unexposed biofilms.

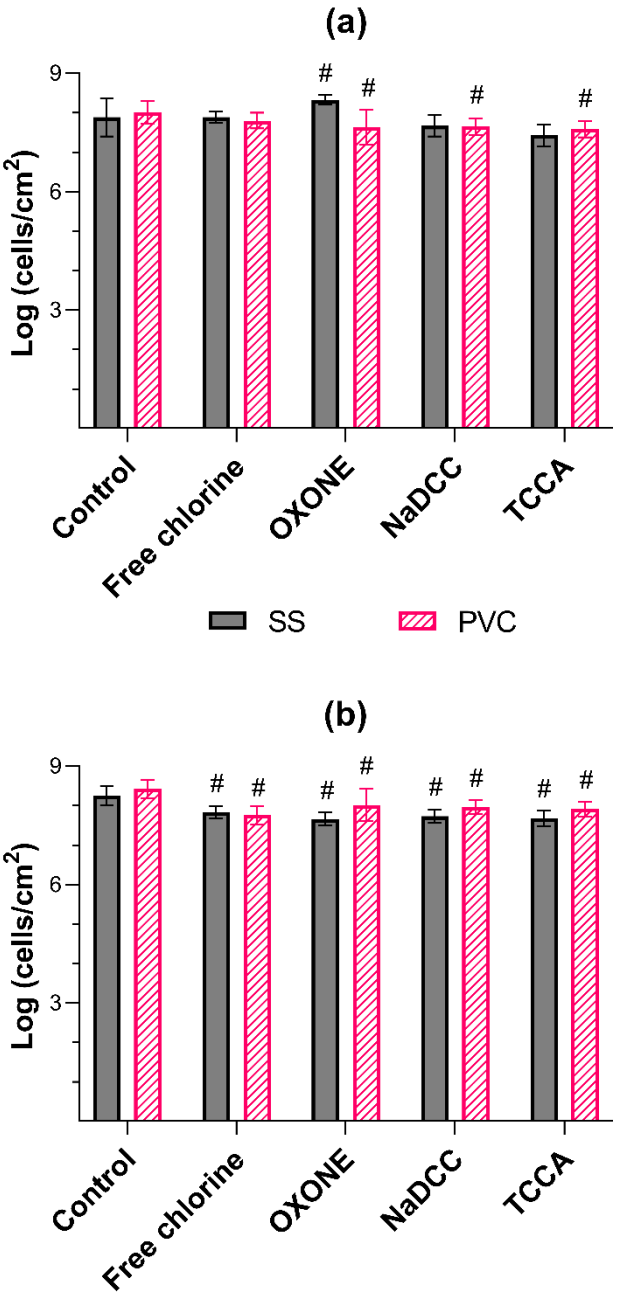

Figure 5-2 – The effects of free chlorine, OXONE, NaDCC and TCCA at 10 × MBC on the total cells of 48 h-old *S. maltophilia* biofilms formed on SS (solid-grey bars) and PVC (patterned bars) coupons. (**a**) After biofilm exposure to the selected disinfectants for 30 min. (**b**) Regrowth for 24 h of biofilms previously exposed to the selected disinfectants for 30 min. # Indicates statistically significant differences to control/unexposed biofilms.

Regrowth events can impact the quality of DW because it is associated with the proliferation of bacteria within the DWDS, particularly at the pipe walls and consequently in the bulk water (Camper, 1994). Even with the application of disinfection measures, the

remaining biofilm-associated bacteria after disinfectant exposure can recover and recolonise the DW network (Fish and Boxall, 2018). Additionally, the development of highly resilient biofilms, which include iron-associated and tolerant bacteria to oxidants, is known to be selected by high-chlorine regimes (Fish et al., 2020; Fish and Boxall, 2018).

The 48 h-old *S. maltophilia* biofilms were resistant to removal, given the similar cell densities observed between the unexposed and exposed biofilms to the selected disinfectants. This phenomenon is in accordance with previous studies that also reported biofilm resistance to removal (Chowdhury et al., 2019; Gomes et al., 2016). A 5 min treatment with chlorine-based products at an equivalent concentration of 1000 mg/L chlorine promoted a 2.8 log reduction in culturability of *S. aureus* biofilms, but the removal of biofilm mass was less than 30% (Chowdhury et al., 2019). The disinfection of 24 h-old *S. maltophilia* biofilms on PVC with NaOCl at 0.5 and 175 mg/L for 30 min resulted in a 2.1 log CFU/cm^2 reduction and total CFU reduction, respectively (Gomes et al., 2016). However, the biofilm removal was only up to 0.5 log in the number of total cells (Gomes et al., 2016). The exposure of 48 h-old *A. calcoaceticus* biofilms formed on PVC or SS to TCCA at 3.8 mg/L and OXONE at 690 mg/L for 30 min caused approximately 2 and 5 log CFU/cm^2 reduction, respectively, yet the decrease in the number of total cells was below 1 log (**subsection 4.1.4**).

In the present work, NaDCC, TCCA, and OXONE proved to be efficient in *S. maltophilia* inactivation with biofilm culturability reduction up to 7 log after 30 min of disinfectant exposure. Events of biofilm regrowth were observed in the subsequent 24 h, under more favourable conditions: without chemical stress and with nutrient availability. Nevertheless, the regrown biofilms on SS previously exposed to OXONE showed notably less biofilm culturability than the unexposed biofilms or the biofilms previously exposed

to free chlorine ($P < 0.05$), with a CFU difference up to 5 log. In spite of the fact that the free chlorine concentration used in the present work (8 mg/L) was above the guideline value of chlorine for the use in water treatment or materials in contact with DW that is of health significance (WHO, 2022).

The effects of the selected disinfectants on biofilms can be related to their different chemical structure and mode of action. NaDCC and TCCA are chlorine-based disinfectants that in water rapidly provide an equilibrium between cyanuric acid and the dissociation products, which includes free chlorine in the form of hypochlorous acid (HOCl) and chlorinated cyanurates (Wahman, 2018). The principal microbicidal activity is attributed to the oxidizing action of HOCl (E^0 =1.48 V), unlike chlorinated cyanurates that have minimal disinfecting efficiency (Clasen and Edmondson, 2006; Fukuzaki, 2006; Wahman, 2018). The advantage of the use of NaDCC and TCCA instead of NaOCl or $Ca(OCl)_2$ is that chlorinated cyanurates act as a reservoir of free chlorine until the total available is depleted (Clasen and Edmondson, 2006). OXONE is a potassium salt of peroxymonosulphate with a strong oxidizing action via two-electron reduction $E^0(HSO_5^-/SO_4^{2-})$ = 1.85 V_{NHE} and decomposition into sulphate and hydroxyl radicals by cleaving the peroxide bond in the persulphate molecule [$E^0(SO_4^{\bullet-}/ SO_4^{2-})$ = 2.60 – 3.10 V_{NHE}; $E^0(^{\bullet}OH / OH^-)$ = 1.90 – 2.70 V_{NHE}] (Lee et al., 2020; Liu et al., 2021; Wacławek et al., 2017). Although OXONE was the lowest efficient disinfectant in a dose-response relationship from planktonic experiments, given the higher value of MBC than for free chlorine, NaDCC, and TCCA (**subsection 4.1.1**), it allowed the best inactivation of bacterial biofilms. The action of OXONE against biofilms may be due to its effects on the EPS coupled with its antimicrobial activity. Accordingly, a possible more pronounced alteration of the biofilm matrix properties than the effects of other disinfectants can expose the biofilm embedded cells to chemical stress and limit their capability to recover.

In the present work, the selected disinfectants were generally more efficient against biofilms formed on SS than on PVC. Even though the number of culturable cells and the cellular densities were similar in biofilms formed on both materials, the different susceptibility could be related to distinct characteristics of the biofilms formed on SS and PVC. It is known that the surface material influences biofilm characteristic, such as biomass, bacterial composition, and biofilm structure (Learbuch et al., 2021; Rożej et al., 2015; Yan et al., 2022), which may be the cause for different responses to disinfection processes. In addition, the chemical reactions of disinfectants with pipe materials and biofilms on the pipe surface are known to be affected by the type of pipe materials (Hallam et al., 2002; Li et al., 2019).

5.1.2 Effects on mechanical properties and structure of biofilms

To evaluate the changes in the viscoelastic properties of biofilms resulting from the 30 min exposure to the selected disinfectants, rheometry analysis was performed using 48 h-old colony *S. maltophilia* biofilms (see **Annex C** – characterization of colony biofilms). The results of oscillatory strain sweeps and oscillatory frequency sweeps are presented in **Figure 5-3**, **Figure 5-4**, **Figure 5-5** and **Table 5-1**.

The first step taken to characterize the viscoelastic behaviour of biofilms was the measurement of oscillatory strain sweeps, which established the extent of the biofilm viscoelastic linearity (Gloag et al., 2018; Rosalina and Bhattacharya, 2002). The shear strain increased from 0.01-1000% at a constant frequency of 1 Hz, and the elastic and viscous behaviour of the biofilms were recorded as the storage (G') and loss (G'') moduli, respectively. However, only for the control/unexposed biofilms it was possible to reach values of shear strain higher than 10%, with crossover point G' = G'' at approximately

240% of shear strain (**Figure 5-3**). For the other conditions, the experimental values of G' and G'' were recorded up to 10% of shear strain, the maximum value where it was guaranteed that the biofilm samples completely covered the parallel plates of the rheometer without network rupture of the biofilms under consideration.

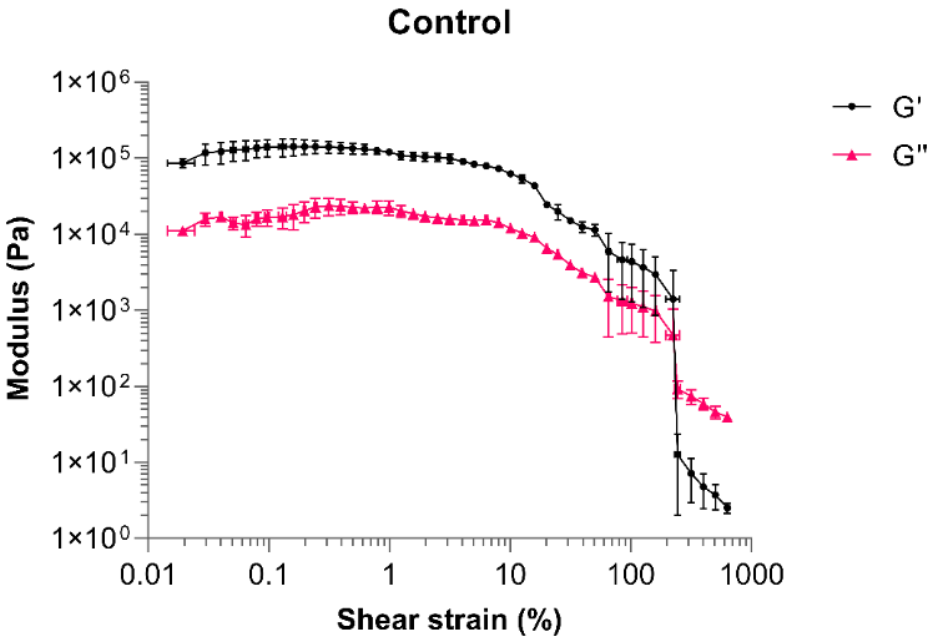

Figure 5-3 – Oscillatory strain sweeps performed on control/unexposed biofilms. The shear strain increased from 0.01-1000% at a constant frequency of 1 Hz. Crossover point G'=G'' at approximately 240% of shear strain.

The linear viscoelastic region (LVR) of the biofilms ranged from 0.02 to 0.8% (**Figure 5-4**), where the deformation of the samples was within the non-destructive deformation limits. Independently of the disinfectant used, the *S. maltophilia* biofilms displayed values of elastic shear modulus (G') approximately 10 times larger than the viscous shear modulus (G'') (**Figure 5-4 (a)**). Therefore, *S. maltophilia* biofilms showed a rheological character reflective of gel-like or solid structure and can be defined as viscoelastic solid materials (Gloag et al., 2018; Kavanagh and Ross-Murphy, 1998; Yan et al., 2018). This is a consequence of the links inside the biofilm matrix, such as chemical

bonds or physical-chemical interactions, that contributed to the solid-state behaviour of the biofilms (Horvat et al., 2019; Jara et al., 2021; Pandit et al., 2020).

The analysis of the complex shear modulus (G*) (**Table 5-1**), which gives a comparative stiffness degree of the materials, revealed a significant decrease in the physical robustness of biofilms after exposure to free chlorine and OXONE ($P < 0.05$). The G* value of control/unexposed biofilms was 140 ± 29 kPa, whereas the G* values for biofilms exposed to free chlorine and OXONE were 104 ± 70 kPa and 69 ± 21 kPa, respectively. Remarkably, the exposure to OXONE promoted a better G* value reduction of *S. maltophilia* biofilms than the exposure to free chlorine ($P < 0.05$). Indeed, these results demonstrated that OXONE could modify the stiffness of the *S. maltophilia* biofilms, weakening its cohesiveness.

Table 5-1 – Complex shear modulus (G*) of 48 h-old *S. maltophilia* colony biofilms after 30 min exposure to free chlorine, NaDCC, TCCA, and OXONE at 10 × MBC. # Indicates statistically significant differences to control/unexposed biofilms. † Indicates statistically significant differences to biofilms exposed to free chlorine.

Disinfectants	**Complex shear modulus (G*, kPa)**
Control	140 ± 29
Free chlorine	104 ± 70[#]
NaDCC	147 ± 51
TCCA	139 ± 65
OXONE	69 ± 21[# †]

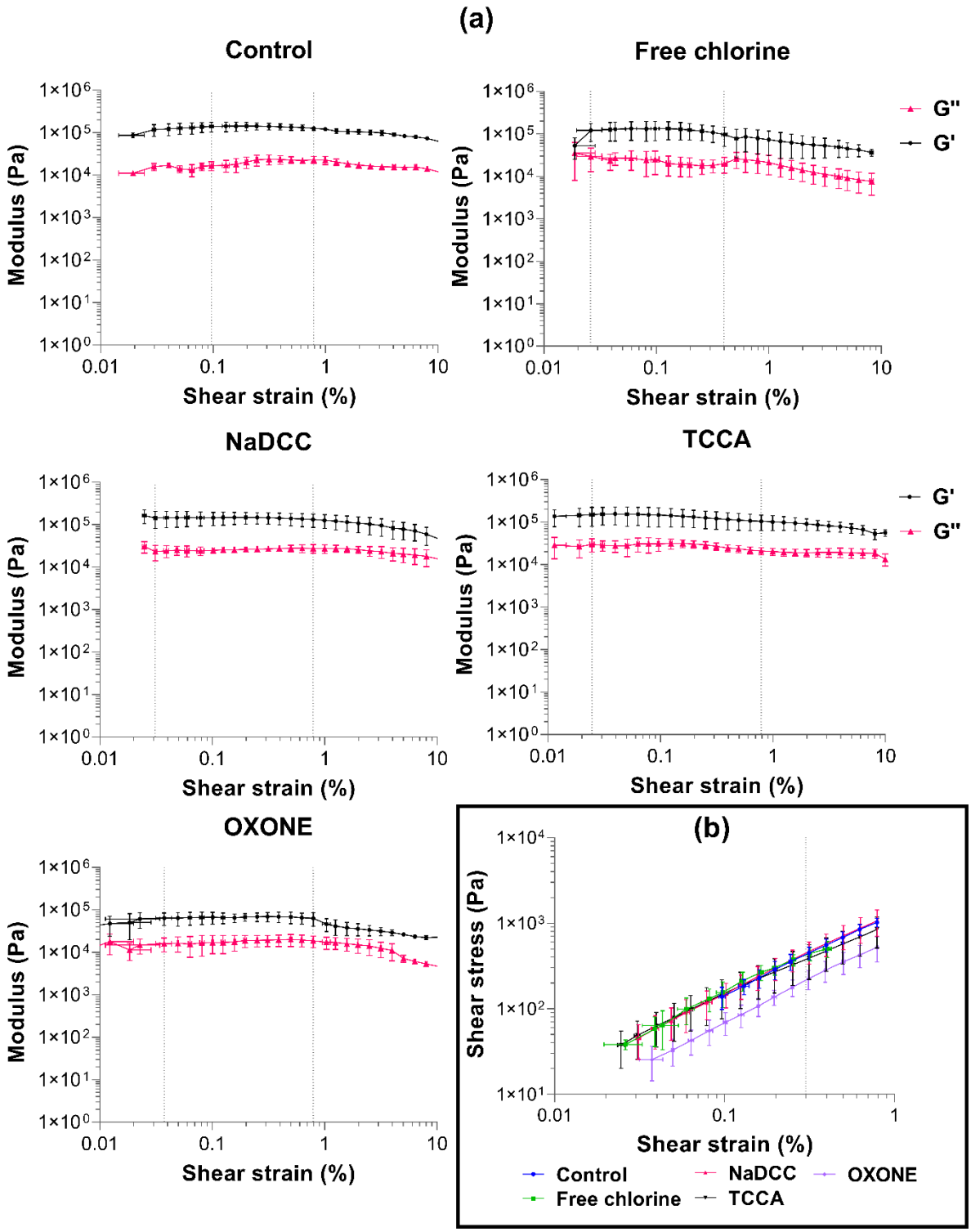

Figure 5-4 – Linear viscoelastic region (LVR) of 48 h-old *S. maltophilia* colony biofilms. **(a)** Oscillatory strain sweeps were performed on control/unexposed biofilms and biofilms exposed to free chlorine, OXONE, NaDCC, and TCCA at 10 × MBC for 30 min. The dashed lines indicate the average LVR for each condition. **(b)** Shear strain values from LVR were depicted in (a) for each condition with the corresponding shear stress. The dashed line indicates the shear strain of 0.3%, the selected value of shear strain within the LVR for all conditions. Control – blue, free chlorine – green, NaDCC – magenta, TCCA – black, OXONE – purple.

For further measurements, the shear strain of 0.3% (**Figure 5-4 (b)**) was selected as a representative value of shear strain within the LVR for each condition. The oscillatory frequency sweeps were performed to evaluate the time-dependent behaviour of the complex viscoelastic parameters of unexposed and exposed biofilms to disinfectants within the non-destructive deformation range (**Figure 5-5**). Across the frequency testing limits of 0.1 to 100 Hz both moduli, G' and G'', were relatively stable for all conditions tested. Additionally, the magnitude of the storage modulus (G') was greater than the loss modulus (G''), as observed for the strain sweeps measurements. Therefore, independently of the chemical treatment, *S. maltophilia* biofilms presented a predominantly solid consistency dimensionally stable at slow motion on long timescales (low frequencies), as well as at fast motion on short timescales (high frequencies).

The quantification of the effects of chemical stress on the viscoelastic properties of biofilms is limited to a few reports. *P. aeruginosa* biofilms presented mechanical properties highly resistant to different chemical perturbations, including chlorine that promoted no effect on biofilm elasticity (Lieleg et al., 2011). Among the chemical agents used in the study, mono- and divalent ions, polyelectrolytes, distinct pH levels and potential nutrients, only citric acid was able to reduce the biofilm elasticity by almost 99.5% (Lieleg et al., 2011). Conversely, when colony biofilms of *P. aeruginosa* were subjected to a classical creep test, different disinfectants increased the peak strain values of the creep curves, even though the treatment with chlorine at 50 mg/L did not show significant changes in the biofilm properties (Jones et al., 2011).

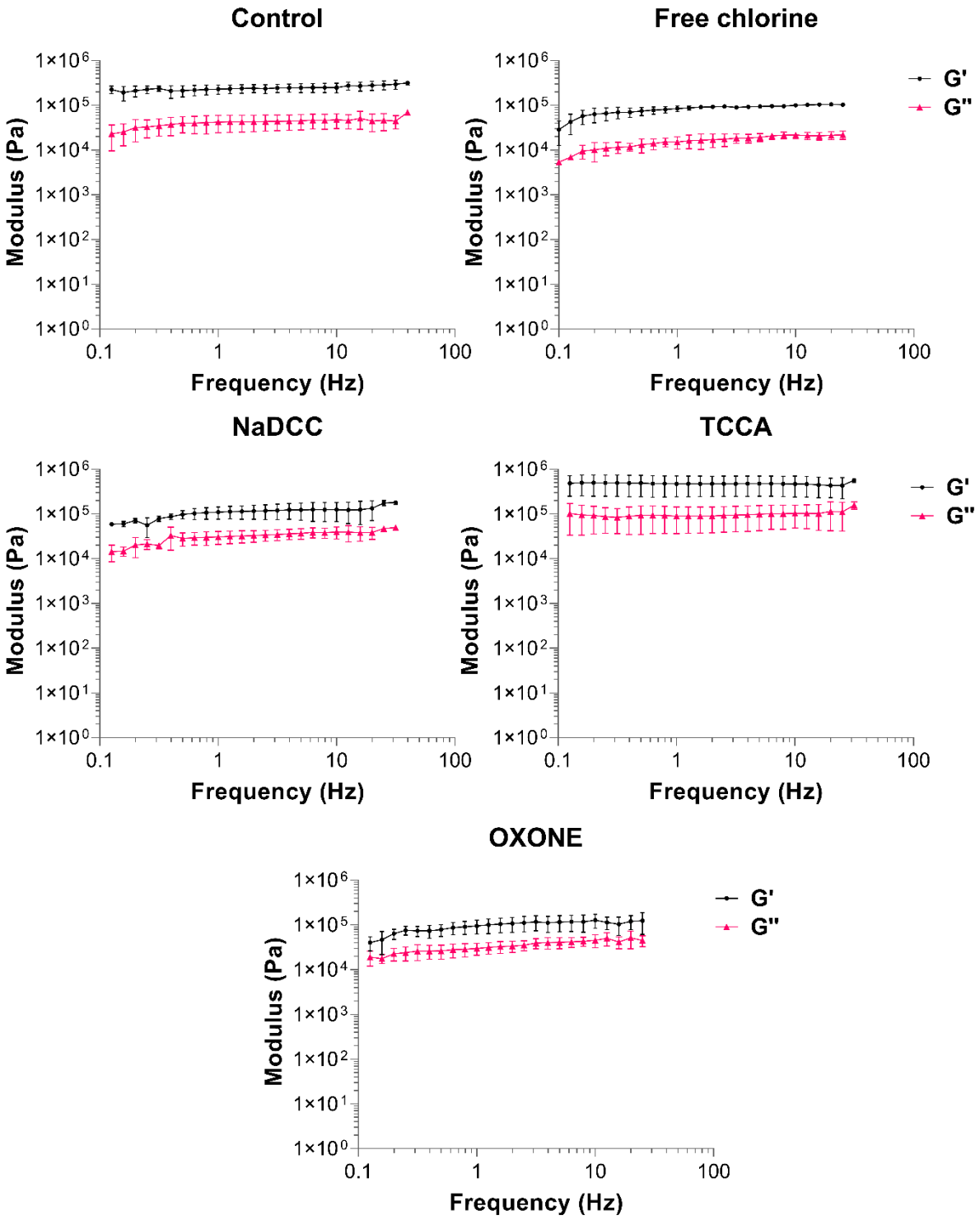

Figure 5-5 – Frequency sweeps of 48 h-old *S. maltophilia* colony biofilms. The oscillatory frequency sweeps were performed by incrementing the frequency from 0.1-100 Hz at a constant shear strain of 0.3% on control/unexposed biofilms and biofilms exposed to free chlorine, OXONE, NaDCC, and TCCA at 10 × MBC for 30 min.

The present work demonstrated that the colony *S. maltophilia* biofilms were significantly weakened by the 30 min exposure to free chlorine or OXONE, although the complex shear modulus (G*) of the biofilms exposed to NaDCC or TCCA was similar to the control/unexposed biofilms. Notably, OXONE reduced the biofilm stiffness by 51%. Consistent with the previous studies, the disinfectant activity on biofilm culturability cannot be directly linked to its ability to change the biofilm mechanical properties (Jones et al., 2011; Lieleg et al., 2011). Besides the oxidative action, OXONE possibly decreased the biofilm cohesiveness by increasing the ionic strength of the biofilm matrix with the addition of potassium ions that could break down crosslinking electrostatic interactions (Chen and Stewart, 2002).

Given the surprising results of biofilm inactivation and the effects on viscoelastic properties of biofilms exposed to OXONE, the AFM analysis aimed to verify the topography of *S. maltophilia* biofilms after disinfectant exposure (**Figure 5-6**). A qualitative analysis of the images revealed that *S. maltophilia* biofilms exposed to OXONE were not removed from the surface of the coupon but presented distinct features. The biofilms exposed to OXONE showed a non-uniform surface with a fractured appearance and small bacterial clusters dispersed on top of the biofilm. Additionally, 50% of the cell clusters on the superior layers of biofilms exposed to OXONE had a surface area approximately between 1 and 2 μm^2, conversely to the cell clusters of control/unexposed biofilms with a surface area approximately between 1.5 and 4.5 μm^2 (**Figure 5-7**). The maximum value of the surface area of the cell clusters after the treatment with OXONE ($\approx 20\ \mu m^2$) was also lower than in the control/unexposed biofilms ($\approx 70\ \mu m^2$). These findings corroborate the above results of the effects of OXONE on biofilm control and mechanical properties. Actually, 30 min exposure to OXONE was not able to remove the biofilm, with the numbers of total cells in the same magnitude as

the control/unexposed biofilm. However, it weakened the biofilm cohesiveness, breaking the cell aggregates into smaller clusters.

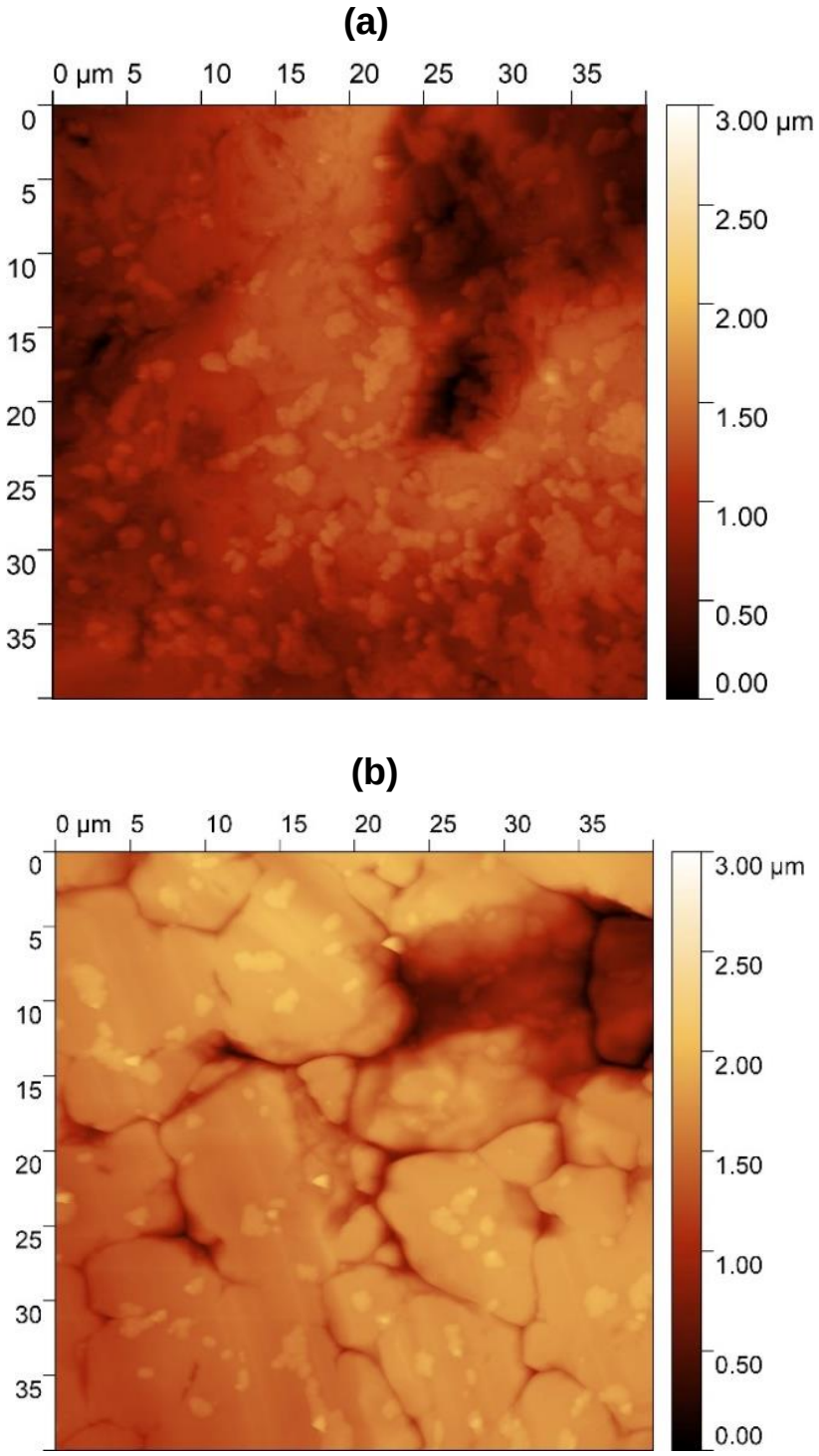

Figure 5-6 – AFM analysis of 48 h-old *S. maltophilia* biofilms on SS exposed to OXONE at 10 × MBC for 30 min. **(a)** Representative AFM height image of the control/unexposed biofilm. **(b)** Representative AFM height image of the biofilm exposed to OXONE.

To the best of my knowledge, this is the first study that demonstrated the changes in biofilm structure by unactivated peroxymonosulphate, particularly by AFM. A previous study evaluated through confocal laser scanning microscope observation the effects of Cu(II)-activated peroxymonosulphate in the structure of biofilms grown on reverse osmosis membranes, but even after 2 h of treatment, the biofilm structure was hardly disrupted (Lee et al., 2020a).

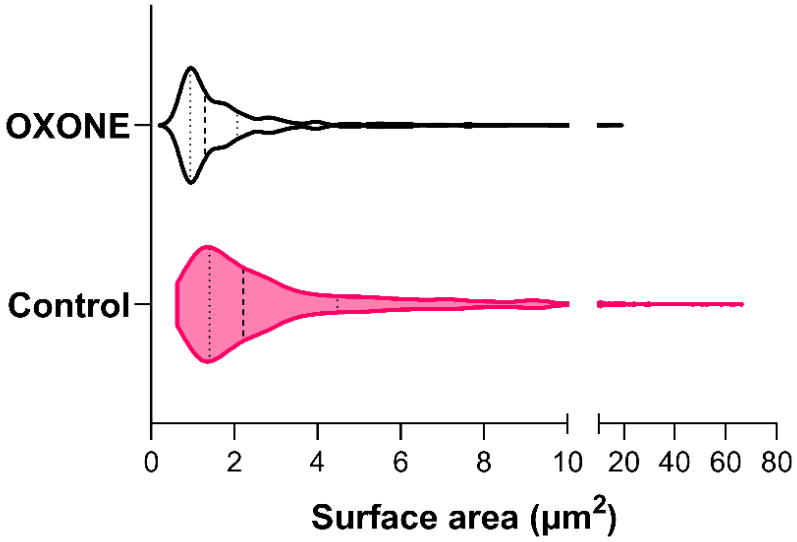

Figure 5-7 – Violin-plot of the surface area of cell clusters on the surface of the control/unexposed biofilms and biofilms exposed to OXONE (data from at least six areas per sample).

5.2 Conclusions

This study investigated the performance of NaDCC, TCCA, and OXONE on biofilm control, prevention of biofilm regrowth, and the ability to change the mechanical properties of *S. maltophilia* biofilms, compared to free chlorine disinfection. The main achievements of this work can be summarized as follows. *S. maltophilia* biofilms were efficiently inactivated by NaDCC, TCCA, and OXONE, being the action against biofilms on SS significantly better than free chlorine. The selected disinfectants did not prevent

biofilm regrowth; however, OXONE was able to limit biofilm regrowth on SS with a decrease in culturable cells remarkably higher than free chlorine. OXONE promoted a reduction of biofilm stiffness, weakening the cohesiveness of the matrix and breaking down the cell clusters on the superior layers of *S. maltophilia* biofilms. The insights gained from this work reinforce OXONE as a promising alternative to free chlorine for DW biofilm disinfection. This study also highlights the importance of understanding biofilm mechanical properties to improve biofilm control strategies.

Chapter 6

Validation of the potential of OXONE as a new alternative to conventional hypochlorite-based disinfection for the control of DW biofilms

The present chapter comprises the realism-based assessment of the potential of OXONE to control DW biofilms in comparison to chlorine disinfection. The effects of disinfectants were evaluated against 7 day-old *S. maltophilia* biofilms formed under conditions mimicking DWDS. The chemical stability of OXONE and chlorine solutions in STW at 25 ºC was evaluated over 40 days. The reactive species produced during the OXONE disinfection in STW were identified by EPR analysis. Additionally, the ecotoxicity of the disinfectants was also examined.

6.1 Results and Discussion

6.1.1 Effects of OXONE on biofilms formed in a benchtop biofilm reactor

The RCR was used for biofilm formation under conditions mimicking DWDS. *S. maltophilia* biofilms were formed for 7 days on PVC cylinders under constant rotation speed similar to the typical water velocity in plumbing systems (0.1 m/s) (Fu et al., 2021; Gomes et al., 2020; Husband and Boxall, 2011; Ragain et al., 2019). Before exposure to disinfectants, biofilms were characterized in terms of wet mass, culturability, total and non-damaged bacteria, and content of extracellular proteins and polysaccharides (**Table 6-1**).

Table 6-1 – Characterization of biofilms formed in the rotating cylinder reactor.

	***S. maltophilia* biofilms on PVC cylinders**
Wet mass, mg/cm^2	4.1 ± 1.2
Culturable cells, log CFU/cm^2	7.6 ± 0.5
Total cells, log cells/cm^2	7.4 ± 0.4
Biofilm viability, log non-damaged cells/cm^2	7.2 ± 0.5
Extracellular proteins, µg/g $_{biofilm}$	519 ± 146
Extracellular polysaccharides, µg/g $_{biofilm}$	460 ± 91

The numbers of culturable and total cells were in the same magnitude, respectively, 7.6 ± 0.5 log CFU/cm^2 and 7.4 ± 0.4 log cells/cm^2. Usually, the level of biofilm cell density is one order of magnitude higher than the number of biofilm culturable cells, however, the results were between the range of CFU and cell densities of biofilms reported within DWDS (Långmark et al., 2005; Olson and Nagy, 1984; Pedersen, 1990). The number of non-damaged cells represented 97% of the total biofilm cell density.

Regarding the content of EPS, the level of extracellular proteins (519 ± 146 μg/g $_{biofilm}$) was approximately equal to the level of extracellular polysaccharides (460 ± 91 μg/g $_{biofilm}$). Conversely, Gomes et al. (2018a, 2020) reported contents of extracellular polysaccharides of *S. maltophilia* biofilms formed in the RCR higher than the levels of extracellular proteins. The different EPS composition of the biofilms could be related to the use of distinct surface materials for biofilm formation (Gomes et al., 2020; Learbuch et al., 2021; Yan et al., 2022) or different medium broth composition for biofilm formation (Gomes et al., 2018a).

The biofilms were exposed to OXONE and free chlorine at 10 × MBC in STW for 30 min and the effects were evaluated in terms of biofilm culturability, biofilm cell density and number of non-damaged cells (**Figure 6-1**). The exposure of the 7 day-old biofilms to the disinfectants promoted a statistically significant reduction of biofilm culturability in comparison to the unexposed/control biofilms of approximately 1 log reduction with free chlorine and 4 log reduction with OXONE ($P < 0.05$). Remarkably, the action of OXONE in decreasing biofilm culturable cells was more efficient than the exposure of biofilms to free chlorine ($P < 0.05$). Considering the biofilm cellular density, no significant differences were observed in the total number of cells on biofilms after the exposure to the disinfectants ($P > 0.05$). Unexposed biofilms (control group) or those exposed to disinfectants presented total levels of cells approximately of 7 log cells/cm^2. However, the exposure of the 7 day-old *S. maltophilia* biofilms to free chlorine and OXONE promoted a significant decrease in the number of non-damaged cells ($P < 0.05$). Notably, biofilms exposed to OXONE presented levels of non-damaged cells below the detection limit of 4.8 log cells/cm^2, whereas the exposure to free chlorine only allowed a decrease of non-damaged cells to 6.4 ± 0.5 log cells/cm^2 ($P < 0.05$).

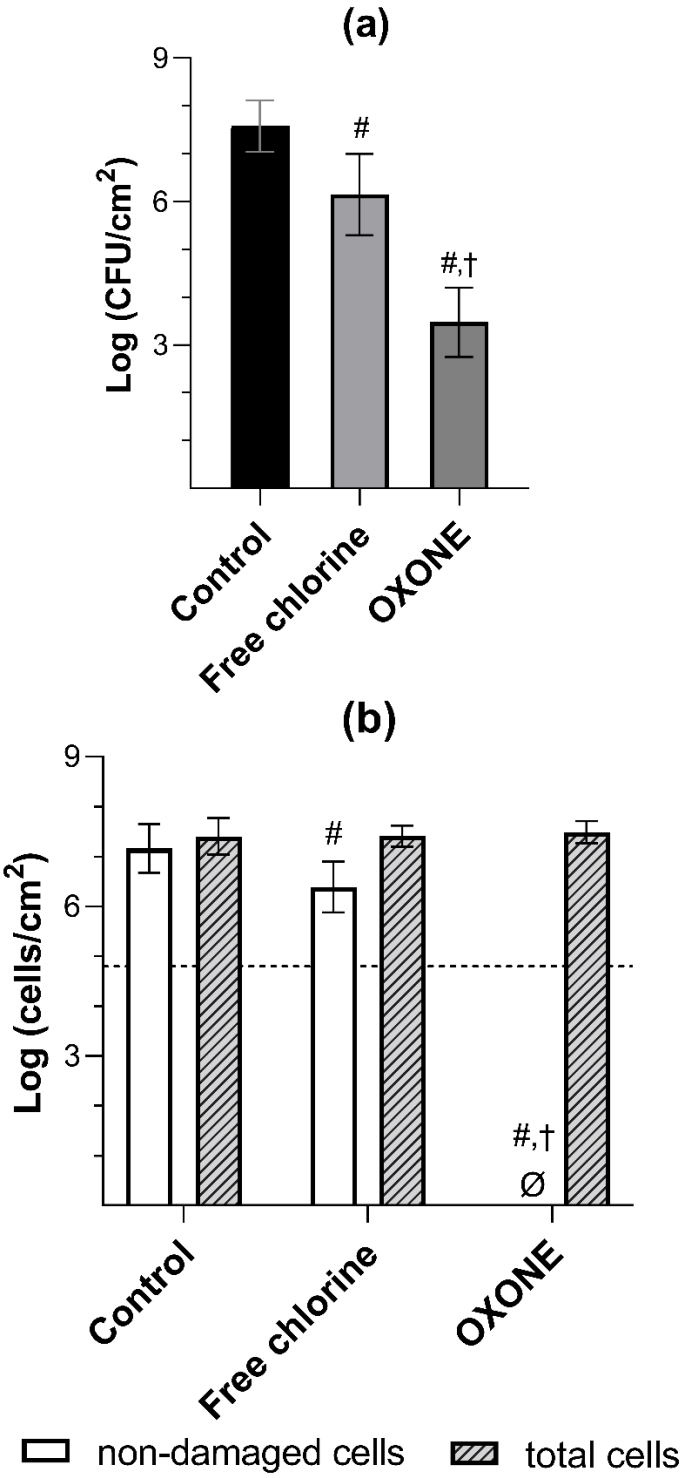

Figure 6-1 – The effects of free chlorine and OXONE at 10 × MBC in STW against 7 day-old *S. maltophilia* biofilms formed in the RCR. **(a)** Biofilm culturable cells. **(b)** Biofilm cellular density: number of non-damaged cells (solid-white bars) and total cells (patterned bars). ø Below the detection limit of 4.8 log cells/cm^2 (dashed line). # Indicates statistically significant differences to control/unexposed biofilms. † Indicates statistically significant differences to biofilms exposed to free chlorine.

The results demonstrated that the treatment with OXONE was efficient to control mature *S. maltophilia* biofilms formed under conditions mimicking DWDS. The biofilms exposed to OXONE were substantially inactivated, resulting in more than 4 log reduction in biofilm culturability and the number of non-damaged cells. However, it was unable to remove the biofilms from the PVC surface, in accordance with previous studies (**subsection 4.1.4** and **subsection 5.1.1**). Moreover, the action of OXONE was significantly better than the exposure to free chlorine, which only allowed a reduction in biofilm culturability and the number of non-damaged cells in the order of 1 log. The inability of chlorine for biofilm control was already reported in previous studies (Assaidi et al., 2020; Gomes et al., 2020; Hemdan et al., 2020). Gomes et al. (2020) demonstrated that free chlorine at 10 mg/L for 10 min did not reduce the number of non-damaged membrane and culturable cells of 7 day-old *S. maltophilia* biofilms grown on SS, copper, and 57% copper alloy. High levels of chlorination (between 50 and 200 mg/L for 2 h) decreased the number of culturable cells in 18 and 30 day-old *L. pneumophila* biofilms on galvanized steel and PVC, however, biofilms were not eradicated and continued to grow on subsequent days (Assaidi et al., 2020). Moreover, detached cells from 90 day-old *E. coli* biofilms formed on plastic-based materials (PVC, polypropylene, and polyethylene) were eradicated by chlorine, but *E. coli* cells from biofilms formed on iron pipes could resist the chlorine treatment (Hemdan et al., 2020). Furthermore, it should be pointed out that the exposure of biofilms to OXONE in STW, which has chloride ions (Cl^-) in its composition, could overestimate the effects of OXONE because the production of hypochlorous acid (HOCl) was reported to be generated from saltwater oxidation of peroxymonosulphate (Feng and Li, 2022; Lee et al., 2020a). Nevertheless, the present results are in agreement with the effects on biofilms exposed to OXONE in ultrapure water, where an approximately 4 log reduction was also observed (see subsection **5.1.1**).

6.1.2 Evaluation of the chemical stability of OXONE and free chlorine solutions

Among different factors, the control of microbial proliferation in DWDS is dependent principally on the maintenance of residual disinfectant concentration through the water distribution network (Liu et al., 2016; Simões and Simões, 2013). Maintaining an effective free chlorine residual is known to be a challenge given the existence of chemical reactions occurring both in the bulk phase and at the pipe walls that contribute to chlorine decay in DWDS (Brown et al., 2011; Kiéné et al., 1998; Shi et al., 2022; Tonev and Dimova, 2020). Therefore, the chemical stability of OXONE solutions in ultrapure water and STW was evaluated as disinfectant depletion over time and compared to the free chlorine decay in the same conditions. The initial disinfectant concentrations were prepared at the correspondent 10 × MBC of each disinfectant against *S. maltophilia* and the temperature was controlled at 25 ºC for 40 days.

The analysis of **Figure 6-2 (a)** demonstrated that after an initial drop of OXONE concentrations during the first 9 days of the experiment, the OXONE solutions were mainly stable over time, both in ultrapure water and in STW. The median values of OXONE concentrations in ultrapure water and in STW were approximately 2700 mg/L and 2500 mg/L, respectively. The interquartile range of OXONE concentrations in ultrapure water was 2600-2800 mg/L. In STW, the interquartile range was 2400-2600 mg/L.

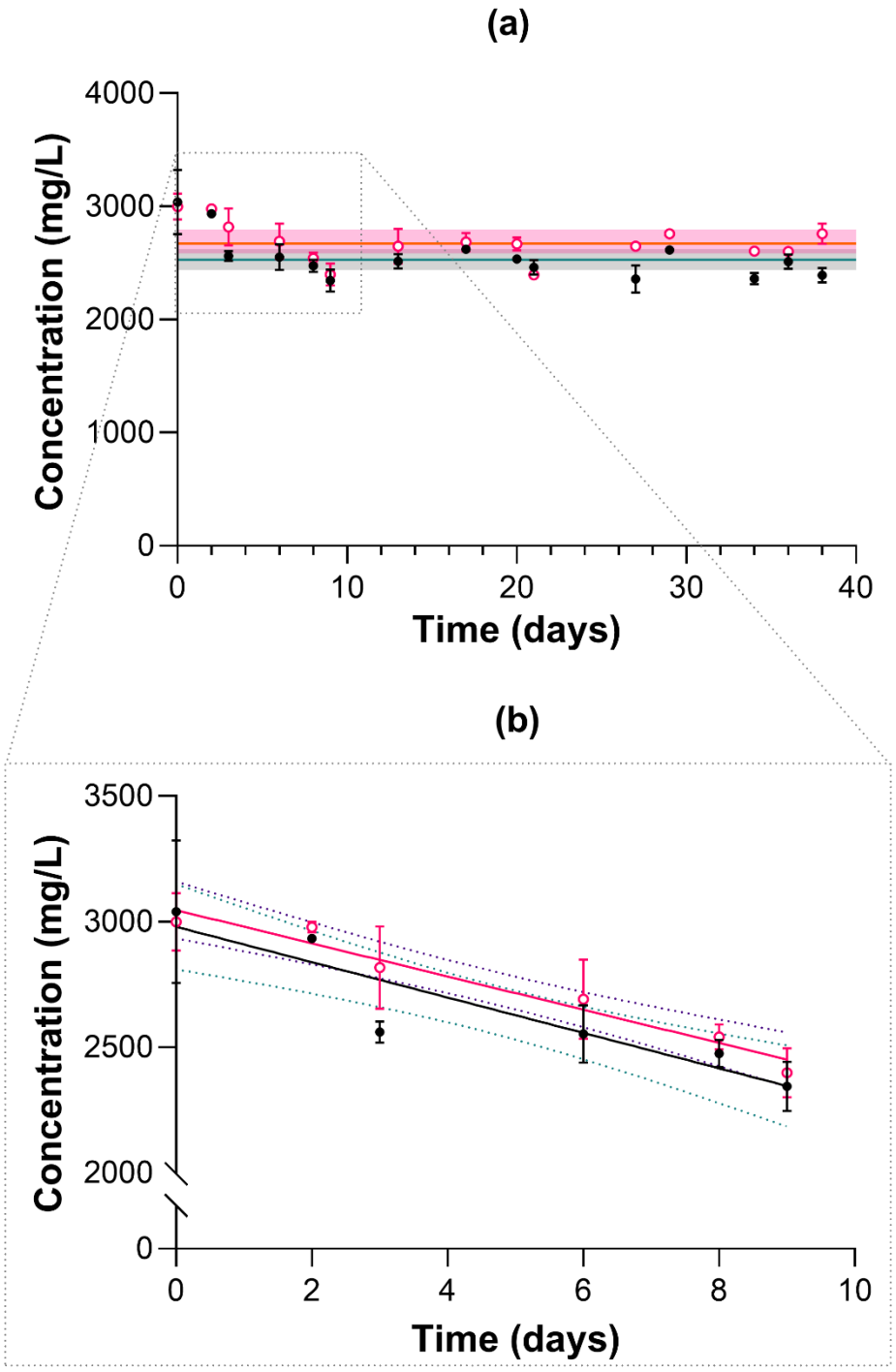

Figure 6-2 – Time course of chemical stability of OXONE in ultrapure water (open magenta circles) and STW (closed black circles) solutions at 25 ºC in light-protected conditions. **(a)** Over the 40 days of the experiment. The blue and orange lines represent the median of OXONE concentrations in STW and in ultrapure water, respectively. Shade zones define the interquartile range of OXONE concentrations in STW and ultrapure water. **(b)** Zoom in on OXONE concentration in the first 9 days of the experiment. Solid lines represent the linear regression of the experimental data. Dashed lines define the 95% confidence band of the model.

To quantify the OXONE depletion during the first 9 days, a linear regression was performed on the experimental data (**Figure 6-2 (b)**). The results of the OXONE loss rate and statistical measures of the linear models are presented in **Table 6-2**. The OXONE loss rate $\left(\frac{dC}{dt}\right)$ in STW and ultrapure water was -70.4 ± 13.4 and -66.1 ± 9.0 mg/L/day, respectively. No statistical difference was observed between the linear regression of OXONE depletion in STW and in ultrapure water ($P > 0.05$). Therefore, the overall results indicate that the presence of inorganic and organic substances in STW had a small impact on OXONE depletion over the 40 days of the experiment, resulting in OXONE concentrations approximately equal to the values obtained in the solution without interfering agents. However, in both conditions, the OXONE solutions presented a disinfectant depletion of approximately 10% of the initial OXONE concentrations within the first 9 days, after this time the values of OXONE concentration became stagnated.

Table 6-2 – Kinetic parameters and statistical measures of the linear regression of the experimental data from the chemical stability evaluation for OXONE over the first 9 days of the experiment.

Parameters	**Ultrapure water**	**STW**
Slope = $\frac{dC}{dt}$, mg/L/day	-66.1 ± 9.0	-70.4 ± 13.4
Y-intercept, mg/L	3046 ± 51	2980 ± 76
R^2	0.8444	0.7347

Regarding the evaluation of the chemical stability of free chlorine, the results of free chlorine concentration over time in ultrapure water and STW are presented in **Figure 6-3**. The linear regression of the experimental data allowed the assessment of the kinetic parameters that quantify chlorine decay (**Table 6-3**).

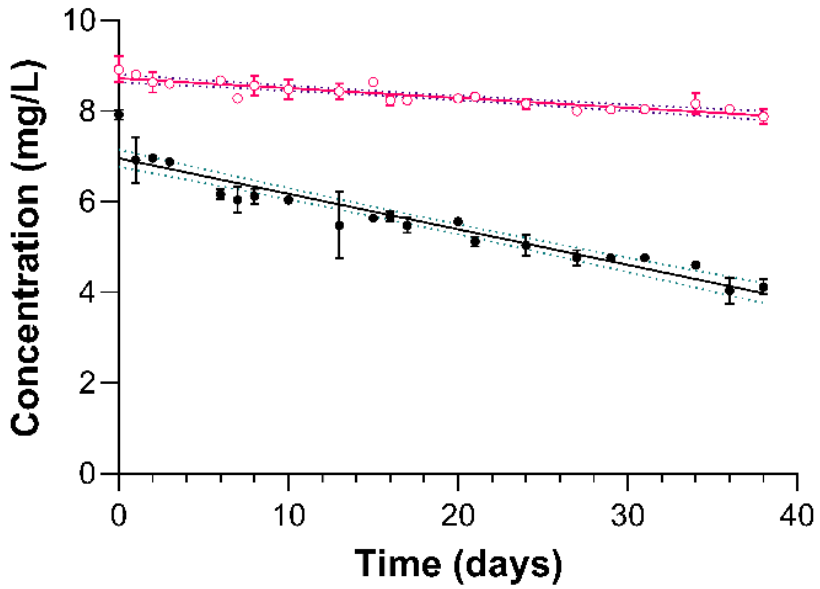

Figure 6-3 – Concentration of free chlorine (mg/L) over 40 days in ultrapure water (open magenta circles) and STW (closed black circles) solutions at 25 ºC in light-protected conditions. Solid lines represent the linear regression of the experimental data. Dashed lines define the 95% confidence band of the model.

The absolute value of the chlorine loss rate $\left(\frac{dC}{dt}\right)$ in STW, 0.078 ± 0.005 mg/L/day, was statistically significantly higher than the loss rate $\left(\frac{dC}{dt}\right)$ in ultrapure water, 0.022 ± 0.002 mg/L/day (P < 0.05). Moreover, the estimated half-life ($t_{1/2}$) for chlorine depletion in STW was approximately 45 days, whereas in ultrapure water the $t_{1/2}$ was approximately 198 days (P < 0.05).

Table 6-3 – Kinetic parameters and statistical measures of the linear regression of the experimental data of free chlorine depletion in ultrapure water and STW.

Parameters	**Ultrapure water**	**STW**
Slope = $\frac{dC}{dt}$, mg/L/day	-0.022 ± 0.002	-0.078 ± 0.005
Y-intercept, mg/L	8.72 ± 0.04	7.00 ± 0.09
R^2	0.7331	0.8834
$t_{1/2}$, days	198	45

Over the 40 days of the experiment, the free chlorine depletion in STW was approximately 48% of the initial value, revealing a possible reaction of chlorine with the inorganic and organic substances of STW (Brown et al., 2011). Indeed, the reactions of chlorine with inorganic substances in natural waters are relatively quick and, generally, involve compounds such as ammonia, halides, iron, and sulphide (Brown et al., 2011; Deborde and von Gunten, 2008). Whereas low chlorine reaction rates with organic compounds are commonly observed during chlorination (Brown et al., 2011; Deborde and von Gunten, 2008). In the present work, chlorine in ultrapure water was mainly stable, with approximately 11% of free chlorine depletion over the 40 days of the experiment. In fact, without interfering substances, sodium hypochlorite at 25 ºC demonstrated to be more stable than neutral electrolysed oxidizing water, chlorine dioxide, and NaDCC solutions (Meireles et al., 2017).

6.1.3 EPR studies for identification of reactive species produced in OXONE disinfection

In **chapter 4** it was demonstrated that OXONE was able to trigger significant bacterial cytoplasmic membrane destabilization and promoted 90% inactivation of the bacterial population of *S. maltophilia* within 10 min, even at a sub-lethal concentration. Research on advanced oxidation processes for oxidative degradation of organic pollutants indicates that persulphates have a strong oxidizing action via two-electron reduction, and decomposition into sulphate and hydroxyl radicals by cleaving the peroxide bond (Lee et al., 2020; Liu et al., 2021; Wacławek et al., 2017). However, the mechanism behind the disinfectant activity of OXONE has not been fully elucidated and is limited to a few studies (Anipsitakis et al., 2008; Lee et al., 2020a). So, in the present work, the activity of OXONE against *S. maltophilia* was monitored by EPR spectroscopy, to get insight into

its mechanism of disinfection. The experiments were performed under STW to simulate microbial disinfection for application in DW treatment.

Studies using spin trap 4-oxo-TEMP were performed aiming to detect singlet oxygen radicals ($^1O_2$) formed during the disinfection of *S. maltophilia* with OXONE. This spin trap forms an adduct with $^1O_2$, which can be detected by EPR (Lopes et al., 2023). The spectra obtained are depicted in **Figure 6-4** and exhibit the typical (1:1:1) triplet signal and *g* value (g = 2.0067) of the adduct 4-oxo-TEMP-singlet oxygen radical (Lopes et al., 2023; Miyaji et al., 2017; Qi et al., 2016; Tian et al., 2019). The relative amount of trapped $^1O_2$ over 30 min is represented in **Figure 6-5 (a)**.

The formation of $^1O_2$ radicals was immediately confirmed at time zero with high-intensity EPR signals registered for OXONE solutions in STW, with and without the presence of bacterial cells (**Figure 6-4 (a)**). Over the 30 min of analysis, the intensity of the signals significantly increased, in both conditions (**Figure 6-4 (b)** and **Figure 6-5 (a)**). However, no statistically significant differences ($P > 0.05$) were observed in the relative amount of $^1O_2$ trapped in the presence or absence of *S. maltophilia* cells. The results suggested that OXONE is activated by the presence of inorganic and organic substances in STW, allowing the generation of $^1O_2$ radicals. During the disinfection process of *S. maltophilia* by OXONE in STW, the presence of $^1O_2$ radicals was also detected, but there was no evidence of an increase in $^1O_2$ generation from the inactivation of *S. maltophilia*.

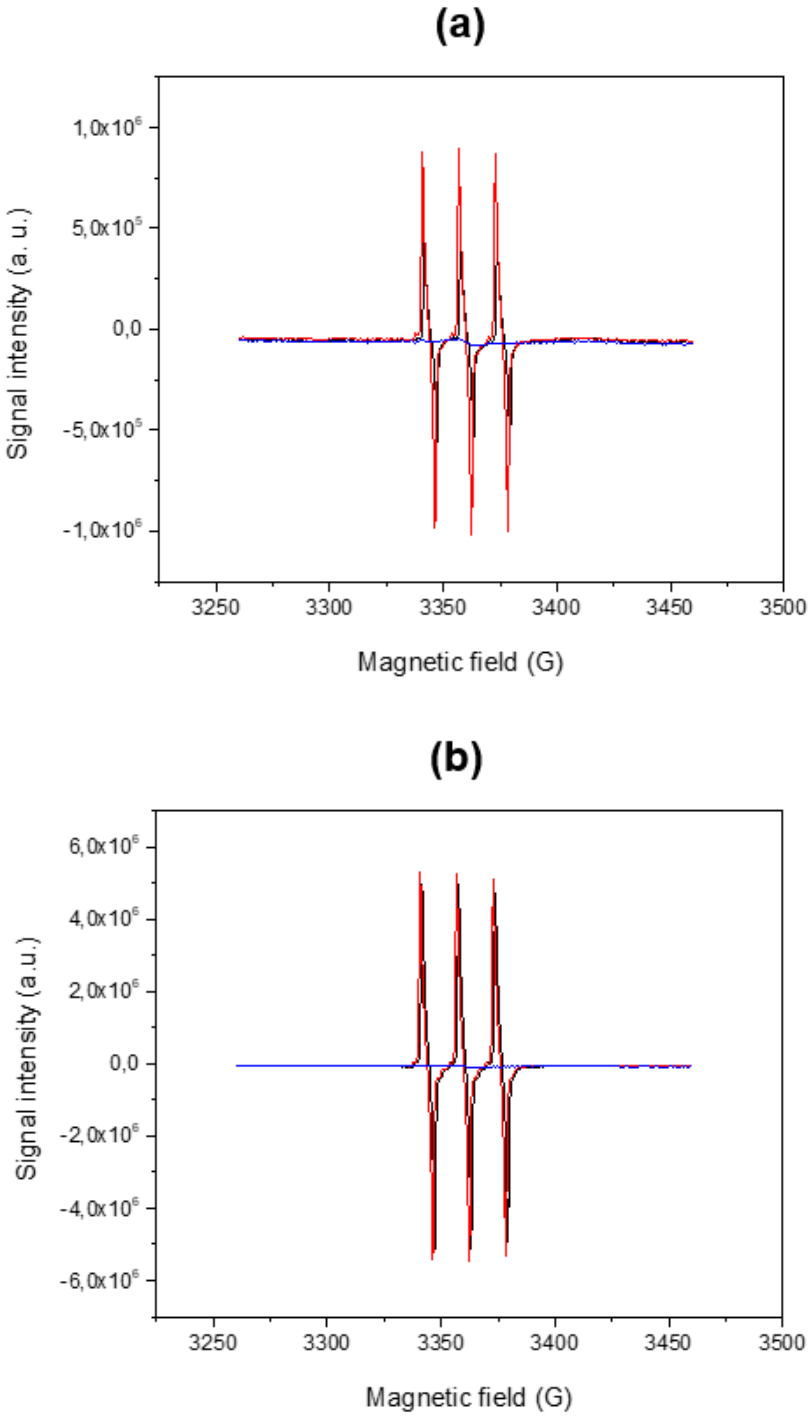

Figure 6-4 – Representative EPR spectra of singlet oxygen radical production at time zero **(a)** and after 30 min **(b)** of *S. maltophilia* exposure to OXONE in STW. A. u. means arbitrary units. The blue line represents the blank sample (bacterial cells in STW without exposure to OXONE); the black line represents the control sample (OXONE in STW without bacterial cells); the red line represents the test sample (bacterial cells exposed to OXONE in STW).

A study on base-catalysed hydrolysis of OXONE to sulphate anion and hydrogen peroxide proved that $^{1}O_2$ and superoxide ($O_2^{\bullet-}$) radicals were the primary reactive oxygen

species in the system, resulting in the degradation of a variety of organic pollutants (Qi et al., 2016). The possible activation mechanism was supported by the radical quenching method (*tert*–butyl alcohol, methanol, sodium azide, and *p*−benzoquinone) and electron spin resonance trapping studies (Qi et al., 2016). The present work also confirmed the presence of $^1O_2$ radicals during microbial exposure to OXONE that may be involved in the mechanism of *S. maltophilia* inactivation. Indeed, $^1O_2$ radicals are known to oxidize many biological molecules, such as proteins, nucleic acids, and lipids, resulting in cell damage (Hamblin and Hasan, 2004; Lee et al., 2009; Manjón et al., 2008; Redmond and Gamlin, 1999).

Superoxide ($O_2^{\bullet-}$), hydroxyl ($HO^{\bullet}$), and sulphate ($SO_4^{\bullet-}$) radicals have been reported to participate in the antimicrobial mechanism of action of activated persulphates, mainly peroxydisulphate (Lee et al., 2020a; Qi et al., 2018; Wordofa et al., 2017; Xia et al., 2017). Therefore, the DMPO spin trap was used to detect the formation of these radicals in the disinfection process by OXONE in STW. The spectra obtained are depicted in **Figure 6-6** and the relative amount of radicals trapped over 30 min is represented in **Figure 6-5 (b)**. A weak EPR signal was detected, and its intensity strengthened over time. After 20 and 30 min of *S. maltophilia* exposure to OXONE in STW, the relative quantity of trapped radicals was statistically significantly higher than in the OXONE solution in STW without bacterial cells ($P < 0.05$). However, it was still not possible to assign the detected EPR signal to specific radical species formed in the process. The obtained signal did not correspond to the typical shapes of DMPO-OH, DMPO-SO_4, and DMPO-OOH adducts (Qi et al., 2016; Wei et al., 2017; Xia et al., 2017), so it must correspond to another non-identified free radical. Qi et al. (2016) and Wei et al. (2017) reported a signal presenting four characteristic peaks which was attributed to a DMPO-OH adduct (1:2:2:1) with hyperfine coupling constants of a_N between 14.9 - 15.0 G and a_H between 14.7 – 14.9 G.

Also, a spectra showing six characteristic peaks was assigned as a DMPO-OOH adduct with $a_N \approx 14$ G and $a_H \approx 8$ G and a DMPO-SO_4 adduct (1:1:1:1:1:1) with $a_N \approx 14$ G, $a_{\beta\text{-H}} \approx 10$ G, $a_{\gamma\text{-H1}} \approx 1.5$ G, and $a_{\gamma\text{-H2}} \approx 0.8$ G (Qi et al., 2016; Wei et al., 2017; Xia et al., 2017).

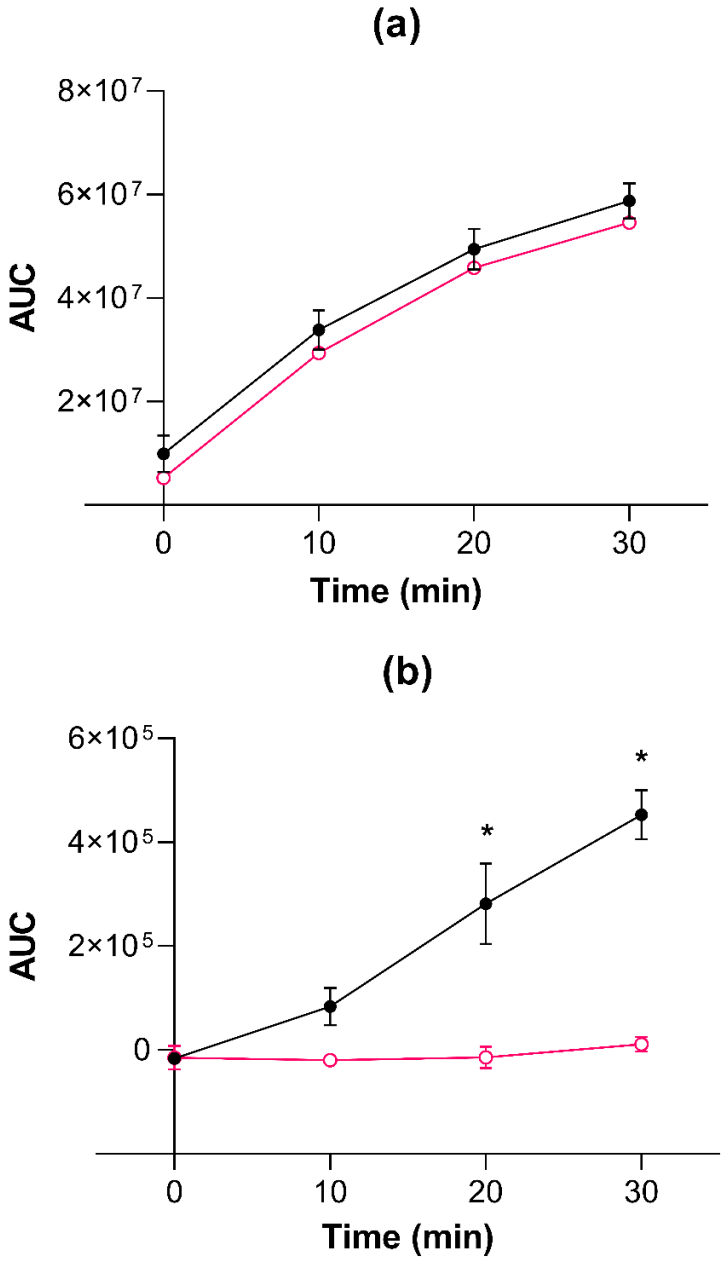

Figure 6-5 – Time course of reactive species generation during the disinfection of *S. maltophilia* by OXONE in STW. **(a)** 4-oxo-TEMP spin trapped singlet oxygen radicals. **(b)** DMPO spin trapped detected other radicals. Closed black circles represent test samples (bacterial cells exposed to OXONE in STW). Open magenta circles represent control samples (OXONE in STW without bacterial cells). The values represent the area under the curve (AUC) of the EPR spectra for each condition subtracted by AUC of the blank samples (bacterial cells in STW without exposure to OXONE). * Indicates statistically significant differences to the control sample ($P < 0.05$).

Regarding the study of the presence and contribution of the specific reactive species on microbial inactivation by persulphates, to the best of the author's knowledge, there is only one published article that has examined the disinfection mechanism through EPR analysis. Xia et al. (2017) reported that the dominant reactive species responsible for the *E. coli* K-12 inactivation with peroxydisulphate activated by magnetic pyrrhotite were sulphate and hydroxyl radicals. In that work, the evaluation of the mechanism of inactivation was based on the integration of EPR analysis and a positive scavenging test using methanol for $SO_4^{\bullet-}$, *tert*-butyl alcohol for $HO^{\bullet}$, Fe(II)-EDTA for H_2O_2, and TEMPOL for $O_2^{\bullet-}$ (Xia et al., 2017).

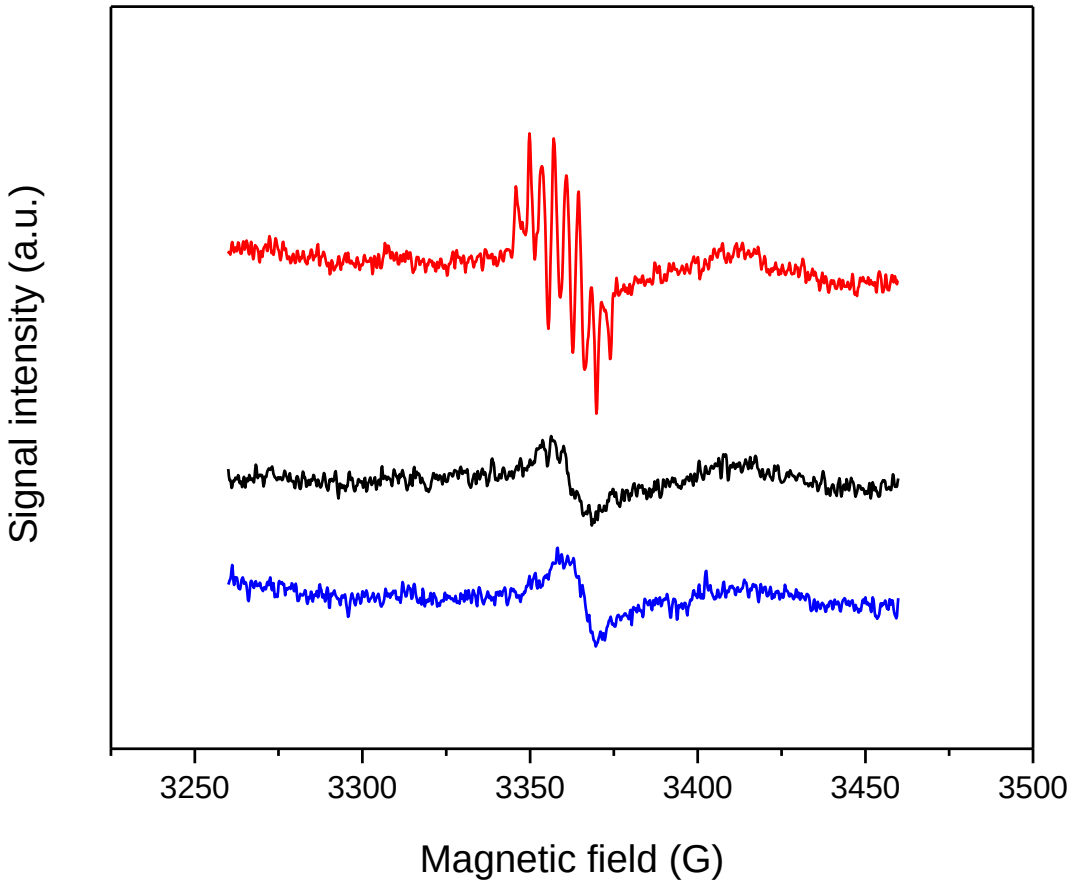

Figure 6-6 – Representative EPR spectra of radicals trapped by DMPO after 30 min of *S. maltophilia* exposure to OXONE in STW. A. u. means arbitrary units. The blue line represents the blank sample (bacterial cells in STW without exposure to OXONE); the black line represents the control sample (OXONE in STW without bacterial cells); the red line represents the test sample (bacterial cells exposed to OXONE in STW).

Other studies evaluated the major contributing radicals in microbial inactivation only by indirect methods, such as through the quantification of the degradation of chemical probes, pathogen survival with the presence of radical scavengers, and theoretical models (Lee et al., 2020a; Qi et al., 2018; Sun et al., 2016; Wordofa et al., 2017). The specific reactive species responsible for the antimicrobial activity appear to be dependent on the method of persulphate activation, for instance, Cu(II) or Fe(II) catalysis, UV photolysis, or alkali activation (Lee et al., 2020a; Qi et al., 2018; Sun et al., 2016; Wordofa et al., 2017). Particularly, in the Cu(II)-activated peroxymonosulphate system, $SO_4^{\bullet-}$ was the dominant reactive oxidant present in the inactivation of *P. aeruginosa* (Lee et al., 2020a). Additionally, *P. aeruginosa* demonstrated to promote the production of reactive oxidants, given the increase in the degradation of a chemical probe (phenol) with an increasing population of bacterial cells (Lee et al., 2020a). However, one should be cautious when interpreting findings of the mechanism of action based on indirect methods, as highlighted in a recent work that proved the invalidity of quenching methods for the persulphate-based processes (Gao et al., 2022). The misinterpretation of the role of the reactive species in these systems can be caused by an increase of peroxymonosulphate decomposition, interfering reactive species generation, and scavenging of non-target reactive species in the presence of high-concentration quenchers (Gao et al., 2022).

6.1.4 Impact on freshwater microalga and considerations on ecotoxicological profile of the disinfectants

A preliminary evaluation of the ecotoxicity of free chlorine and OXONE was performed by the assessment of the impact of residual levels of these disinfectants on freshwater microalga *C. vulgaris*. The microalga was exposed to OXONE and free chlorine at 0.5 mg/L in STW for 72 h. This value was chosen regarding the common

chlorine residual concentrations between 0.2 and 0.5 mg/L at the point of delivery for water that is centrally treated (WHO, 2022). The results of *C. vulgaris* cell concentration over 72 h of exposure to free chlorine and OXONE are presented in **Figure 6-7**. The specific growth rate for each condition is presented in **Table 6-4**.

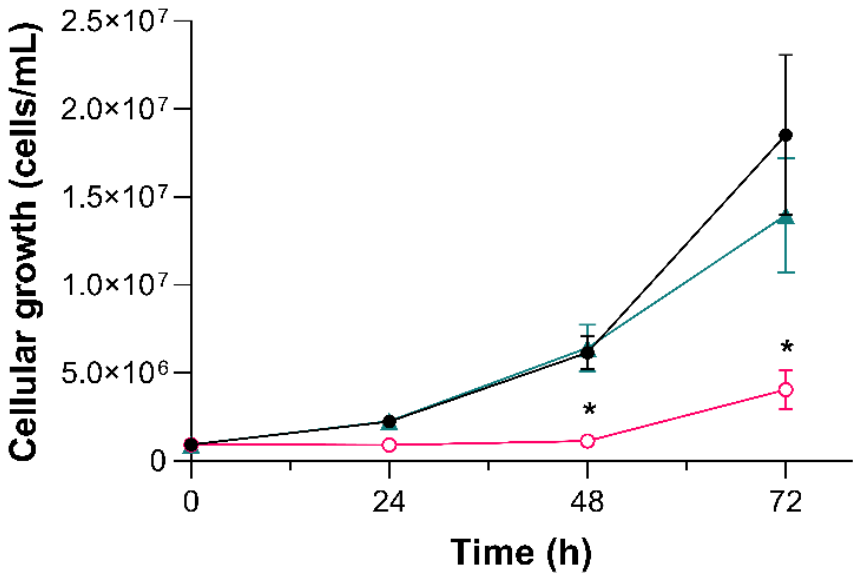

Figure 6-7 – Microalgal cellular growth over 72 h of exposure to free chlorine (open magenta circles) and OXONE (green triangles) at 0.5 mg/L in STW. The closed black circles represent the control samples (unexposed microalga). * Indicates statistically significant differences to the control sample ($P < 0.05$).

The *C. vulgaris* cellular growth in STW presented a similar profile for the control and the microalgal cultures exposed to OXONE at 0.5 mg/L ($P > 0.05$). However, when exposed to free chlorine at 0.5 mg/L, the cellular growth was significantly lower than for the unexposed microalga upon 48 h of incubation ($P < 0.05$). At the end of 72 h, the cellular growth of *C. vulgaris* exposed to free chlorine was significantly reduced by *circa* 78% in comparison to the control ($P < 0.05$). Regarding the microalga specific growth rate (μ), the values observed for the control (0.43 ± 0.04 d^{-1}) and for microalgal cultures exposed to OXONE (0.39 ± 0.04 d^{-1}) were within the range of values reported for lab scale treatment of urban wastewater, between 0.2 and 1 d^{-1} (Matamoros et al., 2016; Vale

et al., 2022). No statistical differences were observed between the unexposed and exposed cultures to OXONE ($P > 0.05$). Nevertheless, the exposure to free chlorine caused a significant decrease in the specific growth rate to 0.20 ± 0.04 d^{-1} ($P < 0.05$), representing a reduction of the growth rate of approximately 54% in comparison to the control cultures. Therefore, the results indicated that under these experimental conditions, the toxicity of OXONE to the freshwater microalga *C. vulgaris* was limited in contrast to the impact of free chlorine.

Table 6-4 – Specific growth rate (μ) of *C. vulgaris* for 72 h of exposure to free chlorine or OXONE at 0.5 mg/L in STW. * Indicates statistically significant differences to the control sample ($P < 0.05$).

Cultures	**μ (d^{-1})**
Control	0.43 ± 0.04
OXONE	0.39 ± 0.04
Free chlorine	0.20 ± 0.04*

Contradictory information was found regarding the acute toxicity of chlorine to microalgae. The median effective concentrations (EC_{50}) of chlorine which resulted in a 50% reduction in marine microalgae growth after 96 h exposure were reported to be 2.91 mg/L for *Isochrysis galbana* and 1.73 mg/L for *Dunaliella salina* (López-Galindo et al., 2010). On the other hand, the EC_{50} values for freshwater microalgae *Pseudokirchneriella subcapitata* and *C. vulgaris* were 1.6 and 5.1 mg/L, respectively, after 72 h of exposure (Pitanga, 2011). In addition, Vannoni et al. (2018) demonstrated that the EC_{50} values for chlorine after 72 h of growth inhibition test using marine diatoms *Achnanthes* spp. and *Navicula pelliculosa* were 2.79 and 0.23 mg/L, respectively. Furthermore, Ebenezer and Ki (2013) observed that chlorine concentrations within the range of DW supply (0.1-0.5 mg/L) promoted a decrease in growth rate and pigment levels of the marine dinoflagellate

microalga *Prorocentrum minimum*. Indeed, the public information within the registration dossier of sodium hypochlorite in the ECHA database indicates an EC_{50} value for freshwater algae of 0.05 mg/L, based on a toxicity study using the microalga *P. subcapitata* according to OECDE 201 (ECHA, 2023b; Liedtke, 2013). Considering the ecotoxicity of OXONE, to the best of my knowledge, there is only one published article that investigated the toxic effect of peroxymonosulphate on water organisms from different trophic levels (Olmez-Hanci et al., 2014). However, the high doses implemented in that study (>1000 mg/L of OXONE) revealed to promote approximately 77% of cell growth inhibition to the freshwater microalga *P. subcapitata*, after 72 h of exposure (Olmez-Hanci et al., 2014).

Concerning the toxicological information for repeated doses via the oral route, a tolerable daily intake (TDI) of 0.15 mg chlorine/kg of body weight is indicated by WHO to be safe for a human being on a long-term basis (WHO, 1996). This TDI value was derived from a no-observed-adverse-effect level (NOAEL) of 15 mg/kg of body weight per day for the absence of toxicity in rodents ingesting chlorinated DW for up to 2 years (NTP, 1992; WHO, 1996). On the other hand, a derived-no-effect level (DNEL) of 1 mg/kg of body weight per day was calculated to OXONE for long-term exposure via the oral route, as declared in the registration dossier of pentapotassium bis(peroxymonosulphate) bis(sulphate) in the public ECHA database (ECHA, 2023c). The DNEL value was derived from a 90-day oral toxicity study in rodents according to the OECD Guideline 408, where a NOAEL of 200 mg/kg of body weight per day was observed for OXONE (ECHA, 2023c). Nevertheless, the toxicological information about OXONE is still under revision by the Biocidal Products Committee (ECHA, 2023a), and therefore careful conclusions should be made. Even so, comparing the NOAEL values of these disinfectants, OXONE demonstrated to be less toxic than chlorine. However, it

remains uncertain if the proposed DNEL value for OXONE, which should be safe for human consumption in DW, guaranties water disinfection and biofilm control as proposed through this work.

6.2 Conclusions

The purpose of the current study was to validate the capability of OXONE to control DW biofilms under realism-based conditions and highlight it as a promising alternative to hypochlorite-based disinfection. The results of this investigation revealed that OXONE was able to promote significant inactivation of 7 day-old biofilms formed under conditions mimicking DWDS, with a reduction of biofilm culturability and the number of non-damaged cells up to approximately 4 log. The relevance of OXONE was supported by the significant effects on biofilm control and its chemical stability in comparison to the results for chlorine. Moreover, during *S. maltophilia* exposure to OXONE, the formation of reactive species was detected by EPR, demonstrating the presence of singlet oxygen and other non-identified radicals. Notwithstanding the preliminary evaluation of the ecotoxicological profile, the findings suggested that OXONE was less toxic to freshwater microalga *C. vulgaris* than chlorine, even at a concentration within the range of DW supply. More information on the toxicological profile of OXONE for long-term exposure via the oral route would help to establish a safe guideline value for routine DW treatment with OXONE. Even though, a possible application of OXONE may be proposed in a first instance for temporary emergency disinfection of DW biofilms.

Chapter 7

General conclusions and future work

The major conclusions of this investigation project are described in this chapter, as well as some recommendations for further research work.

7.1 General conclusions

Although chlorination is widespread for the disinfection of DW, the control of DW biofilms is limited by the increase of biofilm tolerance to chlorine and the persistence of biofilms in the distribution systems. This project was undertaken to extensively analyse and provide new information about the antimicrobial and antibiofilm action of NaDCC, TCCA, and OXONE against two emergent pathogens isolated from DWDS. The antimicrobial activity against planktonic bacteria revealed that the disinfectant concentrations × contact time (*Ct*) for *S. maltophilia* were lower than the *Ct* values obtained for *A. calcoaceticus,* for all disinfectants. The dose-response analysis showed that the efficiency of the selected disinfectants for approximately 3 to 4 log reduction was between 12-15 min·mg/L for free chlorine, 48-63 min·mg/L for NaDCC, 33-57 min·mg/L for TCCA, and 8.4-10.2 ($\times 10^3$) min·mg/L OXONE. The time-response evaluation demonstrated that NaDCC and TCCA had similar inactivation rates against both bacteria and that *S. maltophilia* became more susceptible to OXONE during the disinfection process, while an opposite trend was observed for *A. calcoaceticus*. The disinfectants also triggered significant bacterial cytoplasmic membrane destabilization, even at concentrations below the MBC. On the other hand, in general, no significant alteration was observed in bacterial hydrophobicity, surface tension, and ability to accept and donate electrons. The control of 48 h-old single species biofilms of *A. calcoaceticus* and *S. maltophilia* formed on two representative pipe materials from DW networks, PVC and SS, demonstrated that the selected disinfectants presented similar or better efficiencies in reducing biofilm culturability than free chlorine. Moreover, OXONE showed the best performance against biofilms, with 2 to 4 log CFU/cm^2 reduction. However, none of the disinfectants caused biofilm removal of more than 1 log cells/cm^2. Unlike the

susceptibility profile in the planktonic state, *S. maltophilia* biofilms were more tolerant to the action of disinfectants than those of *A. calcoaceticus*.

Further studies on the effects of OXONE and chlorinated isocyanurates in the biofilm viscoelastic properties and structure revealed that *S. maltophilia* biofilms presented a rheological character of a viscoelastic solid material, regardless of the treatment. One of the most important findings to emerge from this study was that the exposure to OXONE allowed a significant reduction of biofilm stiffness, weakening the cohesiveness of the matrix, even in comparison to biofilms exposed to free chlorine. These results were coherent with the topographic analysis of biofilms that showed a fractured appearance and smaller bacterial clusters dispersed on top of the biofilm structure after exposure to OXONE. However, the selected disinfectants did not prevent biofilm regrowth for 24 h after disinfection. Nevertheless, OXONE was able to remarkably limit biofilm regrowth on SS by 5 and 4 log CFU/cm^2 in comparison to the unexposed and biofilm exposed to free chlorine, respectively.

The realism-based assessment of OXONE performance as an alternative to hypochlorite disinfection was validated using the RCR that allowed the formation of mature 7 day-old biofilms in conditions that mimic real DWDS. These experiments confirmed that the exposure to OXONE effectively inactivated mature *S. maltophilia* biofilms, promoting a reduction of biofilm culturability and the number of non-damaged cells up to approximately 4 log. The effects of OXONE were also of significance in comparison to the conventional disinfection with free chlorine. The second major finding was that OXONE in STW demonstrated to be more stable than chlorine, indicating that the presence of inorganic and organic substances in STW made no significant difference in OXONE depletion over 40 days at 25 ºC. The results showed that after an initial depletion of circa 10%, the OXONE concentrations maintained stable over time, whereas

the free chlorine depletion in STW was approximately 48% of the initial value. The investigation of the reactive species involved in the inactivation of *S. maltophilia* by OXONE confirmed the presence of singlet oxygen and other non-identified radicals. Furthermore, the findings of ecotoxicity against freshwater microalgae suggested that OXONE is less toxic than chlorine, even at a concentration within the range of DW supply. Overall, this project strengthens OXONE as a promising alternative to conventional hypochlorite-based disinfection for the control of DW biofilms. The application for routine DW treatment needs further research given the scarce information about the safe intake for human consumption on a long-term basis via the oral route, but initially, OXONE may be indicated for temporary emergency disinfection of DW biofilms.

7.2 Future work

This work highlighted new information about alternative disinfection strategies to control DW biofilms, but it is recognizable that further research is still needed to achieve an insightful understanding of their effects and practicable application in real scenarios.

In the present project, only single-species biofilms from relevant DW-isolated bacteria were evaluated. Given the high complexity and microbial biodiversity of real DW biofilms, a natural progression of this work would be to analyse the effects of disinfectants on heterogeneous biofilms of the autochthonous DW microbial community. To accomplish this, the RCR or other bench-scale biofilm reactor can be connected to drinking tap water, as well using sampling devices attached to full-scale water mains. These strategies for biofilm formation can approximate the characteristics of laboratory

biofilms to the real DW biofilms, however, some variables such as pH, conductivity, residual chlorine, heterotrophic microorganism population, total organic carbon, which are unique to each DW network, must be monitored to guarantee representativeness and reproducibility of the methods. Another disadvantage is the long experimental time necessary for biofilm formation in these conditions.

Although the results of this study revealed that the selected disinfectants were effective on biofilm control in two representative pipe materials, further experiments with other surfaces for biofilm formation, for example, cast iron, copper, and different plastic-based materials (polypropylene, polyethylene, HDPE), would be of interest. The impact of the surface material on the disinfection action, specifically the greatest performance of OXONE in the limitation of biofilm regrowth in SS, remains to be answered. Further research could usefully explore if metal leaching from SS or copper can act as a synergistic effect of disinfection by metal transition catalysis of OXONE, allowing to decrease disinfectant concentration required for biofilm control. To assess metal leaching, inductively coupled plasma mass spectrometry, flame emission, and atomic absorption spectrometry could be performed (Gomes et al., 2019; Kamerud et al., 2013).

The findings of this research indicate that the exposure to OXONE impacts the biofilm cohesiveness. To better conclude the mechanism of action against biofilms, the study of the effects on EPS production and composition and bacterial phenotypic alterations during biofilm formation would also give relevant information. Additionally, the evaluation of the effects of the combination of biofilm exposure to OXONE and water flushing would be valuable for biofilm removal.

Further work needs to be done to identify the reactive species involved in the disinfection with OXONE. Simulation of the EPR spectra (Chen et al., 2022; Timofeev

et al., 2011; Wang et al., 2022) obtained for the DMPO-radical adducts can fully elucidate the reaction mechanism of disinfection.

A study about the formation and estimated cytotoxicity of DBPs formed during OXONE disinfection would be important to minimize the formation of unintended compounds that have adverse health effects on humans. Chlorine disinfection is widely reported to promote the formation of a long list of DBPs, such as trihalomethanes, and halogenated and non-halogenated organic and inorganic compounds (Li and Mitch, 2018). Nevertheless, the difference between DBP formation during OXONE disinfection and DBP formation in chlorinated DW is a research topic that should be carefully evaluated. With this purpose, collaborative research has been established with Dr. Mourad Harir, from the Helmholtz Zentrum München.

References

Aarnisalo, K., Salo, S., Miettinen, H., Suihko, M.-L., Wirtanen, G., Autio, T., Lundén, J., Korkeala, H., Sjöberg, A.-M., 2000. Bactericidal efficiencies of commercial disinfectants against *Listeria monocytogenes* on surfaces. J. Food Saf. 20, 237–250. https://doi.org/10.1111/j.1745-4565.2000.tb00302.x

Abreu, A.C., Borges, A., Simões, L.C., Saavedra, M.J., Simões, M., 2013. Antibacterial activity of phenyl isothiocyanate on *Escherichia coli* and *Staphylococcus aureus*. Med. Chem. 9, 756–761. https://doi.org/10.2174/1573406411309050016

Aggarwal, S., Gomez-Smith, C.K., Jeon, Y., Lapara, T.M., Waak, M.B., Hozalski, R.M., 2018. Effects of chloramine and coupon material on biofilm abundance and community composition in bench-scale simulated water distribution systems and comparison with full-scale water mains. Environ. Sci. Technol. 52, 13077–13088. https://doi.org/10.1021/acs.est.8b02607

Albuquerque, M.V. da C., Ramos, R. de O., Leite, V.D., de Sousa, J.T., de Araújo, M.C.U., de Ceballos, B.S.O., Lopes, W.S., 2022. Studies of the liposolubility and the ecotoxicity of MC-LR degradation by-products using computational molecular modeling and in-vivo tests with *Chlorella vulgaris* and *Daphnia magna*. Aquat. Toxicol. 245, 106127. https://doi.org/https://doi.org/10.1016/j.aquatox.2022.106127

Alfredo, K., 2021. The "Burn": water quality and microbiological impacts related to limited free chlorine disinfection periods in a chloramine system. Water Res. 197, 117044. https://doi.org/10.1016/j.watres.2021.117044

Altman, S.J., McGrath, L.K., Souza, C.A., Murton, J.K., Camper, A.K., 2009. Integration and decontamination of *Bacillus cereus* in *Pseudomonas fluorescens* biofilms. J. Appl. Microbiol. 107, 287–299. https://doi.org/10.1111/j.1365-2672.2009.04206.x

Álvarez-Arroyo, R., Pérez, J.I., Ruiz, L.M., Gómez, M.A., 2022. Chlorination by-products formation in a drinking water distribution system treated by ultrafiltration associated with pre-ozonation or coagulation/flocculation. J. Water Process Eng. 47, 102779. https://doi.org/https://doi.org/10.1016/j.jwpe.2022.102779

Andersson, A., Harir, M., Gonsior, M., Hertkorn, N., Schmitt-Kopplin, P., Kylin, H., Karlsson, S., Ashiq, M.J., Lavonen, E., Nilsson, K., Pettersson, Ä., Stavklint, H., Bastviken, D., 2019. Waterworks-specific composition of drinking water disinfection by-products. Environ. Sci. Water Res. Technol. 5, 861–872. https://doi.org/10.1039/C9EW00034H

Anipsitakis, G.P., Tufano, T.P., Dionysiou, D.D., 2008. Chemical and microbial decontamination of pool water using activated potassium peroxymonosulfate. Water Res. 42, 2899–2910. https://doi.org/10.1016/j.watres.2008.03.002

Assaidi, A., Ellouali, M., Latrache, H., Zahir, H., Karoumi, A., Mliji, E.M., 2020. Chlorine disinfection against *Legionella pneumophila* biofilms. J. Water, Sanit. Hyg. Dev. 10, 885–893. https://doi.org/10.2166/washdev.2020.151

Batté, M., Mathieu, L., Laurent, P., Prévost, M., 2003. Influence of phosphate and disinfection on the composition of biofilms produced from drinking water, as measured by fluorescence in situ hybridization. Can. J. Microbiol. 49, 741–753. https://doi.org/10.1139/W03-094

Bertelli, C., Courtois, S., Rosikiewicz, M., Piriou, P., Aeby, S., Robert, S., Loret, J.-F., Greub, G., 2018. Reduced chlorine in drinking water distribution systems impacts bacterial biodiversity in biofilms. Front. Microbiol. 9, 1–11. https://doi.org/10.3389/fmicb.2018.02520

Borges, A., Ferreira, C., Saavedra, M.J., Simões, M., 2013. Antibacterial activity and mode of action of ferulic and gallic acids against pathogenic bacteria. Microb. Drug Resist. 19, 256–265. https://doi.org/10.1089/mdr.2012.0244

Broadwater, W.T., Hoehn, R.C., King, P.H., 1973. Sensitivity of three selected bacterial species to ozone. J. Appl. Microbiol. 26, 391–393.

Brooke, J.S., 2012. *Stenotrophomonas maltophilia*: an emerging global opportunistic pathogen. Clin. Microbiol. Rev. 25, 2–41. https://doi.org/10.1128/CMR.00019-11

Brown, D., Bridgeman, J., West, J.R., 2011. Predicting chlorine decay and THM formation in water supply systems. Rev. Environ. Sci. Bio/Technology 10, 79–99. https://doi.org/10.1007/s11157-011-9229-8

Buse, H.Y., Morris, B.J., Struewing, I.T., Szabo, J.G., 2019. Chlorine and monochloramine disinfection of *Legionella pneumophila* colonizing copper and polyvinyl chloride drinking water biofilms. Appl. Environ. Microbiol. 85, 1–16. https://doi.org/10.1128/AEM .02956-18.

Busscher, H.J., Weerkamp, A.H., van der Mei, H.C., van Pelt, A.W.J., de Jong H.P., Arends, J., 1984. Measurement of the surface free energy of bacterial cell surfaces and its relevance for adhesion. Appl. Environ. Microbiol. 48, 980–983. https://doi.org/0099-2240/84/110980-04$02.00/0

Cahoon, L.B., 2019. Water purification: Treatment of microbial contamination, in: Advances in Water Purification Techniques. Elsevier Inc., pp. 385–395. https://doi.org/10.1016/B978-0-12-814790-0.00015-6

Calero-Preciado, C., Soria-Carrasco, V., Boxall, J., Douterelo, I., 2022. Climate change and management of biofilms within drinking water distribution systems. Front. Environ. Sci. 10. https://doi.org/10.3389/fenvs.2022.962514

Camper, A.K., 1994. Coliform regrowth and biofilm accumulation in drinking water systems: A Review, in: Geesey, G.G., Lewandowski, Z., Flemming, H.-C. (Eds.), Biofouling and Biocorrosion in Industrial Water Systems. CRC Press, pp. 91–105.

Cerf, O., 1977. Tailing of survival curves of bacterial spores. J. Appl. Bacteriol. 42, 1–19. https://doi.org/10.1111/j.1365-2672.1977.tb00665.x

Chaillou, K., Gérente, C., Andrès, Y., Wolbert, D., 2011. Bathroom greywater characterization and potential treatments for reuse. Water. Air. Soil Pollut. 215, 31–42. https://doi.org/10.1007/s11270-010-0454-5

Chan, S., Pullerits, K., Keucken, A., Persson, K.M., Paul, C.J., Rådström, P., 2019. Bacterial release from pipe biofilm in a full-scale drinking water distribution system.

npj Biofilms Microbiomes 5, 3–10. https://doi.org/10.1038/s41522-019-0082-9

Characklis, W.G., Marshall, K.C., 1990. Biofilms: a basis for an interdisciplinary approach, in: Characklis, W.G., Marshall, K. (Eds.), Biofilms. John Wiley & Sons, Inc, New York.

Chen, L., Duan, J., Du, P., Sun, W., Lai, B., Liu, W., 2022. Accurate identification of radicals by in-situ electron paramagnetic resonance in ultraviolet-based homogenous advanced oxidation processes. Water Res. 221, 118747. https://doi.org/https://doi.org/10.1016/j.watres.2022.118747

Chen, X., Stewart, P.S., 2002. Role of electrostatic interactions in cohesion of bacterial biofilms. Appl. Microbiol. Biotechnol. 59, 718–720. https://doi.org/10.1007/s00253-002-1044-2

Choi, Y., Byun, S.-H., Jang, H.-J., Kim, S.-E., Choi, Y.-J., 2022. Comparison of disinfectants for drinking water: chlorine gas vs. on-site generated chlorine. Environ. Eng. Res. 27, 200540–200543. https://doi.org/10.4491/eer.2020.543

Chowdhury, D., Rahman, A., Hu, H., Jensen, S.O., Deva, A.K., Vickery, K., 2019. Effect of disinfectant formulation and organic soil on the efficacy of oxidizing disinfectants against biofilms. J. Hosp. Infect. 103, e33–e41. https://doi.org/10.1016/j.jhin.2018.10.019

Ciofu, O., Moser, C., Jensen, P.Ø., Høiby, N., 2022. Tolerance and resistance of microbial biofilms. Nat. Rev. Microbiol. 20, 621–635. https://doi.org/10.1038/s41579-022-00682-4

Ciulli, S., Volpe, E., Pagliarani, A., Zavatta, E., Brunetti, B., Gazzotti, T., Parmeggiani, A., Govoni, N., Nesci, S., Fabbri, M., Mordenti, O., Serratore, P., 2017. A preliminary study on a novel sea water disinfection process by a peroxy-acid compound to complement and improve the microbial depuration of clams (*Ruditapes philippinarum*). Food Control 80, 226–235. https://doi.org/10.1016/j.foodcont.2017.04.031

Clasen, T., Edmondson, P., 2006. Sodium dichloroisocyanurate (NaDCC) tablets as an alternative to sodium hypochlorite for the routine treatment of drinking water at the household level. Int. J. Hyg. Environ. Health 209, 173–181. https://doi.org/10.1016/j.ijheh.2005.11.004

Coroller, L., Leguerinel, I., Mettler, E., Savy, N., Mafart, P., 2006. General model, based on two mixed Weibull distributions of bacterial resistance, for describing various shapes of inactivation curves. Appl. Environ. Microbiol. 72, 6493–6502. https://doi.org/10.1128/AEM.00876-06

Craveiro, S., Alves-Barroco, C., Crespo, M.T.B., Barreto, A.S., Semedo-Lemsaddek, T., 2015. *Aeromonas* biofilm on stainless steel: efficiency of commonly used disinfectants. Int. J. Food Sci. Technol. 1–6. https://doi.org/10.1111/ijfs.12731

Cruz, M.C., Woo, Y., Flemming, H.C., Wuertz, S., 2020. Nitrifying niche differentiation in biofilms from full-scale chloraminated drinking water distribution system. Water Res. 176. https://doi.org/10.1016/j.watres.2020.115738

D'Accolti, M., Soffritti, I., Mazzacane, S., Caselli, E., 2021. Bacteriophages as a potential

360-degree pathogen control strategy. Microorganisms 9. https://doi.org/10.3390/microorganisms9020261

Dallolio, L., Scuderi, A., Rini, M.S., Valente, S., Farruggia, P., Sabattini, M.A.B., Pasquinelli, G., Acacci, A., Roncarati, G., Leoni, E., 2014. Effect of different disinfection protocols on microbial and biofilm contamination of dental unit waterlines in community dental practices. Int. J. Environ. Res. Public Health 11, 2064–2076. https://doi.org/10.3390/ijerph110202064

Deborde, M., von Gunten, U., 2008. Reactions of chlorine with inorganic and organic compounds during water treatment—Kinetics and mechanisms: A critical review. Water Res. 42, 13–51. https://doi.org/https://doi.org/10.1016/j.watres.2007.07.025

Decreto-Lei n.º 152/2017, de 7 de dezembro do Ministério do Ambiente. Diário da República n.º 235/2017, Série I de 2017-12-07, páginas 6555-6576.

Desmond, P., Best, J.P., Morgenroth, E., Derlon, N., 2018. Linking composition of extracellular polymeric substances (EPS) to the physical structure and hydraulic resistance of membrane biofilms. Water Res. 132, 211–221. https://doi.org/https://doi.org/10.1016/j.watres.2017.12.058

Dettori, M., Arghittu, A., Deiana, G., Castiglia, P., Azara, A., 2022. The revised European Directive 2020/2184 on the quality of water intended for human consumption. A step forward in risk assessment, consumer safety and informative communication. Environ. Res. 209, 112773. https://doi.org/https://doi.org/10.1016/j.envres.2022.112773

Directive (EU) 2020/2184 of the European Parliament and of the Council of 16 December 2020 on the quality of water intended for human consumption. (Text with EEA revelance) (OJ L 435, 23.12.2020, p. 1-62, ELI: http://data.europa.eu/eli/dir/2020/2184/oj)

Donlan, R.M., Costerton, J.W., 2002. Biofilms: survival mechanisms of clinically relevant microorganisms. Clin. Microbiol. Rev. 15, 167–193. https://doi.org/10.1128/CMR.15.2.167

Dubois, M., Gilles, K., Hamilton, J.K., Rebers, P.A., Smith, F., 1951. A colorimetric method for the determination of sugars. Nature 168, 167. https://doi.org/https://doi.org/10.1038/168167a0

Ebenezer, V., Ki, J.-S., 2013. Physiological and biochemical responses of the marine dinoflagellate *Prorocentrum minimum* exposed to the oxidizing biocide chlorine. Ecotoxicol. Environ. Saf. 92, 129–134. https://doi.org/https://doi.org/10.1016/j.ecoenv.2013.03.014

Ellis, K. V, 1991. Water disinfection: A review with some consideration of the requirements of the third world. Crit. Rev. Environ. Control 20, 341–407. https://doi.org/10.1080/10643389109388405

Emtiazi, F., Schwartz, T., Marten, S.M., Krolla-Sidenstein, P., Obst, U., 2004. Investigation of natural biofilms formed during the production of drinking water from surface water embankment filtration. Water Res. 38, 1197–1206. https://doi.org/10.1016/j.watres.2003.10.056

Environmental Protection Agency, 2011. Water treatment manual: Disinfection. Johnstown Castle, Co. Wexford, Ireland. ISBN: 978-184095-421-0

European Chemicals Agency (ECHA), 2023a. Pentapotassium bis(peroxymonosulphate) bis(sulphate) factsheet [WWW Document]. https://echa.europa.eu/pt/information-on-chemicals/biocidal-active-substances/-/disas/factsheet/1339/PT05 (accessed 2.20.23).

European Chemicals Agency (ECHA), 2023b. Sodium hypochlorite - toxicity to aquatic algae and cyanobacteria [WWW Document]. https://echa.europa.eu/pt/registration-dossier/-/registered-dossier/15516/6/2/6# (accessed 2.23.23).

European Chemicals Agency (ECHA), 2023c. Toxicological information of pentapotassium bis(peroxymonosulphate) bis(sulphate) [WWW Document]. https://echa.europa.eu/pt/registration-dossier/-/registered-dossier/15990/7/6/1 (accessed 2.23.23).

European Chemicals Agency (ECHA), 2022a. Symclosen factsheet [WWW Document]. https://echa.europa.eu/pt/information-on-chemicals/biocidal-active-substances/-/disas/factsheet/1395/PT05 (accessed 2.20.23).

European Chemicals Agency (ECHA), 2022b. Sodium dichloroisocyanurate dihydrate factsheet [WWW Document]. https://echa.europa.eu/pt/information-on-chemicals/biocidal-active-substances/-/disas/factsheet/1219/PT05 (accessed 2.20.23).

European Chemicals Agency (ECHA), 2020. Article 95 List of active substances and product suppliers [WWW Document]. https://echa.europa.eu/pt/information-on-chemicals/active-substance-suppliers (accessed 7.30.20).

European Standard, 1997. Chemical disinfectants and antiseptics - Quantitative suspension test for the evaluation of bactericidal activity of chemical disinfectants and antiseptics used in food, industrial, domestic, and institutional areas - Test method and requirements (phase 2, step 1).

Farhat, N., Kim, L., Mineta, K., Alarawi, M., Gojobori, T., Saikaly, P., Vrouwenvelder, J., 2022. Seawater desalination based drinking water: Microbial characterization during distribution with and without residual chlorine. Water Res. 210, 117975. https://doi.org/https://doi.org/10.1016/j.watres.2021.117975

Farkas, A., Bocos, B., Bularda, M.D., Craciunas, C., 2014. Effect of different disinfectants against biofilm bacteria. Stud. Univ. Babes-Bolyai Biol. LIX 1, 5–20.

Feng, K., Li, Q., 2022. Chloride-enhanced removal of ammonia nitrogen and organic matter from landfill leachate by a microwave/peroxymonosulfate system. Catalysts. https://doi.org/10.3390/catal12101078

Fernandes, S., Gomes, I.B., Simões, M., 2022. Antibiofilm activity of glycolic acid and glyoxal and their diffusion–reaction interactions with biofilm components. Food Res. Int. 152, 110921. https://doi.org/10.1016/j.foodres.2021.110921

Fish, K.E., Boxall, J.B., 2018. Biofilm microbiome (re)growth dynamics in drinking water distribution systems are impacted by chlorine concentration. Front. Microbiol. 9, 1–21. https://doi.org/10.3389/fmicb.2018.02519

Fish, K.E., Reeves-McLaren, N., Husband, S., Boxall, J., 2020. Unchartered waters: the unintended impacts of residual chlorine on water quality and biofilms. npj Biofilms Microbiomes 6, 34. https://doi.org/10.1038/s41522-020-00144-w

Flemming, H.-C., Wuertz, S., 2019. Bacteria and archaea on Earth and their abundance in biofilms. Nat. Rev. Microbiol. 17, 247–260. https://doi.org/10.1038/s41579-019-0158-9

Frølund, B., Palmgren, R., Keiding, K., Nielsen, P.H., 1996. Extraction of extracellular polymers from activated sludge using a cation exchange resin. Water Res. 30, 1749–1758. https://doi.org/https://doi.org/10.1016/0043-1354(95)00323-1

Fu, Y., Peng, H., Liu, J., Nguyen, T.H., Hashmi, M.Z., Shen, C., 2021. Occurrence and quantification of culturable and viable but non-culturable (VBNC) pathogens in biofilm on different pipes from a metropolitan drinking water distribution system. Sci. Total Environ. 764, 142851. https://doi.org/https://doi.org/10.1016/j.scitotenv.2020.142851

Fukuzaki, S., 2006. Mechanisms of actions of sodium hypochlorite in cleaning and disinfection processes. Biocontrol Sci. 11, 147–157. https://doi.org/10.4265/bio.11.147

Gabe, D.R., Walsh, F.C., 1983. The rotating cylinder electrode: a review of development. J. Appl. Electrochem. 13, 3–21. https://doi.org/10.1007/BF00615883

Gagnon, G.A., 2002. Biofilm control in drinking water distribution systems, in: American Chemistry Council, Sodium Chlorite-Chlorine Dioxide Panel, Awwa Research Foundation (Eds.), Chlorine dioxide: The state of science, regulatory, environmental issues, and case histories - Proceedings of the fourth intenational symposium. Awwa Research Foundation and the American Water Works Association, Las Vegas, 71–86. ISBN: 1-58321-180-2

Gales, A.C., Jones, R.N., Forward, K.R., Liñares, J., Sader, H.S., Verhoef, J., 2001. Emerging importance of multidrug-resistant *Acinetobacter* species and *Stenotrophomonas maltophilia* as pathogens in seriously ill patients: geographic patterns, epidemiological features, and trends in the SENTRY Antimicrobial Surveillance Program (1997-1999). Clin. Infect. Dis. 32. https://doi.org/10.1086/320183

Gao, L., Guo, Y., Zhan, J., Yu, G., Wang, Y., 2022. Assessment of the validity of the quenching method for evaluating the role of reactive species in pollutant abatement during the persulfate-based process. Water Res. 221, 118730. https://doi.org/https://doi.org/10.1016/j.watres.2022.118730

Garvey, M., Rabbitt, D., Stocca, A., Rowan, N., 2015. Pulsed ultraviolet light inactivation of *Pseudomonas aeruginosa* and *Staphylococcus aureus biofilms*. Water Environ. J. 29, 36–42. https://doi.org/10.1111/wej.12088

Geeraerd, A.H., Valdramidis, V.P., Van Impe, J.F., 2005. GInaFiT, a freeware tool to assess non-log-linear microbial survivor curves. Int. J. Food Microbiol. 102, 95–105. https://doi.org/10.1016/j.ijfoodmicro.2004.11.038

Ghanbari, F., Moradi, M., 2017. Application of peroxymonosulfate and its activation methods for degradation of environmental organic pollutants: Review. Chem. Eng.

J. 310, 41–62. https://doi.org/10.1016/j.cej.2016.10.064

Gloag, E.S., German, G.K., Stoodley, P., Wozniak, D.J., 2018. Viscoelastic properties of *Pseudomonas aeruginosa* variant biofilms. Sci. Rep. 8, 9691. https://doi.org/10.1038/s41598-018-28009-5

Gomes, I.B., Lemos, M., Mathieu, L., Simões, M., Simões, L.C., 2018a. The action of chemical and mechanical stresses on single and dual species biofilm removal of drinking water bacteria. Sci. Total Environ. 631–632, 987–993. https://doi.org/10.1016/j.scitotenv.2018.03.042

Gomes, I.B., Simoes, L.C., Simoes, M., 2019. The role of surface copper content on biofilm formation by drinking water bacteria. RSC Adv. 9, 32184–32196. https://doi.org/10.1039/c9ra05880j

Gomes, I.B., Simoes, L.C., Simoes, M., 2018b. The effects of emerging environmental contaminants on *Stenotrophomonas maltophilia* isolated from drinking water in planktonic and sessile states. Sci. Total Environ. 643, 1348–1356. https://doi.org/10.1016/j.scitotenv.2018.06.263

Gomes, I.B., Simões, L.C., Simões, M., 2020. Influence of surface copper content on *Stenotrophomonas maltophilia* biofilm control using chlorine and mechanical stress. Biofouling 36, 1–13. https://doi.org/10.1080/08927014.2019.1708334

Gomes, I.B., Simões, M., Simões, L.C., 2016. The effects of sodium hypochlorite against selected drinking water-isolated bacteria in planktonic and sessile states. Sci. Total Environ. 565, 40–48. https://doi.org/10.1016/j.scitotenv.2016.04.136

Gomes, I.B., Simões, M., Simões, L.C., 2014. An overview on the reactors to study drinking water biofilms. Water Res. 62, 63–87. https://doi.org/10.1016/j.watres.2014.05.039

Gomez-Smith, C.K., LaPara, T.M., Hozalski, R.M., 2015. Sulfate reducing bacteria and mycobacteria dominate the biofilm communities in a chloraminated drinking water distribution system. Environ. Sci. Technol. 49, 8432–8440. https://doi.org/10.1021/acs.est.5b00555

Gompertz, B., 1825. On the nature of the function expressive of the law of human mortality, and on a new mode of determining the value of life contingencies. Philos. Trans. R. Soc. London 115, 513–583.

Gora, S.L., Rauch, K.D., Ontiveros, C.C., Stoddart, A.K., Gagnon, G.A., 2019. Inactivation of biofilm-bound *Pseudomonas aeruginosa* bacteria using UVC light emitting diodes (UVC LEDs). Water Res. 151, 193–202. https://doi.org/10.1016/j.watres.2018.12.021

Gosselin, F., Madeira, L.M., Juhna, T., Block, J.C., 2013. Drinking water and biofilm disinfection by Fenton-like reaction. Water Res. 47, 5631–5638. https://doi.org/10.1016/j.watres.2013.06.036

Gröschel, M.I., Meehan, C.J., Barilar, I., Diricks, M., Gonzaga, A., Steglich, M., Conchillo-Solé, O., Scherer, I.-C., Mamat, U., Luz, C.F., De Bruyne, K., Utpatel, C., Yero, D., Gibert, I., Daura, X., Kampmeier, S., Rahman, N.A., Kresken, M., van der Werf, T.S., Alio, I., Streit, W.R., Zhou, K., Schwartz, T., Rossen, J.W.A., Farhat,

M.R., Schaible, U.E., Nübel, U., Rupp, J., Steinmann, J., Niemann, S., Kohl, T.A., 2020. The phylogenetic landscape and nosocomial spread of the multidrug-resistant opportunist *Stenotrophomonas maltophilia*. Nat. Commun. 11, 2044. https://doi.org/10.1038/s41467-020-15123-0

Haas, C.M., Engelbrecht, R.S., 1980. Physiological alterations of vegetative microorganisms resulting from chlorination. J. Water Pollut. Control Fed. 52, 1976–1989.

Haas, C.N., 1999. Benefits of using a disinfectant residual. J. Am. Water Work. Assoc. 91, 65–69. https://doi.org/10.1002/j.1551-8833.1999.tb08569.x

Hallam, N.B., West, J.R., Forster, C.F., Powell, J.C., Spencer, I., 2002. The decay of chlorine associated with the pipe wall in water distribution systems. Water Res. 36, 3479–3488. https://doi.org/https://doi.org/10.1016/S0043-1354(02)00056-8

Hamblin, M.R., Hasan, T., 2004. Photodynamic therapy: a new antimicrobial approach to infectious disease? Photochem. Photobiol. Sci. Off. J. Eur. Photochem. Assoc. Eur. Soc. Photobiol. 3, 436–450. https://doi.org/10.1039/b311900a

Hemdan, B., Azab El-Liethy, M., El-Taweel, G.E., 2020. The destruction of *Escherichia coli* adhered to pipe surfaces in a model drinking water distribution system via various antibiofilm agents. Water Environ. Res. 92, 2155–2167. https://doi.org/10.1002/wer.1388

Hemdan, B.A., El-Taweel, G.E., Goswami, P., Pant, D., Sevda, S., 2021. The role of biofilm in the development and dissemination of ubiquitous pathogens in drinking water distribution systems: an overview of surveillance, outbreaks, and prevention. World J. Microbiol. Biotechnol. 37, 1–18. https://doi.org/10.1007/s11274-021-03008-3

Hindré, T., Brüggemann, H., Buchrieser, C., Héchard, Y., 2008. Transcriptional profiling of *Legionella pneumophila* biofilm cells and the influence of iron on biofilm formation. Microbiology 154, 30–41. https://doi.org/https://doi.org/10.1099/mic.0.2007/008698-0

Horvat, M., Pannuri, A., Romeo, T., Dogsa, I., Stopar, D., 2019. Viscoelastic response of *Escherichia coli* biofilms to genetically altered expression of extracellular matrix components. Soft Matter 15, 5042–5051. https://doi.org/10.1039/c9sm00297a

Hozalski, R.M., Bouwer, E.J., Goel, S., 1999. Removal of natural organic matter (NOM) from drinking water supplies by ozone-biofiltration. Water Sci. Technol. 40, 157–163. https://doi.org/https://doi.org/10.1016/S0273-1223(99)00652-6

Huo, L., Zhao, S., Shi, B., He, S., Wang, H., 2021. Effects of GAC and UV/H_2O_2 -GAC filtration on the bacterial community and opportunistic pathogens in simulated drinking water systems. Environ. Sci. Water Res. Technol. 7, 1611–1621. https://doi.org/10.1039/D1EW00222H

Husband, P.S., Boxall, J.B., 2011. Asset deterioration and discolouration in water distribution systems. Water Res. 45, 113–124. https://doi.org/https://doi.org/10.1016/j.watres.2010.08.021

Inkinen, J., Jayaprakash, B., Ahonen, M., Pitkänen, T., Mäkinen, R., Pursiainen, A.,

Domingo, J.W.S., Salonen, H., Elk, M., Keinänen-Toivola, M.M., 2017. Bacterial community changes in copper and PEX drinking water pipeline biofilms under extra disinfection and magnetic water treatment. J. Appl. Microbiol. 124, 610–623. https://doi.org/10.1111/jam.13662

Inkinen, J., Jayaprakash, B., Siponen, S., Hokajarvi, A.M., Pursiainen, A., Ikonen, J., Ryzhikov, I., Taubel, M., Kauppinen, A., Paananen, J., Miettinen, I.T., Torvinen, E., Kolehmainen, M., Pitkanen, T., 2019. Active eukaryotes in drinking water distribution systems of ground and surface waterworks. Microbiome 7. https://doi.org/10.1186/s40168-019-0715-5

Inkinen, J., Siponen, S., Jayaprakash, B., Tiwari, A., Hokajärvi, A.-M., Pursiainen, A., Ikonen, J., Kauppinen, A., Miettinen, I.T., Paananen, J., Torvinen, E., Kolehmainen, M., Pitkänen, T., 2021. Diverse and active archaea communities occur in non-disinfected drinking water systems–Less activity revealed in disinfected and hot water systems. Water Res. X 12, 100101. https://doi.org/10.1016/j.wroa.2021.100101

Janczuk, B., Chibowski, E., Bruque, J.M., Kerkeb, M.L., González Caballero, F., 1993. On the consistency of surface free energy components as calculated from contact angles of different liquids: an application to the cholesterol surface. J. Colloid Interface Sci. 159, 421–428.

Jara, J., Alarcón, F., Monnappa, A.K., Santos, J.I., Bianco, V., Nie, P., Ciamarra, M.P., Canales, Á., Dinis, L., López-Montero, I., Valeriani, C., Orgaz, B., 2021. Self-adaptation of *Pseudomonas fluorescens* biofilms to hydrodynamic stress. Front. Microbiol. 11, 588884. https://doi.org/10.3389/fmicb.2020.588884

Jones, W.L., Sutton, M.P., McKittrick, L., Stewart, P.S., 2011. Chemical and antimicrobial treatments change the viscoelastic properties of bacterial biofilms. Biofouling 27, 207–215. https://doi.org/10.1080/08927014.2011.554977

Jungfer, C., Friedrich, F., Villarreal, J.V., Brändle, K., Gross, H.-J., Obst, U., Schwartz, T., 2013. Drinking water biofilms on copper and stainless steel exhibit specific molecular responses towards different disinfection regimes at waterworks. Biofouling 29, 891–907. https://doi.org/10.1080/08927014.2013.813936

Kamerud, K.L., Hobbie, K.A., Anderson, K.A., 2013. Stainless steel leaches nickel and chromium into foods during cooking. J. Agric. Food Chem. 61, 9495–9501. https://doi.org/10.1021/jf402400v

Kavanagh, G.M., Ross-Murphy, S.B., 1998. Rheological characterisation polymer gels. Prog. Polym. Sci. 23, 533–562. https://doi.org/10.1016/S0079-6700(97)00047-6

Kekeç, Ö., Gökalsin, B., Karalti, I., Kayhan, F.E., Sesal, N.C., 2016. Effects of chlorine stress on *Pseudomonas aeruginosa* biofilm and analysis of related gene expressions. Curr. Microbiol. 73, 228–235. https://doi.org/10.1007/s00284-016-1056-2

Kelly, J.J., Minalt, N., Culotti, A., Pryor, M., Packman, A., 2014. Temporal variations in the abundance and composition of biofilm communities colonizing drinking water distribution pipes. PLoS One 9, e98542. https://doi.org/10.1371/journal.pone.0098542

Keshvardoust, P., Huron, V.A.A., Clemson, M., Barraud, N., Rice, S.A., 2020. Nitrite

production by ammonia-oxidizing bacteria mediates chloramine decay and resistance in a mixed-species community. Microb. Biotechnol. 13, 1847–1859. https://doi.org/10.1111/1751-7915.13628

Khan, S., Beattie, T.K., Knapp, C.W., 2019. Rapid selection of antimicrobial - resistant bacteria in complex water systems by chlorine and pipe materials. Environ. Chem. Lett. 17, 1367–1373. https://doi.org/10.1007/s10311-019-00867-z

Kiéné, L., Lu, W., Lévi, Y., 1998. Relative importance of the phenomena responsible for chlorine decay in drinking water distribution systems. Water Sci. Technol. 38, 219–227. https://doi.org/https://doi.org/10.1016/S0273-1223(98)00583-6

Kim, C.M., Kim, S.J., LH, K., Shin, M.S., Yu, H.W., Kim, I.S., 2014. Effects of phosphate limitation in feed water on biofouling in forward osmosis (FO) process. Desalination 349, 51–59. https://doi.org/10.1016/j.desal.2014.06.013

Kuechler, T.C., 2009. Use of chlorinated isocyanurates for drinking water chlorination, in: Proceedings of the Water Environment Federation. pp. 942–949. https://doi.org/10.2175/193864709793848356

Långmark, J., Storey, M. V, Ashbolt, N.J., Stenström, T.-A., 2005. Accumulation and fate of microorganisms and microspheres in biofilms formed in a pilot-scale water distribution system. Appl. Environ. Microbiol. 71, 706–712. https://doi.org/10.1128/AEM.71.2.706

Learbuch, K.L.G., Smidt, H., van der Wielen, P.W.J.J., 2021. Influence of pipe materials on the microbial community in unchlorinated drinking water and biofilm. Water Res. 194, 116922. https://doi.org/https://doi.org/10.1016/j.watres.2021.116922

LeChevallier, M.W., Au, K.-K., 2004. Water treatment and pathogen control - Process efficiency in acheiving safe drinking water. Published on behalf of the World Health Organization by IWA Publishing, London.

LeChevallier, M.W., Cawthon, C.D., Lee, R.G., 1988. Inactivation of Biofilm Bacteria. Appl. Environ. Microbiol. 54, 2492–2499.

LeChevallier, M.W., Lowry, C.D., Lee, R.G., 1990. Disinfecting biofilms in a model distribution system. J. Am. Water Work. Assoc. 82, 87–99. https://doi.org/10.1002/j.1551-8833.1990.tb06996.x

Lee, H.-J., Kim, H.-E., Kim, M.S., de Lannoy, C.-F., Lee, C., 2020a. Inactivation of bacterial planktonic cells and biofilms by Cu(II)-activated peroxymonosulfate in the presence of chloride ion. Chem. Eng. J. 380, 122468. https://doi.org/https://doi.org/10.1016/j.cej.2019.122468

Lee, J., Mackeyev, Y., Cho, M., Li, D., Kim, J.-H., Wilson, L.J., Alvarez, P.J.J., 2009. Photochemical and antimicrobial properties of novel C60 derivatives in aqueous systems. Environ. Sci. Technol. 43, 6604–6610. https://doi.org/10.1021/es901501k

Lee, J., Von Gunten, U., Kim, J.H., 2020. Persulfate-based advanced oxidation: Critical assessment of opportunities and roadblocks. Environ. Sci. Technol. 54, 3064–3081. https://doi.org/10.1021/acs.est.9b07082

Lemos, M., Gomes, I., Mergulhão, F., Melo, L., Simões, M., 2015. The effects of surface type on the removal of *Bacillus cereus* and *Pseudomonas fluorescens* single and dual

species biofilms. Food Bioprod. Process. 93, 234–241. https://doi.org/10.1016/j.fbp.2014.08.009

Li, N., Li, X., Yang, Y., Shang, S., Fan, X., Liu, Y., Zhao, L., Zhou, Z., 2020. Secondary disinfection ensures biosafety of domestic hot water and its impact on biofilm bacterial community. Desalin. Water Treat. 173, 186–196. https://doi.org/10.5004/dwt.2020.24818

Li, R.A., McDonald, J.A., Sathasivan, A., Khan, S.J., 2019. Disinfectant residual stability leading to disinfectant decay and by-product formation in drinking water distribution systems: A systematic review. Water Res. 153, 335–348. https://doi.org/10.1016/j.watres.2019.01.020

Li, W., Tan, Q., Zhou, W., Chen, J., Li, Y., Wang, F., Zhang, J., 2020a. Impact of substrate material and chlorine/chloramine on the composition and function of a young biofilm microbial community as revealed by high-throughput 16S rRNA sequencing. Chemosphere 242, 125310. https://doi.org/10.1016/j.chemosphere.2019.125310

Li, X.-F., Mitch, W.A., 2018. Drinking water disinfection byproducts (DBPs) and human health effects: Multidisciplinary challenges and opportunities. Environ. Sci. Technol. 52, 1681–1689. https://doi.org/10.1021/acs.est.7b05440

Li, X., Wang, H., Zhang, Y., Hu, C., Yang, M., 2014. Characterization of the bacterial communities and iron corrosion scales in drinking groundwater distribution systems with chlorine/chloramine. Int. Biodeterior. Biodegradation 96, 71–79. https://doi.org/10.1016/j.ibiod.2014.09.014

Liedtke, A., 2013. Sodium hypochlorite: toxicity to *Pseudokirchneriella subcapitata* in a 72-hour algal growth inhibition test. Harlan Laboraties Ltd., Switserland, Euro Chlor.

Lieleg, O., Caldara, M., Baumgartel, R., Ribbeck, K., 2011. Mechanical robustness of *Pseudomonas aeruginosa* biofilms. Soft Matter 7, 3307–3314. https://doi.org/10.1039/c0sm01467b.Mechanical

Ling, F., Liu, W.-T., 2013. Impact of chloramination on the development of laboratory-grown biofilms fed with filter-pretreated groundwater. Microbes Environ. 28, 50–57. https://doi.org/10.1264/jsme2.ME12095

Liu, L., Xing, X., Hu, C., Wang, H., Lyu, L., 2019a. Effect of sequential UV/free chlorine disinfection on opportunistic pathogens and microbial community structure in simulated drinking water distribution systems. Chemosphere 219, 971–980. https://doi.org/10.1016/j.chemosphere.2018.12.067

Liu, L.Z., Xing, X.C., Hu, C., Wang, H.B., 2019b. O_3-BAC-Cl_2 : A multi-barrier process controlling the regrowth of opportunistic waterborne pathogens in drinking water distribution systems. J. Environ. Sci. 76, 142–153. https://doi.org/10.1016/j.jes.2018.04.017

Liu, S., Gunawan, C., Barraud, N., Rice, S.A., Harry, E.J., Amal, R., 2016. Understanding, monitoring, and controlling biofilm growth in drinking water distribution systems. Environ. Sci. Technol. 50, 8954–8976. https://doi.org/10.1021/acs.est.6b00835

Liu, Y., Tay, J.H., 2002. The essential role of hydrodynamic shear force in the formation of biofilm and granular sludge. Water Res. 36, 1653–1665. https://doi.org/10.1016/S0043-1354(01)00379-7

Liu, Y., Wang, L., Dong, Y., Peng, W., Fu, Y., Li, Q., Fan, Q., Wang, Y., Wang, Z., 2021. Current analytical methods for the determination of persulfate in aqueous solutions: A historical review. Chem. Eng. J. 416. https://doi.org/10.1016/j.cej.2021.129143

Lopes, J.C., Moniz, T., Sampaio, M.J., Silva, C.G., Rangel, M., Faria, J.L., 2023. Efficient synthesis of imines using carbon nitride as photocatalyst. Catal. Today 418, 114045. https://doi.org/https://doi.org/10.1016/j.cattod.2023.114045

López-Galindo, C., Garrido, M.C., Casanueva, J.F., Nebot, E., 2010. Degradation models and ecotoxicity in marine waters of two antifouling compounds: Sodium hypochlorite and an alkylamine surfactant. Sci. Total Environ. 408, 1779–1785. https://doi.org/https://doi.org/10.1016/j.scitotenv.2010.01.029

Lowry, O.H., Rosebrough, N.J., Farr, A.L., Randall, R.J., 1951. Protein measurement with the folin phenol reagent. J. Biol. Chem. 193, 265–275. https://doi.org/https://doi.org/10.1016/S0021-9258(19)52451-6

Lugo, J.L., Lugo, E.R., De La Puente, M., 2021. A systematic review of microorganisms as indicators of recreational water quality in natural and drinking water systems. J. Water Health 19, 20–28. https://doi.org/10.2166/WH.2020.179

Luo, L.-W., Wu, Y.-H., Yu, T., Wang, Y.-H., Chen, G.-Q., Tong, X., Bai, Y., Xu, C., Wang, H.-B., Ikuno, N., Hu, H.-Y., 2021. Evaluating method and potential risks of chlorine-resistant bacteria (CRB): A review. Water Res. 188, 116474. https://doi.org/10.1016/j.watres.2020.116474

Ma, B., Seyedi, S., Wells, E., McCarthy, D., Crosbie, N., Linden, K.G., 2022. Inactivation of biofilm-bound bacterial cells using irradiation across UVC wavelengths. Water Res. 217, 118379. https://doi.org/https://doi.org/10.1016/j.watres.2022.118379

Ma, X., Li, G., Chen, R., Yu, Y., Tao, H., Zhang, G., Shi, B., 2020. Revealing the changes of bacterial community from water source to consumers tap: A full-scale investigation in eastern city of China. J. Environ. Sci. 87, 331–340. https://doi.org/10.1016/j.jes.2019.07.017

Maes, S., Vackier, T., Huu, S.N., Heyndrickx, M., Steenackers, H., Sampers, I., Raes, K., Verplaetse, A., De Reu, K., 2019. Occurrence and characterisation of biofilms in drinking water systems of broiler houses. BMC Microbiol. 19. https://doi.org/10.1186/s12866-019-1451-5

Magin, V., Garrec, N., Andrés, Y., 2019. Selection of bacteriophages to control *in vitro* 24 h old biofilm of *Pseudomonas aeruginosa* isolated from drinking and thermal water. Viruses 11, 749. https://doi.org/10.3390/v11080749

Mancilla, E., Palacios-Muñoz, A., Salinas-Vázquez, M., Vicente, W., Ascanio, G., 2019. A level set method for capturing interface deformation in immiscible stratified fluids. Int. J. Heat Fluid Flow 76, 170–186. https://doi.org/https://doi.org/10.1016/j.ijheatfluidflow.2019.01.014

Manjón, F., Villén, L., García-Fresnadillo, D., Orellana, G., 2008. On the factors

influencing the performance of solar reactors for water disinfection with photosensitized singlet oxygen. Environ. Sci. Technol. 42, 301–307. https://doi.org/10.1021/es071762y

Matamoros, V., Uggetti, E., García, J., Bayona, J.M., 2016. Assessment of the mechanisms involved in the removal of emerging contaminants by microalgae from wastewater: a laboratory scale study. J. Hazard. Mater. 301, 197–205. https://doi.org/https://doi.org/10.1016/j.jhazmat.2015.08.050

Mathieu, L., Bertrand, I., Abe, Y., Angel, E., Block, J.C., Skali-lami, S., Francius, G., 2014. Drinking water biofilm cohesiveness changes under chlorination or hydrodynamic stress. Water Res. 55, 175–184. https://doi.org/10.1016/j.watres.2014.01.054

Meier, T., Bendinger, B., 2016. Survival of pathogens in drinking water plumbing systems: impact factors and sanitation options. Water Sci. Technol. Water Supply 16.4, 931–941. https://doi.org/10.2166/ws.2016.040

Meireles, A., Ferreira, C., Melo, L., Simões, M., 2017. Comparative stability and efficacy of selected chlorine-based biocides against *Escherichia coli* in planktonic and biofilm states. Food Res. Int. 102, 511–518. https://doi.org/10.1016/j.foodres.2017.09.033

Menetrey, Q., Sorlin, P., Jumas-Bilak, E., Chiron, R., Dupont, C., Marchandin, H., 2021. *Achromobacter xylosoxidans* and *Stenotrophomonas maltophilia*: Emerging pathogens well-armed for life in the cystic fibrosis patients' lung. Genes (Basel). https://doi.org/10.3390/genes12050610

Mezule, L., Denisova, V., Briedis, A., Reimanis, M., Ozolins, J., Juhna, T., 2015. Disinfection effect of electrochemically generated chlorine on surface associated *Escherichia coli* in a drinking water system. Desalin. Water Treat. 53, 3704–3710. https://doi.org/10.1080/19443994.2013.873742

Miao, X., Han, X., Liu, C., Bai, X., 2022. Intrinsic chlorine resistance of bacteria modulated by glutaminyl-tRNA biosynthesis in drinking water supply systems. Chemosphere 308, 136322. https://doi.org/10.1016/j.chemosphere.2022.136322

Miller, H.C., Wylie, J., Dejean, G., Kaksonen, A.H., Sutton, D., Braun, K., Puzon, G.J., 2015. Reduced efficiency of chlorine disinfection of *Naegleria fowleri* in a drinking water distribution biofilm. Environ. Sci. Technol. 49, 11125–11131. https://doi.org/10.1021/acs.est.5b02947

Mir, J., Morató, J., Ribas, F., 1997. Resistance to chlorine of freshwater bacterial strains. J. Appl. Microbiol. 82, 7–18. https://doi.org/10.1111/j.1365-2672.1997.tb03292.x

Mirnasab, M.A., Hashemi, H., Samaei, M.R., Azhdarpoor, A., 2021. Advanced removal of water NOM by pre-ozonation, enhanced coagulation and bio-augmented granular activated carbon. Int. J. Environ. Sci. Technol. 18, 3143–3152. https://doi.org/10.1007/s13762-020-03039-7

Miyaji, A., Gabe, Y., Kohno, M., Baba, T., 2017. Generation of hydroxyl radicals and singlet oxygen during oxidation of rhododendrol and rhododendrol-catechol. J. Clin. Biochem. Nutr. 60, 86–92. https://doi.org/10.3164/jcbn.16-38

Mohammadi, A., Dobaradaran, S., Schmidt, T.C., Malakootian, M., Spitz, J., 2022. Emerging contaminants migration from pipes used in drinking water distribution systems: a review of the scientific literature. Environ. Sci. Pollut. Res. 29, 75134–75160. https://doi.org/10.1007/s11356-022-23085-7

Moher, D., Liberati, A., Tetzlaff, J., Altman, D.G., 2009. Preferred reporting items for systematic reviews and meta-analyses: the PRISMA statement. PLoS Med. 6, e1000097. https://doi.org/10.1371/journal.pmed.1000097

Moreira, J., Teodósio, J., Silva, F., Simões, M., Melo, L., Mergulhão, F., 2013. Influence of flow rate variation on the development of *Escherichia coli* biofilms. Bioprocess Biosyst. Eng. 36, 1787–1796. https://doi.org/10.1007/s00449-013-0954-y

Morgenthau, A., Nicolae, A.M., Laursen, A.E., Foucher, D.A., Wolfaardt, G.M., Hausner, M., 2012. Assessment of the working range and effect of sodium dichloroisocyanurate on *Pseudomonas aeruginosa* biofilms and planktonic cells. Biofouling 28, 111–120. https://doi.org/10.1080/08927014.2011.654335

Moye, Z.D., Woolston, J., Sulakvelidze, A., 2018. Bacteriophage applications for food production and processing. Viruses 10. https://doi.org/10.3390/v10040205

Munoz, S., Trueman, B.F., Li, B., Gagnon, G.A., 2022. Effect of sodium silicate on drinking water biofilm development. Environ. Sci. Water Res. Technol. 8, 1300–1311. https://doi.org/10.1039/D1EW00682G

Murphy, J.L., Arrowood, M.J., Lu, X., Hlavsa, M.C., Beach, M.J., Hill, V.R., 2015. Effect of cyanuric acid on the inactivation of *Cryptosporidium parvum* under hyperchlorination conditions. Environ. Sci. Technol. 49, 7348–7355. https://doi.org/10.1021/acs.est.5b00962

Murray, K.E., Manitou-Alvarez, E.I., Inniss, E.C., Healy, F.G., Bodour, A.A., 2015. Assessment of oxidative and UV-C treatments for inactivating bacterial biofilms from groundwater wells. Front. Environ. Sci. Eng. 9, 39–49. https://doi.org/10.1007/s11783-014-0699-0

National Toxicology Program (NTP), 1992. Toxicology and carcinogenesis studies of chlorinated water (CAS Nos. 7782-50-5 and 7681-52-9) and chloraminated water (CAS No. 10599-90-3) (deionized and charcoal-filtered) in F344/N Rats and B6C3F1 Mice (drinking water studies). Technical report series. 392, 1–466.

Navada, S., Knutsen, M.F., Bakke, I., Vadstein, O., 2020. Nitrifying biofilms deprived of organic carbon show higher functional resilience to increases in carbon supply. Sci. Rep. 10, 7121. https://doi.org/10.1038/s41598-020-64027-y

Ng, W.J., Tan, C.T., Bae, S., 2021. Effects of monochloramine on culturability, viability and persistence of *Pseudomonas putida* and tap water mixed bacterial community. Appl. Microbiol. Biotechnol. 105, 3799–3810. https://doi.org/10.1007/s00253-021-11251-9

Nizer, W.S. da C., Inkovskiy, V., Overhage, J., 2020. Surviving reactive chlorine stress: Responses of gram-negative bacteria to hypochlorous acid. Microorganisms 8, 1–27. https://doi.org/10.3390/microorganisms8081220

Novak Babič, M., Gostinčar, C., Gunde-Cimerman, N., 2020. Microorganisms populating

the water-related indoor biome. Appl. Microbiol. Biotechnol. 104, 6443–6462. https://doi.org/10.1007/s00253-020-10719-4

NSF, 2018. Drinking water treatment chemicals - Health effects of trichloroisocyanuric acid [WWW Document]. The Public Healthe Safety Organization http://info.nsf.org/Certified/PwsChemicals/Listings.asp?ChemicalName=Trichloroisocyanuric+Acid& (accessed 11.22.20).

OECD, 2011. OECD Guidelines for the testing of chemicals, freshwater alga and cyanobacteria, growth inhibition test [WWW Document]. https://www.oecd.org/chemicalsafety/testing/1946914.pdf

Ohashi, A., de Silva, D. V, Mobarry, B., Manem, J.A., Stahl, D., Rittmann, B.E., 1995. Influence of substrate C/N ratio on the structure of multi-species biofilms consisting of nitrifiers and heterotrophs. Water Sci. Technol. 32, 75–84. https://doi.org/10.1016/0273-1223(96)00010-8

Oliveira, I.M., Gomes, I.B., Simoes, L.C., Simoes, M., 2022. Chlorinated cyanurates and potassium salt of peroxymonosulphate as antimicrobial and antibiofilm agents for drinking water disinfection. Sci. Total Environ. 811. https://doi.org/10.1016/j.scitotenv.2021.152355

Olmez-Hanci, T., Arslan-Alaton, I., Dursun, D., 2014. Investigation of the toxicity of common oxidants used in advanced oxidation processes and their quenching agents. J. Hazard. Mater. 278, 330–335. https://doi.org/https://doi.org/10.1016/j.jhazmat.2014.06.021

Olson, B.H., Nagy, L.A., 1984. Microbiology of potable water, advances in applied microbiology. Academic Press. https://doi.org/10.1016/S0065-2164(08)70053-4

Pan, R., Zhang, K., Cen, C., Zhou, X., Xu, J., Wu, J., Wu, X., 2021. Characteristics of biostability of drinking water in aged pipes after water source switching: ATP evaluation, biofilms niches and microbial community transition. Environ. Pollut. 271, 116293. https://doi.org/https://doi.org/10.1016/j.envpol.2020.116293

Pandit, S., Fazilati, M., Gaska, K., Derouiche, A., Nypelö, T., Mijakovic, I., Kádár, R., 2020. The exo-polysaccharide component of extracellular matrix is essential for the viscoelastic properties of *Bacillus subtilis* biofilms. Int. J. Mol. Sci. 21, 6755. https://doi.org/10.3390/ijms21186755

Parasion, S., Kwiatek, M., Gryko, R., Mizak, L., Malm, A., 2014. Bacteriophages as an alternative strategy for fighting biofilm development. Polish J. Microbiol. 63, 137–145.

Pedersen, K., 1990. Biofilm development on stainless steel and PVC surfaces in drinking water. Water Res. 24, 239–243. https://doi.org/10.1016/0043-1354(90)90109-J

Pelleieux, S., Mathieu, L., Block, J.C., Gantzer, C., Bertrand, I., 2016. The effect of chlorination and hydrodynamic shear stress on the persistence of bacteriophages associated with drinking water biofilms. J. Appl. Microbiol. 121, 1189–1197. https://doi.org/10.1111/jam.13243

Penna, T.C., Mazzola, P.G., Silva Martins, A.M., 2001. The efficacy of chemical agents in cleaning and disinfection programs. BMC Infect. Dis. 1, 1–16.

https://doi.org/10.1186/1471-2334-1-16

Pérez, M.F.L., Cárdenas, J.A., Leon, A.J.M., Susa, M.S.R., 2019. Changes on Eubacteria 338I, Gamma-, Betaproteobacteria in biofilms from drinking water systems according to operational conditions. Environ. Process. 6, 85–106. https://doi.org/10.1007/s40710-019-00355-0

Pérez, M.F.L., Susa, M.R., 2017. Exopolymeric substances from drinking water biofilms: Dynamics of production and relation with disinfection by products. Water Res. 116, 304–315. https://doi.org/10.1016/j.watres.2017.03.036

Peterson, E.S., Summers, R.S., 2021. Removal of effluent organic matter with biofiltration for potable reuse: A review and meta-analysis. Water Res. 199, 117180. https://doi.org/https://doi.org/10.1016/j.watres.2021.117180

Peterson, G.L., 1977. A simplification of the protein assay method of Lowry et al. which is more generally applicable. Anal. Biochem. 83, 346–356. https://doi.org/10.1016/0003-2697(77)90043-4

Pichel, N., Vivar, M., Fuentes, M., 2019. The problem of drinking water access: A review of disinfection technologies with an emphasis on solar treatment methods. Chemosphere 218, 1014–1030. https://doi.org/10.1016/j.chemosphere.2018.11.205

Pickering, C., Byrne, J., 2014. The benefits of publishing systematic quantitative literature reviews for PhD candidates and other early-career researchers. High. Educ. Res. Dev. 33, 534–548. https://doi.org/10.1080/07294360.2013.841651

Pitanga, F., 2011. The effect of sodium hypochlorite in different aquatic organisms. MSc Thesis, Biology Department, University of Aveiro. 1-58.

Proctor, C.R., Hammes, F., 2015. Drinking water microbiology - from measurement to management. Curr. Opin. Biotechnol. 33, 87–94. https://doi.org/10.1016/j.copbio.2014.12.014

Qi, C., Liu, X., Ma, J., Lin, C., Li, X., Zhang, H., 2016. Activation of peroxymonosulfate by base: Implications for the degradation of organic pollutants. Chemosphere 151, 280–288. https://doi.org/https://doi.org/10.1016/j.chemosphere.2016.02.089

Qi, H., Huang, Q., Hung, Y.-C., 2018. Efficacy of activated persulfate in inactivating *Escherichia coli* O157:H7 and *Listeria monocytogenes*. Int. J. Food Microbiol. 284, 40–47. https://doi.org/https://doi.org/10.1016/j.ijfoodmicro.2018.06.021

Ragain, L., Masters, S., Bartrand, T.A., Clancy, J.L., Whelton, A.J., 2019. Analysis of building plumbing system flushing practices and communications. J. Water Health 17, 196–203. https://doi.org/10.2166/wh.2019.024

Rand, J.L., Sharafimasooleh, M., Walsh, M.E., 2013. Effect of water hardness and pipe material on enhanced disinfection with UV light and chlorine. J. Water Supply Res. Technol. 62, 426–432. https://doi.org/10.2166/aqua.2013.060

Rebelo, S.L.H., Moniz, T., Medforth, C.J., de Castro, B., Rangel, M., 2019. EPR spin trapping studies of H_2O_2 activation in metaloporphyrin catalyzed oxygenation reactions: Insights on the biomimetic mechanism. Mol. Catal. 475, 110500. https://doi.org/https://doi.org/10.1016/j.mcat.2019.110500

Redmond, R.W., Gamlin, J.N., 1999. A compilation of singlet oxygen yields from biologically relevant molecules. Photochem. Photobiol. 70, 391–475.

Regulation (EU) No 528/2012 of the European Parliament and of the Council of 22 May 2012 concerning the making available on the market and use of biocidal products (Text with EEA relevance) (OJ L 167, 27.6.2012, p. 1–123, ELI: http://data.europa.eu/eli/reg/2012/528/oj)

Rosalina, I., Bhattacharya, M., 2002. Dynamic rheological measurements and analysis of starch gels. Carbohydr. Polym. 48, 191–202. https://doi.org/https://doi.org/10.1016/S0144-8617(01)00235-1

Rożej, A., Cydzik-Kwiatkowska, A., Kowalska, B., Kowalski, D., 2015. Structure and microbial diversity of biofilms on different pipe materials of a model drinking water distribution systems. World J. Microbiol. Biotechnol. 31, 37–47. https://doi.org/10.1007/s11274-014-1761-6

Schwering, M., Song, J., Louie, M., Turner, R.J., Ceri, H., 2013. Multi-species biofilms defined from drinking water microorganisms provide increased protection against chlorine disinfection. Biofouling 29, 917–928. https://doi.org/10.1080/08927014.2013.816298

Sedgwick, S.G., 1973. Inducible error-prone repair in *Escherichia coli*. Proc. Natl. Acad. Sci. U.S.A. 72, 2753–2757. https://doi.org/10.1073/pnas.72.7.2753

Sharafimasooleh, M., Rand, J.L., Walsh, M.E., 2016. Effect of high chloride concentrations on microbial regrowth in drinking water distribution systems. J. Environ. Eng. 142, 1–7. https://doi.org/10.1061/(ASCE)EE.1943-7870.0001027

Shen, Y., Huang, C., Lin, J., Wu, W., Ashbolt, N.J., Liu, W.-T., Nguyen, T.H., 2017. Effect of disinfectant exposure on *Legionella pneumophila* associated with simulated drinking water biofilms: release, inactivation, and infectivity. Environ. Sci. Technol. 51, 2087–2095. https://doi.org/10.1021/acs.est.6b04754

Shen, Y., Huang, C., Monroy, G.L., Janjaroen, D., Derlon, N., Lin, J., Espinosa-Marzal, R., Morgenroth, E., Boppart, S.A., Ashbolt, N.J., Liu, W.-T., Nguyen, T.H., 2016. Response of simulated drinking water biofilm mechanical and structural properties to long-term disinfectant exposure. Environ. Sci. Technol. 50, 1779–1787. https://doi.org/10.1021/acs.est.5b04653

Shi, X., Clark, G.G., Huang, C., Nguyen, T.H., Yuan, B., 2022. Chlorine decay and disinfection by-products formation during chlorination of biofilms formed with simulated drinking water containing corrosion inhibitors. Sci. Total Environ. 815, 152763. https://doi.org/10.1016/j.scitotenv.2021.152763

Shi, Y., Babatunde, A., Bockelmann-Evans, B., Webster, G., 2019. Influence of hydraulic regimes and Cl_2/NH_3-N mass ratios on the bacterial structure and composition in an experimental flow cell chloraminated drinking water system. Environ. Sci. Water Res. Technol. 5, 977–992. https://doi.org/10.1039/c9ew00015a

Silva, A., Figueiredo, S.A., Sales, M.G., Delerue-Matos, C., 2009. Ecotoxicity tests using the green algae *Chlorella vulgaris*—A useful tool in hazardous effluents management. J. Hazard. Mater. 167, 179–185. https://doi.org/https://doi.org/10.1016/j.jhazmat.2008.12.102

Simões, L.C., Chaves, A.F.A., Simões, M., Lima, N., 2023. Interactions between *Penicillium brevicompactum*/*Penicillium expansum* and *Acinetobacter calcoaceticus* isolated from drinking water in biofilm development and control. Int. J. Food Microbiol. 384, 109980. https://doi.org/https://doi.org/10.1016/j.ijfoodmicro.2022.109980

Simões, L.C., Simões, M., 2013. Biofilms in drinking water: problems and solutions. RSC Adv. 3, 2520–2533. https://doi.org/10.1039/c2ra22243d

Simões, L.C., Simões, M., Oliveira, R., Vieira, M.J., 2007a. Potential of the adhesion of bacteria isolated from drinking water to materials. J. Basic Microbiol. 47, 174–183. https://doi.org/10.1002/jobm.200610224

Simões, L.C., Simões, M., Vieira, M.J., 2010a. Adhesion and biofilm formation on polystyrene by drinking water-isolated bacteria. Antonie van Leeuwenhoek, Int. J. Gen. Mol. Microbiol. 98, 317–329. https://doi.org/10.1007/s10482-010-9444-2

Simões, L.C., Simões, M., Vieira, M.J., 2007b. Biofilm interactions between distinct bacterial genera isolated from drinking water. Appl. Environ. Microbiol. 73, 6192–6200. https://doi.org/10.1128/AEM.00837-07

Simões, M., Pereira, M.O., Vieira, M.J., 2005. Effect of mechanical stress on biofilms challenged by different chemicals. Water Res. 39, 5142–5152. https://doi.org/10.1016/j.watres.2005.09.028

Simões, M., Simões, L.C., Cleto, S., Machado, I., Pereira, M.O., Vieira, M.J., 2007. Antimicrobial mechanisms of ortho-phthalaldehyde action. J. Basic Microbiol. 47, 230–242. https://doi.org/10.1002/jobm.200610280

Simões, M., Simões, L.C., Vieira, M.J., 2010. A review of current and emergent biofilm control strategies. LWT - Food Sci. Technol. 43, 573–583. https://doi.org/10.1016/j.lwt.2009.12.008

Sinha, P., Mukherji, S., 2022. Biofiltration process for treatment of water and wastewater. Trans. Indian Natl. Acad. Eng. 7, 1069–1091. https://doi.org/10.1007/s41403-022-00360-0

Song, C., Zhao, C., Wang, Q., Lu, S., She, Z., Zhao, Y., Jin, C., Guo, L., Li, K., Gao, M., 2021. Impact of carbon/nitrogen ratio on the performance and microbial community of sequencing batch biofilm reactor treating synthetic mariculture wastewater. J. Environ. Manage. 298, 113528 . https://doi.org/https://doi.org/10.1016/j.jenvman.2021.113528

Soto-Giron, M.J., Rodriguez-R, L.M., Luo, C.W., Elk, M., Ryu, H., Hoelle, J., Domingo, J.W.S., Konstantinidis, K.T., 2016. Biofilms on hospital shower hoses: Characterization and implications for nosocomial infections. Appl. Environ. Microbiol. 82, 2872–2883. https://doi.org/10.1128/AEM.03529-15

Stüken, A., Haverkamp, T.H.A., Dirven, H.A.A.M., Gilfillan, G.D., Leithaug, M., Lund, V., 2018. Microbial community composition of tap water and biofilms treated with or without copper-silver ionization. Environ. Sci. Technol. 52, 3354–3364. https://doi.org/10.1021/acs.est.7b05963

Sun, H., Shi, B., Bai, Y., Wang, D., 2014. Bacterial community of biofilms developed

under different water supply conditions in a distribution system. Sci. Total Environ. 472, 99–107. https://doi.org/10.1016/j.scitotenv.2013.11.017

Sun, P., Tyree, C., Huang, C.-H., 2016. Inactivation of *Escherichia coli*, Bacteriophage MS2, and *Bacillus* Spores under UV/H_2O_2 and UV/peroxydisulfate advanced disinfection conditions. Environ. Sci. Technol. 50, 4448–4458. https://doi.org/10.1021/acs.est.5b06097

Szabo, J., Rodgers, M., Mistry, J., Steenbock, J., Hall, J., 2019. The effectiveness of disinfection and flushing procedures to prevent coliform persistence in aircraft water systems. Water Supply 19, 1339–1346. https://doi.org/10.2166/ws.2018.195

Tian, F., Li, J., Nazir, A., Tong, Y., 2021. Bacteriophage - a promising alternative measure for bacterial biofilm control. Infect. Drug Resist. 14, 205–217. https://doi.org/10.2147/IDR.S290093

Tian, X., Sun, Y., Fan, S., Boudreau, M.D., Chen, C., Ge, C., Yin, J.-J., 2019. Photogenerated charge carriers in molybdenum disulfide quantum dots with enhanced antibacterial activity. ACS Appl. Mater. Interfaces 11, 4858–4866. https://doi.org/10.1021/acsami.8b19958

Timofeev, V.P., Misharin, A.Y., Tkachev, Y. V, 2011. Simulation of EPR spectra of the radical TEMPO in water-lipid systems in different microwave ranges. Biophysics (Oxf). 56, 407–417. https://doi.org/10.1134/S0006350911030274

Tonev, R., Dimova, G., 2020. Investigation of chlorine wall decay in an old, decommissioned metallic pipe using a pipe section reactor. Water Supply 20, 953–962. https://doi.org/10.2166/ws.2020.017

Tsaridou, C., Karabelas, A.J., 2021. Drinking water standards and their implementation - A critical assessment. Water. https://doi.org/10.3390/w13202918

United Nations (UN) General Assembly, 2010. Resolution A/RES/64/292 The human right to water and sanitation.

United States Environmental Protection Agency (U.S. EPA), 2011. Development and testing of methods to decontaminate a building's plumbing system impacted by water contamination event: Decontamination of *Bacillus* spores (No. EPA/600/R-09/089). Washington, DC.

Vale, F., Sousa, C.A., Sousa, H., Santos, L., Simões, M., 2022. Impact of parabens on microalgae bioremediation of wastewaters: A mechanistic study. Chem. Eng. J. 442, 136374. https://doi.org/https://doi.org/10.1016/j.cej.2022.136374

van Oss, C.J., Chaudhury, M.K., Good, R.J., 1987. Monopolar Surfaces. Adv. Colloid Interface Sci. 28, 35–64. https://doi.org/10.1016/0001-8686(87)80008-8

van Oss, C.J., Good, R.J., Chaudhury, M.K., 1988. Additive and nonadditive surface tension components and the interpretation of contact angles. Langmuir 4, 884–891. https://doi.org/10.1021/la00082a018

van Oss, C.J., Ju, L., Chaudhury, M.K., Good, R.J., 1989. Estimation of the polar parameters of the surface tension of liquids by contact angle measurements on gels. J. Colloid Interface Sci. 128, 313–319. https://doi.org/10.1016/0021-9797(89)90345-7

Vannoni, M., Creach, V., Barry, J., Sheahan, D., 2018. Chlorine toxicity to *Navicula pelliculosa* and *Achnanthes* spp. in a flow-through system: The use of immobilised microalgae and variable chlorophyll fluorescence. Aquat. Toxicol. 202, 80–89. https://doi.org/https://doi.org/10.1016/j.aquatox.2018.06.013

Verner-Jeffreys, D.W., Joiner, C.L., Bagwell, N.J., Reese, R.A., Husby, A., Dixon, P.F., 2009. Development of bactericidal and virucidal testing standards for aquaculture disinfectants. Aquaculture 286, 190–197. https://doi.org/10.1016/j.aquaculture.2008.10.001

Waak, M.B., Hozalski, R.M., Hallé, C., LaPara, T.M., 2019. Comparison of the microbiomes of two drinking water distribution systems - with and without residual chloramine disinfection. Microbiome 7, 1–14. https://doi.org/10.1186/s40168-019-0707-5

Wacławek, S., Lutze, H. V., Grübel, K., Padil, V.V.T., Černík, M., Dionysiou, D.D., 2017. Chemistry of persulfates in water and wastewater treatment: A review. Chem. Eng. J. 330, 44–62. https://doi.org/10.1016/j.cej.2017.07.132

Wahman, D.G., 2018. Chlorinated cyanurates: review of water chemistry and associated drinking water implications. J. Am. Water Works Assoc. 110, E1–E15. https://doi.org/10.1002/awwa.1086

Wan, K., Zhang, M., Ye, C., Lin, W., Guo, L., Chen, S., Yu, X., 2019. Organic carbon: An overlooked factor that determines the antibiotic resistome in drinking water sand filter biofilm. Environ. Int. 125, 117–124. https://doi.org/https://doi.org/10.1016/j.envint.2019.01.054

Wang, H., Hu, C., Zhang, S., Liu, L., Xing, X., 2018. Effects of O_3/Cl_2 disinfection on corrosion and opportunistic pathogens growth in drinking water distribution systems. J. Environ. Sci. 73, 38–46. https://doi.org/10.1016/j.jes.2018.01.009

Wang, H., Pryor, M.A., Edwards, M.A., Falkinham, J.O., Pruden, A., 2013. Effect of GAC pre-treatment and disinfectant on microbial community structure and opportunistic pathogen occurrence. Water Res. 47, 5760–5772. https://doi.org/10.1016/j.watres.2013.06.052

Wang, H., Zhu, Y., Hu, C., 2017. Impacts of bacteria and corrosion on removal of natural organic matter and disinfection byproducts in different drinking water distribution systems. Int. Biodeterior. Biodegrad. 117, 52–59. https://doi.org/10.1016/j.ibiod.2016.11.023

Wang, H.B., Hu, C., Hu, X.X., 2014. Effects of combined UV and chlorine disinfection on corrosion and water quality within reclaimed water distribution systems. Eng. Fail. Anal. 39, 12–20. https://doi.org/10.1016/j.engfailanal.2014.01.009

Wang, L., Fu, Y., Li, Q., Wang, Z., 2022. EPR Evidence for mechanistic diversity of Cu(II)/peroxygen oxidation systems by tracing the origin of DMPO spin adducts. Environ. Sci. Technol. 56, 8796–8806. https://doi.org/10.1021/acs.est.2c00459

Wang, Z., Li, L., Ariss, R.W., Coburn, K.M., Behbahani, M., Xue, Z., Seo, Y., 2021. The role of biofilms on the formation and decay of disinfection by-products in chlor(am)inated water distribution systems. Sci. Total Environ. 753, 141606. https://doi.org/10.1016/j.scitotenv.2020.141606

Wei, Z., Villamena, F.A., Weavers, L.K., 2017. Kinetics and mechanism of ultrasonic activation of persulfate: An *in situ* EPR spin trapping study. Environ. Sci. Technol. 51, 3410–3417. https://doi.org/10.1021/acs.est.6b05392

Wojtowicz, J.A., 2001. Relative bactericidal effectiveness of hypochlorous acid and chloroisocyanurates. J. Swim. Pool Spa Ind. 2, 34–41.

Wordofa, D.N., Walker, S.L., Liu, H., 2017. Sulfate radical-induced disinfection of pathogenic *Escherichia coli* O157:H7 via iron-activated persulfate. Environ. Sci. Technol. Lett. 4, 154–160. https://doi.org/10.1021/acs.estlett.7b00035

World Health Organization (WHO), 1996. Guidelines for drinking-water quality. Vol. 2, Health criteria and other supporting information. International Program on Chemical Safety. Geneva. ISBN: 9241544805

World Health Organization (WHO), 2022. Guidelines for drinking-water quality: fourth edition incorporating the first and second addenda. Licence: CC BY-NC-SA 3.0 IGO. ISBN: 978-92-4-004506-4

Wu, H.T., Zhang, J.X., Mi, Z.L., Xie, S.G., Chen, C., Zhang, X.J., 2015. Biofilm bacterial communities in urban drinking water distribution systems transporting waters with different purification strategies. Appl. Microbiol. Biotechnol. 99, 1947–1955. https://doi.org/10.1007/s00253-014-6095-7

Xia, D., Li, Y., Huang, G., Yin, R., An, T., Li, G., Zhao, H., Lu, A., Wong, P.K., 2017. Activation of persulfates by natural magnetic pyrrhotite for water disinfection: Efficiency, mechanisms, and stability. Water Res. 112, 236–247. https://doi.org/https://doi.org/10.1016/j.watres.2017.01.052

Xing, X.C., Wang, H.B., Hu, C., Liu, L.Z., 2018. Effects of phosphate-enhanced ozone/biofiltration on formation of disinfection byproducts and occurrence of opportunistic pathogens in drinking water distribution systems. Water Res. 139, 168–176. https://doi.org/10.1016/j.watres.2018.03.073

Xue, Z., Lee, W.H., Coburn, K.M., Seo, Y., 2014. Selective reactivity of monochloramine with extracellular matrix components affects the disinfection of biofilm and detached clusters. Environ. Sci. Technol. 48, 3832–3839. https://doi.org/10.1021/es405353h

Xue, Z., Seo, Y., 2013. Impact of chlorine disinfection on redistribution of cell clusters from biofilms. Environ. Sci. Technol. 47, 1365–1372. https://doi.org/10.1021/es304113e

Yan, J., Moreau, A., Khodaparast, S., Perazzo, A., Feng, J., Fei, C., Mao, S., Mukherjee, S., Košmrlj, A., Wingreen, N.S., Bassler, B.L., Stone, H.A., 2018. Bacterial biofilm material properties enable removal and transfer by capillary peeling. Adv. Mater. 30. https://doi.org/10.1002/adma.201804153

Yan, X., Lin, T., Wang, X., Zhang, S., Zhou, K., 2022. Effects of pipe materials on the characteristic recognition, disinfection byproduct formation, and toxicity risk of pipe wall biofilms during chlorination in water supply pipelines. Water Res. 210, 117980. https://doi.org/https://doi.org/10.1016/j.watres.2021.117980

Ye, X., Wang, P., Wu, Y., Zhou, Y., Sheng, Y., Lao, K., 2020. Microplastic acts as a

vector for contaminants: the release behavior of dibutyl phthalate from polyvinyl chloride pipe fragments in water phase. Environ. Sci. Pollut. Res. 27, 42082–42091. https://doi.org/10.1007/s11356-020-10136-0

Yu, J., Baek, Y., Yoon, H., Yoon, J., 2013. New disinfectant to control biofouling of polyamide reverse osmosis membrane. J. Memb. Sci. 427, 30–36. https://doi.org/10.1016/j.memsci.2012.09.057

Yu, Z., Li, X., Guo, J., 2022. Combat antimicrobial resistance emergence and biofilm formation through nanoscale zero-valent iron particles. Chem. Eng. J. 444, 136569. https://doi.org/https://doi.org/10.1016/j.cej.2022.136569

Yuan, L., Sadiq, F.A., Wang, N., Yang, Z., He, G., 2020. Recent advances in understanding the control of disinfectant-resistant biofilms by hurdle technology in the food industry. Crit. Rev. Food Sci. Nutr. 0, 1–16. https://doi.org/10.1080/10408398.2020.1809345

Zhang, H.J., Yang, Y.L., Li, X., Liu, Y.W., Zhao, L., 2018. Evaluation of biofilm development on various pipelines in the domestic hot water system. Water Sci. Technol. Supply 18, 638–647. https://doi.org/10.2166/ws.2017.138

Zhang, X., Lin, T., Wang, X., 2022. Investigation of microplastics release behavior from ozone-exposed plastic pipe materials. Environ. Pollut. 296, 118758. https://doi.org/https://doi.org/10.1016/j.envpol.2021.118758

Zhu, Y., Chen, L., Xiao, H., Shen, F., Deng, S.H., Zhang, S.R., He, J.S., Song, C., Wang, X., Zhang, J.H., Gong, L., Hu, C., 2020. Effects of disinfection efficiency on microbial communities and corrosion processes in drinking water distribution systems simulated with actual running conditions. J. Environ. Sci. 88, 273–282. https://doi.org/10.1016/j.jes.2019.09.009

Zhu, Y., Wang, H.B., Li, X.X., Hu, C., Yang, M., Qu, J.H., 2014. Characterization of biofilm and corrosion of cast iron pipes in drinking water distribution system with UV/Cl_2 disinfection. Water Res. 60, 174–181. https://doi.org/10.1016/j.watres.2014.04.035

Zhu, Z., Shan, L., Hu, F., Li, Z., Zhong, D., Yuan, Y., Zhang, J., 2020a. Biofilm formation potential and chlorine resistance of typical bacteria isolated from drinking water distribution systems. RSC Adv. 10, 31295–31304. https://doi.org/10.1039/D0RA04985A

Zhu, Z., Shan, L., Zhang, X., Hu, F., Zhong, D., Yuan, Y., Zhang, J., 2021. Effects of bacterial community composition and structure in drinking water distribution systems on biofilm formation and chlorine resistance. Chemosphere 264, 128410. https://doi.org/10.1016/j.chemosphere.2020.128410

Zou, J., Huang, Y., Zhu, L., Cui, Z., Yuan, B., 2019. Multi-wavelength spectrophotometric measurement of persulfates using 2,2′-azino-bis(3-ethylbenzothiazoline-6-sulfonate) (ABTS) as indicator. Spectrochim. Acta Part A Mol. Biomol. Spectrosc. 216, 214–220. https://doi.org/https://doi.org/10.1016/j.saa.2019.03.019

Zuo, P., Metz, J., Yu, P., Alvarez, P.J.J., 2022. Biofilm-responsive encapsulated-phage coating for autonomous biofouling mitigation in water storage systems. Water Res.

224, 119070. https://doi.org/10.1016/j.watres.2022.119070

Annex A – Bacterial concentration and optical density relationship

Throughout this work, the antimicrobial and antibiofilm assays were typically run at bacterial concentrations of 10^8 or 10^6 CFU/mL. To achieve the proper dilution, initially, a curve that relates optical density ($OD_{610\ nm}$) to bacteria concentration (CFU/mL) was generated for *S. maltophilia* and *A. calcoaceticus*. The procedure was based on the protocol reported by Campbell (2010), with some modifications. Bacteria were grown overnight in batch cultures using R2A broth at 25 ± 2 ºC and under agitation (150 rpm). Cells were harvested by centrifugation at 3220 ×*g*, 10 min, washed, and resuspended in PBS (pH 7.4) until $OD_{610\ nm} \approx 1.0$. The cultures were then diluted in proportions 4:1, 3:2, 2:3, 1:4, and 1:9 into PBS and the optical density at 610 nm of each sample was measured, including the original sample where $OD_{610\ nm} \approx 1.0$. Finally, the samples were 10-fold serially diluted in PBS, and 10 µL of each dilution was placed on R2A agar plates. Colony counting was carried out after 48 h of incubation at 25 ± 2 ºC, and bacterial concentration (CFU/mL) was determined. A linear regression was performed on the data and the equation representing bacterial concentration (CFU/mL) vs. optical density $OD_{610\ nm}$ was recorded (**Figures A-1** and **A-2**).

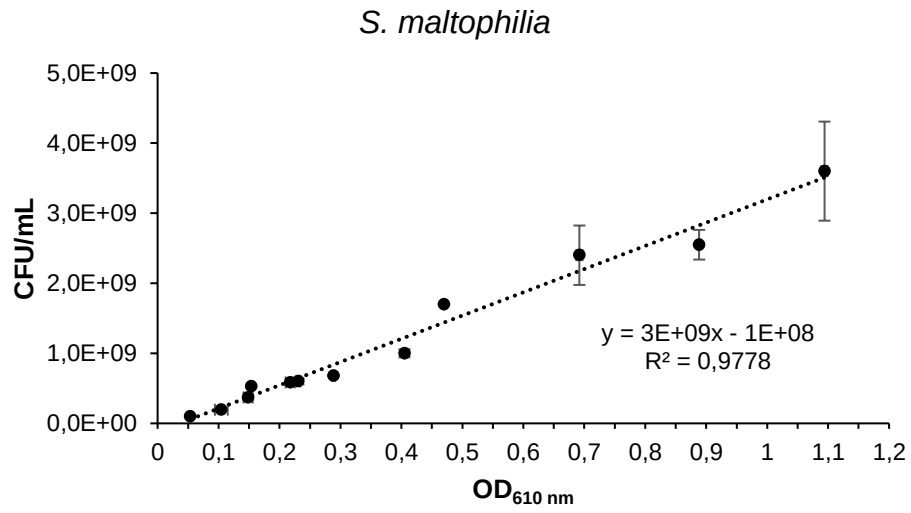

Figure A-1 – Graph depicting *S. maltophilia* concentration (CFU/mL) vs. optical density (OD_{610nm}).

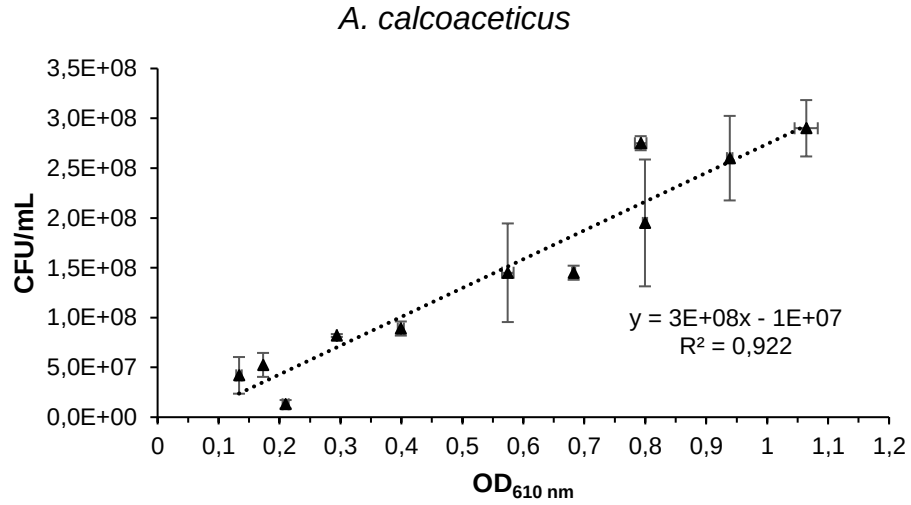

Figure A-2 – Graph depicting *A. calcoaceticus* concentration (CFU/mL) vs. optical density (OD_{610nm}).

References

Campbell, J., 2010. High-throughput assessment of bacterial growth inhibition by optical density measurements. Curr Protoc Chem Biol. 2, 195–208. https://doi.org/10.1002/9780470559277.ch100115

Annex B – Test for validation of dilution-neutralization method

The validation of the dilution-neutralization method for each disinfectant and bacteria was performed according to the European Standard EN 1276 (European Standard, 1997). The pre-cultures grown as described in subsection **3.1** were adjusted to a cellular density between 6×10^2 and 3×10^3 CFU/mL in PBS. A 10^{-1} dilution with ultrapure water was performed and 100 µL samples were plated on R2A agar plates. Colony counting of the suspensions were carried out after 48 h of incubation at 25 ± 2 ºC, and log CFU/mL in the experimental conditions validation (A) was determined.

For neutralizer toxicity validation, 1 mL of the cell suspension, containing approximately 10^3 CFU/mL, was added to 1 mL of sterile distilled water and 8 mL of neutralizer (described in subsection **3.3**). At the end of 5 min of incubation at room temperature (23 ± 2 ºC), 100 µL samples were plated on R2A agar plates and colony counting was carried out after 48 h of incubation at 25 ± 2 ºC for determination of log CFU/mL in the neutralizer toxicity conditions validation (B).

For dilution-neutralization validation, the disinfectants were prepared at the highest strength used in the test (according to subsection **3.3**). In a sterile tube, 1 mL of distilled water, 1 mL of PBS, and 8 mL of disinfectant solution were added and leaved in contact for 30 min at room temperature (23 ± 2 ºC). Then, 1 mL of the mixture was transferred into a test tube containing 8 mL of neutralizer. At the end of further 5 min of incubation at room temperature (23 ± 2 ºC), 1 mL of the cell suspension, containing approximately 10^3 CFU/mL, was added into the test tube. After 30 min of incubation at room temperature (23 ± 2 ºC), 100 µL samples were plated on R2A agar plates. Colony counting was carried

out after 48 h of incubation at 25 ± 2 ºC for determination of log CFU/mL in the dilution-neutralization validation (C).

The results of the test for validation of the dilution-neutralization method for each disinfectant and bacteria are presented in the following table. It was concluded that the test results complied the relevant requirements for validation of the method.

Table B-1 – Validation of the dilution-neutralization method

	A. calcoaceticus	***S. maltophilia***
A log CFU/mL	2.5	2.5
B log CFU/mL	2.5	2.4
C log CFU/mL		
NaDCC	2.5	2.5
TCCA	2.6	2.6
OXONE	2.6	2.7

Annex C – Characterization of colony biofilms

The 48 h-old *S. maltophilia* colony biofilms used in the rheological measurements presented diameters of approximately 8 mm and thickness of 70-170 μm. The magnitude of culturable cells and total cells were higher than the corresponding values for biofilms formed on PVC and SS coupons. However, these results are in accordance with other studies using colony biofilms (Fernandes et al., 2022).

Table C-1 – Characteristics of 48 h-old colony biofilms of *S. maltophilia*.

	Colony biofilms
Culturable cells, log CFU/cm^2	9.8 ± 0.1
Total cells, log cells/cm^2	10.1 ± 0.2
Biofilm matrix proteins, μg/cm^2	153.6 ± 34.0
Biofilm matrix polysaccharides, μg/cm^2	84.1 ± 37.3

References

Fernandes, S., Gomes, I.B., Simões, M., 2022. Antibiofilm activity of glycolic acid and glyoxal and their diffusion–reaction interactions with biofilm components. Food Res. Int. 152, 110921. https://doi.org/10.1016/j.foodres.2021.110921

Annex D – Antimicrobial activity of other disinfectants

During the first task of the project to accomplish the first objective of the work, other disinfectants were also tested for screening the antimicrobial activity against *S. maltophilia* and *A. calcoaceticus* in the planktonic states. However, in the following tasks, these disinfectants were not further evaluated given their lower biocidal efficacy than the disinfectants studied throughout this work. Below are described the results obtained for the disinfectants that were declined during the screening task.

Sodium N-chlorobenzenesulfonamide (chloramin B) from Sigma-Aldrich (St. Louis MO, USA) was also selected from the product type 5 Article 95 List of the Biocidal Products Regulation published by ECHA (2020). A similar dose-response relationship was performed as described in subsection **3.3**. The results are presented in **Figure D-1**. However, this disinfectant did not show antimicrobial activity in the range of the concentrations tested. On the other hand, even though at the time of disinfectant selection, the initial application for approval of chloramin B was under competent authority evaluation, on 24 November 2022 the European Commission adopted the decision to not approve this disinfectant as an active substance for the use in biocidal products of product-types 2, 3, 4, and 5 (private area and public health area disinfectants and other biocidal products, veterinary hygiene biocidal products, food and feed area disinfectants, drinking water disinfectants) (Commission Implementing Decision (EU) 2022/2327).

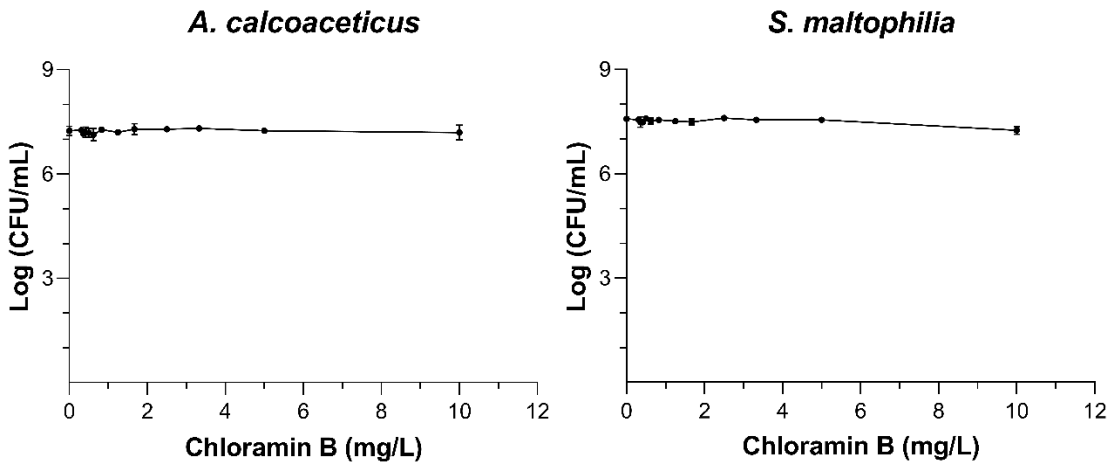

Figure D-1 – Dose-response relationship after 30 min of exposure to chloramine B against *A. calcoaceticus* and *S. maltophilia*.

Additional disinfectants (*e.g.* cinnamaldehyde, gallic acid, ferulic acid, syringic acid, vanillic acid) were selected based on the results from the FCT project Phytodisinfectants (FCT|PTDC/DTP-SAP/1078/2012) on the testing of phytochemical products for disinfection. The off-label use of chemical molecules currently applied as additives and preservatives in industrial products is a strategy of potential interest to replenish the pipeline of disinfectants (Tajkarimi and Ibrahim, 2012). Herbal-based treatments have been employed for coagulation processes and disinfection of DW in rural areas of developing countries for several centuries (Pandit and Kumar, 2015). Details of structures and sources of many antimicrobial phytochemicals have been widely compiled, and evidence of the functions of these products has also been reviewed (Cowan, 1999; Simões et al., 2009).

The minimum inhibitory concentrations (MIC) of cinnamaldehyde, gallic acid, ferulic acid, syringic acid, and vanillic acid (Sigma-Aldrich, St. Louis MO, USA) for *A. calcoaceticus* and *S. maltophilia* were determined by the broth microdilution method according to Gomes et al. (2016) and Oliveira et al. (2019), with some modifications. Pre-culture as described in subsection **3.1** were used as inoculum (≈ 10^8 CFU/mL) in R2A

broth. Then, 96-well polystyrene microtiter plates were filled with 20 µL of phytochemical solution at a range of different concentrations (final concentrations between 12.5 and 1000 mg/L in DMSO) and 180 µL of the bacterial suspension. Bacterial suspensions without phytochemicals and with DMSO were used as controls. The highest DMSO concentration remaining after dilution was 5% (v/v). The optical density was measured in a microtiter plate reader at 610 nm (FLUOstar Omega; BMG LABTECH, Germany) before and after 24 h incubation at 25 ± 2 °C and 150 rpm. The MIC was defined as the lowest concentration that prevented bacterial growth. Then, for MBC determination, a volume of 10 µL of bacterial suspension was directly removed from the wells containing phytochemical concentrations equal to and above the MIC and placed onto R2A agar. Plates were incubated at 25 ± 2 °C for 24 h and bacterial growth was visually inspected. MBC was considered to be the lowest concentration in which complete growth absence was detected on the solid culture medium after exposure to phytochemicals. The results are presented in **Table D-1**.

Table D-1 – MIC and MBC values of selected phytochemicals against *A. calcoaceticus* and *S. maltophilia*.

	A. calcoaceticus		***S. maltophilia***	
	MIC (mg/L)	MBC (mg/L)	MIC (mg/L)	MBC (mg/L)
cinnamaldehyde	400	800	200	>1000
ferulic acid	800	>1000	800	>1000
gallic acid	800	>1000	1000	>1000
syringic acid	800	>1000	800	>1000
vanillic acid	800	>1000	800	>1000

The MIC values were between 200 and 1000 mg/L, the MIC of cinnamaldehyde against *S. maltophilia* was the lowest value, and the MIC of gallic acid against *S.*

maltophilia was the highest. Cinnamaldehyde presented the best results against both bacteria. However, in general, the selected phytochemicals did not show biocidal activity within the range of concentrations tested (MBC > 1000 mg/L), except for the case of cinnamaldehyde that exhibited MBC equal to 800 mg/L against *A. calcoaceticus*. The results are under MIC and MBC values reported for other bacteria (*S. aureus*, *E. coli*, *P. aeruginosa*, and *L. monocytogenes*) with food and biomedical relevance (Borges et al., 2013; Malheiro et al., 2016).

References

Borges, A., Ferreira, C., Saavedra, M.J., Simões, M., 2013. Antibacterial activity and mode of action of ferulic and gallic acids against pathogenic bacteria. Microb. Drug Resist. 19, 256–265. http://doi.org/10.1089/mdr.2012.0244

Commission Implementing Decision (EU) 2022/2327 of 24 November 2022 not approving chloramin B as an active substance for use in biocidal products of product-types 2, 3, 4 and 5 in accordance with Regulation (EU) No 528/2012 of the European Parliament and of the Council (Text with EEA relevance) (OJ L 307 28.11.2022, p. 271-272, ELI: http://data.europa.eu/eli/dec_impl/2022/2327/oj).

Cowan, M.M., 1999. Plant Products as Antimicrobial Agents, Clin. Microbiol. Rev. 12, 564–582.

European Chemicals Agency (ECHA), 2020. Article 95 List of active substances and product suppliers [WWW document]. https://echa.europa.eu/pt/information-on-chemicals/active-substance-suppliers. (Accessed 30 July 2020).

Gomes, I.B., Simões, M., Simões, L.C., 2016. The effects of sodium hypochlorite against selected drinking water-isolated bacteria in planktonic and sessile states. Sci. Total Environ. 565, 40–48. https://doi.org/10.1016/j.scitotenv.2016.04.136

Malheiro, J., Gomes, I., Borges, A., Bastos, M.M.S.M., Maillard, J.-Y., Borges, F., Simões, M., 2016. Phytochemical profiling as a solution to palliate disinfectant limitations. Biofouling. 32, 1007–1016. http://dx.doi.org/10.1080/08927014.2016.1220550

Oliveira, I.M., Borges, A., Borges, F., Simões, M., 2019. Repurposing ibuprofen to control *Staphylococcus aureus* biofilms. Eur. J. Med. Chem. 166, 197-205. https://doi.org/10.1016/j.ejmech.2019.01.046

Pandit, A.B. and Kumar, J.K., 2015. Clean water for developing countries, Annu. Rev. Chem. Biomol. Eng. 6, 217–246. https://doi.org/10.1146/annurev-chembioeng-061114-123432

Simões, M., Bennett, R.N., Rosa, E.A.S., 2009. Understanding antimicrobial activities of phytochemicals against multidrug resistant bacteria and biofilms, Nat. Prod. Rep. 26, 746–757. https://doi.org/10.1039/b821648g

Tajkarimi, M. and Ibrahim, S., 2012. Phytochemicals as antimicrobial food preservatives, in: Dietary phytochemicals and microbes. A. Patra (Ed.), Springer. 207–235.

Annex E – AFM-based measurement of biofilm stiffness

The AFM-based indentation experiments were performed on 48 h-old *S. maltophilia* biofilms formed on SS equally prepared and treated as mentioned in subsections **3.7.1** and **3.7.2**. After exposure to OXONE, biofilms were rinsed two times with PBS to remove loosely attached fragments of the surface. Indentation measurements were executed on biofilms under ultrapure water using a custom-made chamber, an atomic force microscope TT-AFM from AFM Workshop, and DNP-10 probes (Bruker) in non-vibrating (contact) mode. After the acquisition of deflection-distance curves, the software MountainsSPIP 8 was used to perform the data treatment – the conversion of deflection to force and the calculation of Young's modulus. At least 8 curves from at least 16 different zones on the biofilm surface were recorded for each sample. The deflection sensitivity (nm/V) was obtained by measuring the slope of the deflection signal versus vertical piezo displacement plot on the SS coupon without biofilms. The spring constant of the cantilever (N/m) was calibrated at the beginning of the experiments.

The following figure illustrates examples of raw data obtained in the indentation experiments of biofilms and a deflection-calibration curve.

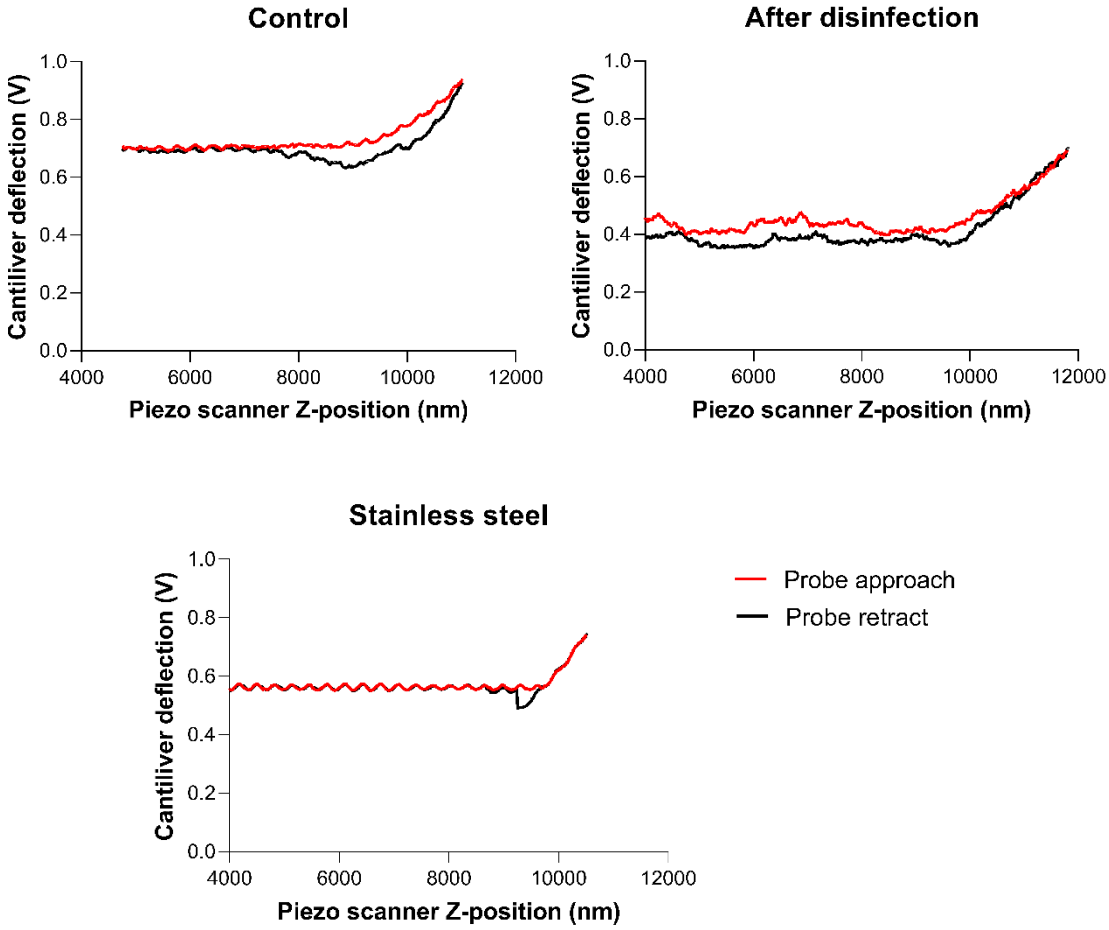

Figure E-1 – Examples of deflection-distance curves (raw data) obtained in the indentation measurements with AFM.

The values of Young's modulus calculated for unexposed and exposed biofilms to OXONE are represented in the form of histograms in **Figure E-2**. The descriptive statistics are shown in the following table.

Table E-1 – Descriptive statistics of the results obtained for Young's modulus (stiffness) of unexposed biofilms (control) and biofilms after 30 min treatment with OXONE at 10 × MBC.

Young's Modulus (kPa)	Control	After disinfection
Mean ± SD	319 ± 414	370 ± 404
Minimum	23	4
Maximum	3336	2324
Median	238	203

The results revealed a high discrepancy of Young's modulus within each sample, principally in the unexposed biofilms (control), compromising further conclusions of the effect of disinfection on biofilm stiffness. The challenges to obtaining representative results in these experiments could be related to the heterogeneity of the biofilm surface. A different silicon nitride probe (Novascan Technologies) with a 5 µm borosilicate particle was also tested but the experimental curves were similar to the deflection-calibration curve performed with SS. Therefore, the indentation of the biofilm samples by this probe was not guaranteed. Further optimizations of the protocol would be needed to study the effects of disinfection on biofilm stiffness by the AFM-based indentation technique.

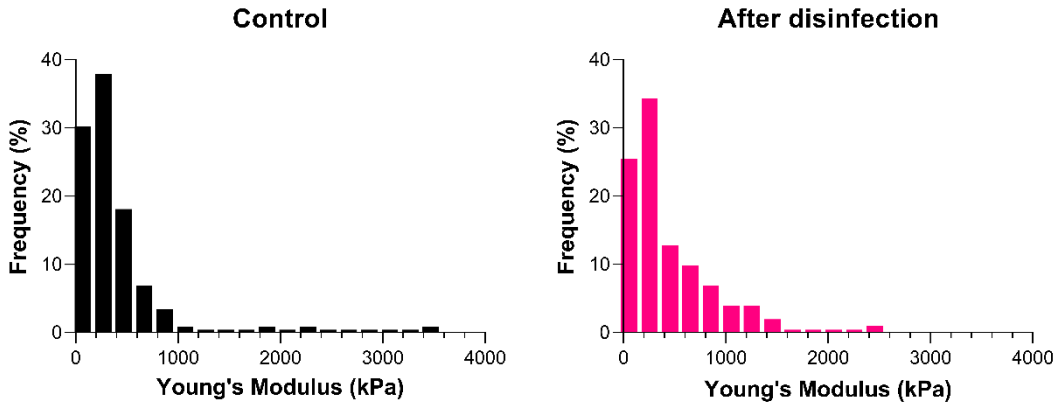

Figure E-2 – Example of histograms of Young's modulus obtained for unexposed biofilms (control) and biofilms after 30 min treatment with OXONE at 10 × MBC.